

ADDITION OF COMPLEX FUNCTIONALITY TO SURFACES VIA SULFONYL
NITRENES AND SUFEX CLICK REACTIONS

by

JEREMY MARC YATVIN

(Under the Direction of Dr. Jason Locklin)

ABSTRACT

The development of new grafting and attachment chemistries is of high importance in the materials science community. This work looks at the functionalization of the highly inert substrate Kevlar using sulfonyl azide containing polymers to generate sulfonyl nitrene groups for aryl C-H insertion. The covalent coating of polymers is demonstrated, as well as the retention of critical mechanical properties.

In addition the use of Sulfur(VI) Fluoride Exchange (SuFEx) chemistry in functionalizing polymer brushes is examined. SuFEx is a new form of click chemistry that uses sulfonyl fluorides or fluorosulfates and silyl ethers in the presence of certain bases to form sulfonate or sulfate linkages. It is highly orthogonal to most other described forms of click chemistry, and the precursors are generally redox, thermally, radical, and UV stable. This post-polymerization modification technique provides access to the inclusion of free-radical incompatible moieties in polymer brush in a single step. Using this motif, new pathways for orthogonal functionalization and patterning of polymer brush surfaces should be possible.

INDEX WORDS: polymer; surface chemistry; brushes; nitrene; click; SuFEx;

ADDITION OF COMPLEX FUNCTIONALITY TO SURFACES VIA SULFONYL
NITRENES AND SUFEX CLICK REACTIONS

By

JEREMY MARC YATVIN

BS, College of Charleston, 2011

A Dissertation Submitted to the Graduate Faculty of the University of Georgia in
Partial Fulfillment of the Requirements for the Degree

DOCTOR OF PHILOSOPHY

ATHENS, GEORGIA

2016

© 2016

Jeremy Marc Yatvin

All Rights Reserved

ADDITION OF COMPLEX FUNCTIONALITY TO SURFACES VIA SULFONYL
NITRENES AND SUFEX CLICK REACTIONS

by

JEREMY MARC YATVIN

Major Professor: Jason Locklin

Committee: Jin Xie

Sergiy Minko

Branson Ritchie

Electronic Version Approved:

Suzanne Barbour

Dean of the Graduate School

The University of Georgia

August 2016

ACKNOWLEDGEMENTS

First and foremost, I would like to thank my advisor Jason Locklin. He has constantly been in my corner, and supported me through every step of the Ph.D. experience. He knew that sometimes pressure makes diamonds, and also that sometimes a little help up is what it takes to get over the top.

Thank you also to my mentor Evan, who taught me how do synthesis, use each of our instruments, and basically be an effective and conscientious scientist. I don't think I had a single research idea I didn't run by you in the last 5 years, and your superhuman patience and good humor was beyond helpful.

Thank you to Anandi and Jing for being my partners in misery through the tough times, and for providing high fives during the good times. And yes, I am still sick of your attitudes.

Karson, I'm not even sure what to say here. We grew very close during grad school, and I will miss spending seemingly every minute around each other. You're going to do just great without me around, you're a blossoming researcher with the all the skills to succeed.

And finally, thank you to my parents. They spent uncountable hours and resources guiding and cultivating my often intense interests in science. This work is dedicated to both of them: my father Alan, who allowed me to read his sci-fi books even as I destroyed many of them in the process, and taught me to prize logic, reason, and a strong moral compass; and to my mother Laura who knew early on that I was destined for science. She taught me how to be passionate about my own work and compassionate for others, and never shirked from letting me spend "just a few more minutes" on the helicopter flight simulator game at the Franklin Institute.

TABLE OF CONTENTS

	Page
ACKNOWLEDGEMENTS	iv
LIST OF TABLES	vii
LIST OF FIGURES	ix
CHAPTER	
1 INTRODUCTION AND LITERATURE REVIEW	1
Introduction.....	1
Grafting to vs grafting from	2
High reactivity grafting to chemistries	5
Postpolymerization modification and click chemistry.....	6
Generation of complex surfaces.....	8
Mechanism of antimicrobial polyquaternary amine biocidal activity	9
Objectives and outline.....	11
References.....	13
2 ADDITION OF COPOLYMERS TO AN INERT ARAMID SURFACE VIA	
SULFONYL NITRENES	21
Abstract.....	22
Introduction.....	23
Materials and Procedure	27
Results and Discussion	33

Conclusion	40
References.....	41
3 POSTPOLYMERIZATION MODIFICATION OF POLYMER BRUSHES VIA THE SULFUR(VI) FLUORIDE EXCHANGE REACTION	47
Abstract	48
Introduction.....	49
Equipment and Materials	51
Synthesis	52
Gel permeation chromatography.....	56
Absorbance data.....	57
Grafting density calculation.....	58
Rate constant calculation	59
Dye functional group density calculation	59
EDX Spectroscopy.....	60
Results and discussion	61
Conclusion	66
References.....	68
4 FORMATION OF TRI-FUNCTIONAL SURFACES WITH THREE ORTHOGONAL CLICK REACTIONS ON POLYMER BRUSHES	72
Abstract	73
Introduction.....	74
Experimental Section	76
Results and Discussion	82

Conclusion	90
References.....	91
5 DURABLE DEFENSE: ROBUST AND VARIED ATTACHMENT OF NON-LEACHING POLY“-ONIUM” BACTERICIDAL COATINGS TO REACTIVE AND INERT SURFACES.....	95
Abstract	96
Introduction.....	97
Bacterial membrane physiology	98
Mechanism of bactericidal action with leaching “-onium” salts	98
Mechanism of bactericidal action with non-leaching “-onium” salts.....	99
Attachment chemistry	100
Polymer surfaces.....	102
Inorganic surfaces	111
Conclusions.....	117
References.....	120
6 CONCLUSIONS AND OUTLOOK.....	130
Analysis and future prospects	130
Conclusion	131
References.....	132

LIST OF TABLES

	Page
Table 2:1 Kevlar Tensile Data	36
Table 3.1: SuFEx brush thicknesses and contact angles.....	66
Table 4.1: Tri-functional brush thicknesses and contact angles	82

LIST OF FIGURES

	Page
Figure 1.1: Grafting to vs grafting from	4
Figure 1.2: Structure of Kevlar	6
Figure 1.3: Bacteria SEMs	10
Figure 2.1: Nitrene aryl insertion mechanism.....	24
Figure 2.2: Monomer selection	31
Figure 2.3: SEM and EDX of TiO ₂ functionalized Kevlar	34
Figure 2.4: TGA data for Kevlar coatings	37
Figure 2.5: FTIR of PMMA and PMMA-co-SSAz coated Kevlar	38
Figure 2.6: Fluorescent images of coated Kevlar	39
Figure 3.1: Brush PPM with SuFEx scheme	49
Figure 3.2: ¹ H NMR of 3-(fluorosulfonyl)propyl methacrylate	53
Figure 3.3: ¹⁹ F NMR of 3-(fluorosulfonyl)propyl methacrylate.....	54
Figure 3.4: GPC of poly(3-(fluorosulfonyl)propyl methacrylate)	56
Figure 3.5: Absorbance vs. time of DR1-TMS surface SuFEx catalyzed by DBU.....	57
Figure 3.6: Absorbance vs. time of DR1-TBDMS surface SuFEx catalyzed by DBU.....	57
Figure 3.7: Absorbance vs time of DR1-TBDMS surface SuFEx catalyzed by TBD	58
Figure 3.8: EDX of pFPSMA brush	60
Figure 3.9: EDX of pFSPMA brush after SuFEx with TBDMS mercaptoethanol.....	60
Figure 3.10: EDX of pFSPMA brush after SuFEx with TBDMS propargyl alcohol	61

Figure 3.11: EDX of pFSPMA brush after SuFEx with TBDMS fufuryl alcohol	61
Figure 3.12: FTIR of pFSPMA before and after PPM.....	63
Figure 3.13: Kinetic plot of SuFEx reactions	64
Figure 4.1: Reaction scheme of tri-reactive surface	75
Figure 4.2: FTIR of click reactive brush surfaces.....	84
Figure 4.3: Raman of click reactive surface	85
Figure 4.4: Kinetic plot of aminolysis, SPAAC, and SuFEx.....	86
Figure 4.5: Fluorescent microscopy of tri-functional surface.....	88
Figure 4.6: AFM images of tri-morphological surface.....	89
Figure 5.1: Phospholipid sponge diagram	100
Figure 5.3: Vinyl sulfone grafting	104
Figure 5.4: BPAMP coated substrates antimicrobial tests.....	106
Figure 5.5: SEM of <i>E. coli</i> on PET and alkylated P4VP films	108
Figure 5.6: Polycation configuration on surfaces	109
Figure 5.7: AFM of PDAEMA on surfaces	113
Figure 5.8: SFG spectra of polycation surfaces	116
Figure 5.9: Synthesis of partially quaternized catechol antimicrobial polymer	117

CHAPTER 1

INTRODUCTION AND LITERATURE REVIEW

Introduction

Protective or decorative coatings are of significant interest in polymer chemistry. Coatings from lacquer to paint are produced on a massive scale, and utilized in every facet of daily life. In the U.S. alone, the coatings market produces 1.2 billion gallons of product yearly.¹ Most of these coatings depend on noncovalent interactions such as hydrogen bonding and van der Waals forces to maintain adhesion between the coating and the substrate. However, these coatings and films have limited resistance to mechanical wear and are highly susceptible to dissolution in solvents. While simple coatings like paint are generally easy to reapply, advanced “smart” coatings often necessitate covalent attachment to a substrate to retain their usefulness.

Covalent attachment of coatings can take advantage of a wide variety of chemistries. Virtually any coupling reaction can be used if an appropriate partner functional group is on the surface; however, for coating applications, only a few specific reactions are the most widely used. Epoxides are the most common grafting chemistry and are excellent at forming tightly crosslinked network polymers. They react with surface nucleophiles as well as themselves in the presence of catalytic water.² In fact, epoxides are so reactive and dependable that they form the main ingredient in common “epoxy” glues, used in both commercial and residential applications.³ This high reactivity, however, means that epoxides will react indiscriminately with several functionalities in a polymer, and once exposed to ambient conditions they must be used quickly.

A similar surface grafting chemistry is the use of chloro- or alkoxy silanes.⁴⁻⁶ Polymers or small molecules incorporating these functional groups can condense with surface -OHs and form covalent bonds to the substrate. However, silane chemistry is sensitive to water, so while it is extremely flexible and widely used, it is not appropriate for functionalizing substrates without native -OH's or surfaces prone to exposure to aqueous solution.

While commercially relevant and dependable, grafting polymers to surfaces with these popular chemistries have significant drawbacks aside from their water sensitivity. Foremost, there is a necessity of the surface containing a nucleophile or -OH. Additionally, films made by this method tend to be very thin (<10 nm) and of low functional group density.⁷ Finally, the high reactivity and nonspecific nature of the grafting reactions limits the ability to include or add new functional groups to the polymer in a precise manner. Addressing these concerns is a major topic in the polymer thin film community, and new approaches are discussed herein.

Grafting to vs grafting from functionalization

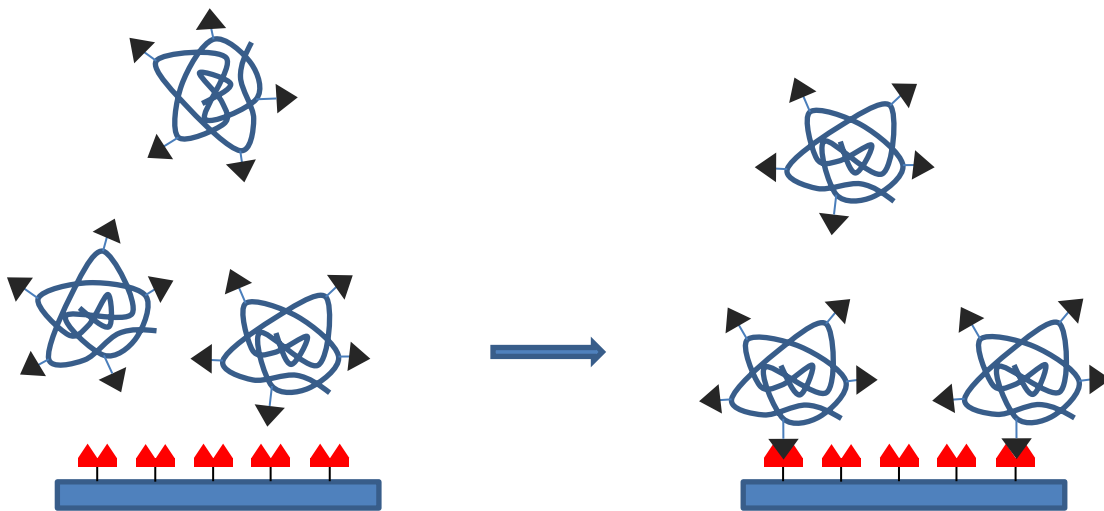
In solution, an ordinary polymer chain naturally exists in a random coil formation which can be thought of occupying, on average, a spherical volume of space. The amount of space being occupied is dependent on the functional groups, molecular weight, and solvent interactions. This space is known as the hydrodynamic volume. When deposited in the dry state on a surface, solvent interactions are removed, and the polymer will have a different, but still roughly spherical shape. Polymers that are grafted to a surface will retain this spherical shape, but, more importantly, block any underlying, unreacted functional groups, rendering these groups unreachable by the reactive moieties on still dissolved polymer and further grafting to the surface. This self-limiting process will result only in very thin films consisting of polymer in its random coil state. The number of chains per unit area is characterized by the grafting density, σ :

$$\sigma = \frac{h\rho N_a}{M_n} \quad (\text{Equation 1.1})$$

where h is the height, ρ is the bulk density, N_a is Avogadro's number, and M_n is the molecular weight of the attached polymer chain. At low grafting densities, there is minimal interaction between neighboring chains on the surface.

To achieve higher grafting densities, a different approach to surface functionalization must be used, namely grafting from. In grafting from, a surface bound initiator is activated in the presence of a monomer solution, causing polymer to grow directly from the surface. Low molecular weight monomers are not blocked from the surface even sterically congested environment, allowing them to diffuse towards a growing chain end, which means new chains can grow beneath the steric shadow of already formed surface-bound polymer. As more chains grow on the surface, polymers must extend normal to the surface due to excluded volume effects (Figure 1.1). This upward stretching of chains leads to a polymer architecture known as "brushes." Brushes afford thicker films (up to hundreds of nm), high functional group density, and unique interfacial properties.⁷

Grafting to



Grafting from

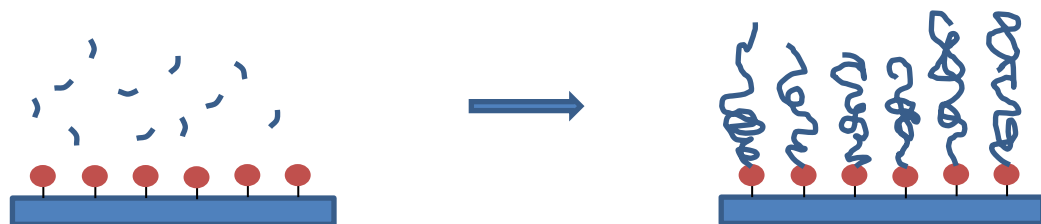


Figure 1.1. Illustration demonstrating the differences of grafting from surfaces vs grafting to surfaces.

polymerizations, such as free radical polymerization, require moderately specialized conditions such as the removal of oxygen.⁸ Also, the initiator molecule typically must be grafted to the surface.. As such, grafting to is a more commercially viable method for functionalizing large surface areas, whereas grafting from is most useful for conducting specialized small surface area

experiments in the biomedical and material science fields. Most grafting techniques involve dip or spray coating, followed by curing.

High reactivity grafting to chemistries

While silane and epoxide grafting reactions are usually spontaneous in the presence of their reactive counterparts, some of the most useful grafting reactions are ones that require a stimulus such as light or heat. Benzophenone is a prime example of such a reaction. Benzophenone is a generally inert aryl ketone that, upon exposure to UV light can be excited to a diradicaloid triplet state.⁹ In this triplet state, the oxygen abstracts a nearby alkyl hydrogen, leaving two carbon centered radicals, which can then recombine to form a covalent bond. If the benzophenone is attached along a polymer backbone, then the result of this is to graft to polymer to wherever the carbon center is being created, such as an inert plastic surface like polypropylene. Our group previously took advantage of this chemistry to attach non-leaching antimicrobial quaternary amine polymers to a variety of inert substrates.¹⁰

However, some substrates are even more inert than polypropylene, which contains only alkyl C-H bonds. Polyaramids like Kevlar® (Figure 1.2) consist of aryl groups connected by conjugated amides. Conjugated amides are poor reactive handles. Also, the amides serve as electron withdrawing groups to make the benzene rings of the aramid less reactive to electrophilic aromatic substitution reactions. There are techniques for covalently coating Kevlar; however, these techniques usually involve purposeful degradation of the backbone with acid or base to create reactive handles or electrophilic aromatic substitution reactions that have byproducts, which may cause chain scission along the backbone and degrade the mechanical properties of the material.¹¹⁻

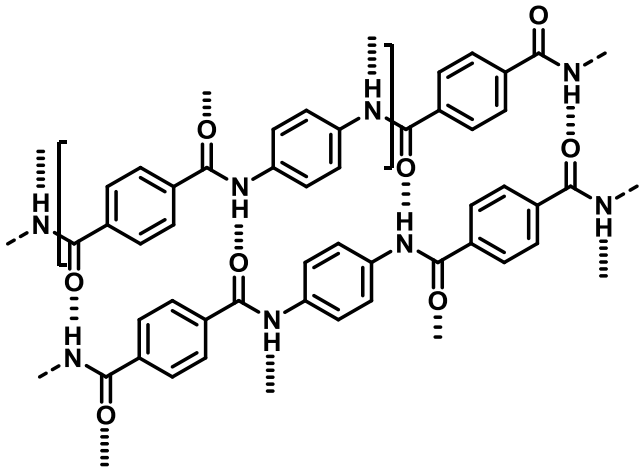


Figure 1.2. Structure of Kevlar.

To react with such a unique inert substrate, new attachment chemistries must be explored. The use of nitrenes, an excited state of nitrogen, is promising in this field *and is one of the topics of this dissertation.*¹⁵

Post-polymerization modification and click chemistry

As discussed earlier, polymer brushes are a unique surface functionalization methodology that allows for exquisite control of the surface chemistry. Brushes can be grown using free-radical polymerization,¹⁶ atom transfer radical polymerization,¹⁷ nitroxide mediated polymerization,¹⁸ reversible addition-fragmentation transfer polymerization,¹⁹ ring opening polymerization,²⁰ and ring opening metathesis polymerization.²¹ With such a huge selection of types of surface initiated polymerizations for brushes, the monomer scope, reactivity, and polymer architecture control of polymer brushes is immense.²² While it is possible through many of these techniques to synthesize monomers with unique or stimuli responsive pendant groups, this can be time consuming, synthetically inefficient, or simply incompatible with polymerization conditions. A simpler and more effective method to produce specialized polymer brush films is to find easily accessible

reactive monomers to polymerize, then add advanced functionality to the brushes using reactive chemistry, a technique known as post-polymerization modification.

While many reactions are suitable for post polymerization modification, “click” reactions are uniquely qualified.²³ A click reaction is defined by Barry Sharpless as:

“The reaction must *be modular, wide in scope, give very high yields, generate only inoffensive byproducts* that can be removed by nonchromatographic methods, and be *stereospecific* (but not necessarily enantioselective). The required process characteristics include simple reaction conditions (ideally, the process should be insensitive to oxygen and water), *readily available starting materials and reagents*, the use of *no solvent or a solvent that is benign* (such as water) or *easily removed*, and *simple product isolation*. Purification--if required--must be by nonchromatographic methods, such as crystallization or distillation, and the product must be stable under physiological conditions.”²⁴ Furthermore, he asserts that the reaction should be “spring-loaded” with a thermodynamic driving force of higher than 20 kcal/mol, giving the reaction a single trajectory.

The premier examples of click chemistry involve the formation of triazoles from azides and alkynes. The copper(I) mediated (terminal)alkyne-azide cycloaddition (CuAAC) reaction was discovered concurrently by Sharpless and Meldal.^{25, 26} The immense modularity of this reaction was immediately apparent, as both azides and alkynes have orthogonal reactivity to biologically present functional groups, the reaction is efficient and high-yielding in water, and as long as some effort is made to limit oxidation of the copper species (oxygen exclusion, including a reducing agent), the reaction appears quantitative at room temperature over reasonable times. A copper-free version of this reaction involves the use of strained internal alkynes. Strain-promoted alkyne-azide

cycloaddition (SPAAC) reactions have the same advantages of CuAAC, except that they are insensitive to oxygen, since no metal catalyst is needed. The downside of SPAAC is that strained alkynes can complex to synthesize and can also suffer from stability issues.

There are multiple click-type reactions that have been used to modify brush substrates, such as the aforementioned CuAAC and SPAAC,²⁷⁻²⁹ activated esters,³⁰ thio-Michael addition,³¹ thiolene,³² thiol-yne,^{33, 34} and Diels-Alder.^{35, 36} However, most click reactions have flaws that whereby critical functionality involves thermally unstable, chain transferring, or polymerizable groups, which make them unsuitable for polymerizations involving radical chemistry. *The use of a new type of click chemistry to circumvent this issue, the sulfur(VI) fluoride exchange reaction (SuFEx) in post polymerization modification is another aspect of this dissertation.*³⁷

Generation of complex surfaces

In order to create surfaces that truly mimic biological substrates, a methodology for imparting complexity onto synthetic surfaces is a useful development. Observation on how individual cells interact with complex surfaces is a critical tool for deconvoluting biological processes.³⁸⁻⁴⁰ The growth pattern of tissues such as nerves and bone has already been studied using artificially patterned surfaces, which allows scientists to make structure/property deductions about such interactions.^{41, 42} Complex surfaces may also be useful as a method to produce multifunctional biosensors, which can give signals in response to a complex physiological fluid.⁴³ Additionally, the modulus and micro- or nanomorphology of a surface can also influence cellular behavior.⁴⁴,
^{45,46}

Polymer brushes offer a unique platform for multifunctional surfaces due to their ability to incorporate widely varying functional groups in a closely controlled environment. Both statistical distributions, and patterning are relatively easily attainable, especially using click reactions.^{27, 29,}

⁴⁷⁻⁴⁹ While the concept of patterning functionalities onto brush surfaces using click chemistry is not new, the expansion in the complexity of the surfaces able to be generated from a single reaction solution is a crucial step forward in our ability to begin to mimic the immense complexity of true biological surface. Our work in the field of *orthogonal multi-surface functionalization by click reactions makes up another part of this dissertation.*⁵⁰

Mechanism of antimicrobial polyquaternary amine biocidal activity

As mentioned earlier, our lab previously synthesized an antimicrobial polymer capable of covalent attachment to surfaces via benzophenone chemistry.¹⁰ This work represents a unique fusion of two known concepts: the C-H insertion chemistry of benzophenone with polymers invented by Ruhe⁵¹, and the non-leaching biocidal activity of poly-quaternary amines on surface discovered by Klibanov.^{52, 53} However, the mechanism by which these coatings destroy bacteria (and perhaps fungi and viruses), and the times scales over which they are effective, are poorly studied.

There are two main hypothesized mechanisms of action involving leaching alkyl “-onium” biocidal activity. Both rely on the electrostatic attraction between the net-negatively charged lipid bilayer surface and the positive charge of the “-onium” cations. First, the alkyl “-onium” functionality must permeate through the peptidoglycan layer of Gram-positive bacteria, or through the lipopolysaccharide and peptidoglycan of Gram-negative bacteria. The first mechanism suggests an electrostatic interaction in which the alkyl “-onium” cations displace the divalent cations of the lipid bilayer (primarily Mg²⁺ and Ca²⁺) which serve as counterions to the anionic phosphate groups which populate the membrane.⁵⁴ This displacement damages the structural integrity and organization of the surface of the lipid bilayer, which increases its permeability and facilitates leaking of internal cellular content out of the cell.

However, there is some indication that neither of these are mechanism of *surface-bound* quaternary amines. Work by Klibanov demonstrated that some bacteria, such as *P. aeruginosa*, that are immune to quaternary amines (QA) in solution,⁵⁵ are still susceptible to similar functionalities that are tethered to a surface.⁵³ Klibanov also demonstrated that *S. aureus* and *E.*

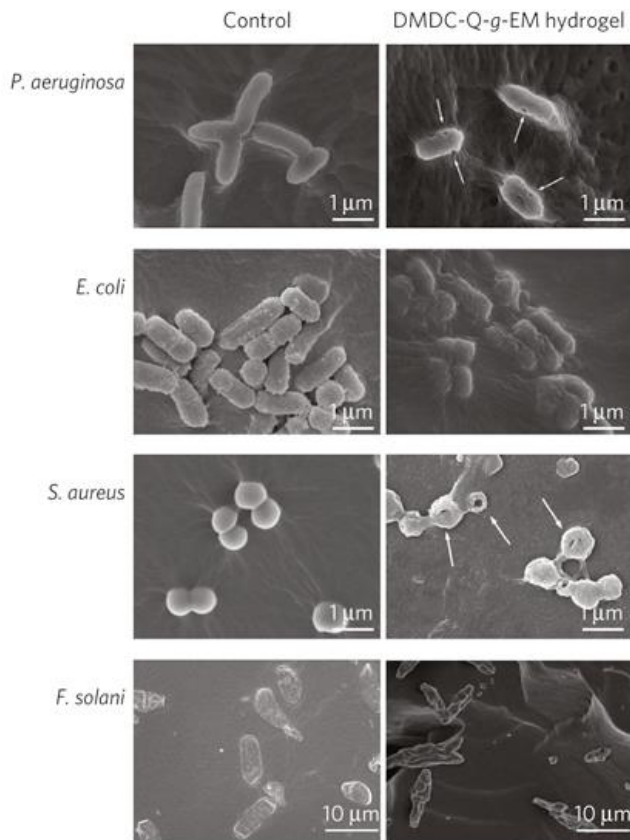


Figure 1.3. SEM of bacteria on a control sample (left) and on a quaternary amine hydrogel (right). Arrows indicate hole formation in cellular membrane. There is also notable deformation of the cell membrane of each bacterium on the hydrogel surface. Reprinted by permission from Macmillan Publishers Ltd: *Nature Materials* (P. Li, Y. F. Poon, W. Li, H.-Y. Zhu, S. H. Yeap, Y. Cao, X. Qi, C. Zhou, M. Lamrani, R. W. Beuerman, E.-T. Kang, Y. Mu, C. M. Li, M. W. Chang, S. S. Jan Leong and M. B. Chan-Park, *Nat. Mater.*, 2011, **10**, 149. Copyright 2011.

coli do not develop resistance to surface bound polyquaternary amines.⁵⁶ Based on this evidence,

it is possible that the biocidal mechanism of action in surface bound, non-leaching “-onium” cations may deviate from that of free, solvated, “-onium” salts.

It is still too early to definitively identify one mechanism as the primary biocidal route of surface tethered “-onium” cations, although there appear to be differences between the mechanism of action of solutions containing poly”-onium” salts and cations that are confined to a surface. However, the ultimate result involving any of these mechanisms is formation of holes in the cell membrane, which has been demonstrated by several groups, and is illustrated by the excellent scanning electron microscope (SEM) images published by the Li group.⁵⁷ *The final topic of this dissertation is a comprehensive literature review of the methods of attachment chemistry for such compounds and their effectiveness.*⁵⁸

Objectives and Outline

This dissertation has two main focuses. The first is on the use of sulfonyl nitrene chemistry to attach copolymers covalently to Kevlar surfaces. This unique chemistry allows for thermal curing of a thin coating onto an unusually inert fabric substrate. It is also a classic example of small molecule chemistry which has received little attention since the late 1960s being revived for more advanced applications in modern materials science.

The second major focus is the use of the SuFEx reaction along with other click functionalities to post-polymerization modify polymer brush substrates. This work focuses on using click reactions on the surface to create polymer surfaces that would be difficult to synthesize by other methods. It also opens the door for the use of such chemistries to make micropatterned surfaces.

The final section is a literature examination to direct the field in elucidating the mechanism of biocidal activity and chronicle the state of the art of tethering chemistries of poly“-onium” cations

to both organic surface such as polyethylene or cellulose, and inorganic surfaces such as gold or steel.

References

1. Paint & Coatings - Demand and Sales Forecasts, Market Share, Market Size, Market Leaders. *Freedonia 2015*.
2. Heublein, G.; Heublein, B.; Hortschansky, P.; Meissner, H.; Schutz, H., Reaction Composites from Polyfunctional Macromolecules and Inorganic Solids. *Journal of Macromolecular Science: Part A - Chemistry* **1988**, *25*, 183-200.
3. Hughes, J. D. H., The carbon fibre/epoxy interface—A review. *Compos. Sci. Technol.* **1991**, *41*, 13-45.
4. Xie, Y.; Hill, C. A. S.; Xiao, Z.; Militz, H.; Mai, C., Silane coupling agents used for natural fiber/polymer composites: A review. *Composites Part A: Applied Science and Manufacturing* **2010**, *41*, 806-819.
5. Witucki, G. L., A silane primer: chemistry and applications of alkoxy silanes. *Journal of coatings technology* **1993**, *65*, 57-57.
6. Der Voort, P. V.; Vansant, E. F., Silylation of the Silica Surface A Review. *J. Liq. Chromatogr. Relat. Technol.* **1996**, *19*, 2723-2752.
7. Advincula, R. C.; Brittain, W. J.; Caster, K. C.; Rühe, J., *Polymer Brushes*. Wiley Online Library **2004**.
8. Matyjaszewski, K.; Davis, T. P., *Handbook of radical polymerization*. Wiley Online Library **2002**; Vol. 5.
9. Dormán, G.; Prestwich, G., Benzophenone photophores in biochemistry. *Biochemistry* **1994**, *33*, 5661-5673.

10. Dhende, V. P.; Samanta, S.; Jones, D. M.; Hardin, I. R.; Locklin, J., One-Step Photochemical Synthesis of Permanent, Nonleaching, Ultrathin Antimicrobial Coatings for Textiles and Plastics. *ACS Appl. Mater. Interfaces* **2011**, *3*, 2830-2837.

11. Li, G.; Zhang, C.; Wang, Y.; Li, P.; Yu, Y.; Jia, X.; Liu, H.; Yang, X.; Xue, Z.; Ryu, S., Interface correlation and toughness matching of phosphoric acid functionalized Kevlar fiber and epoxy matrix for filament winding composites. *Compos. Sci. Technol.* **2008**, *68*, 3208-3214.

12. Wu, Y.; Tesoro, G. C., Chemical modification of Kevlar fiber surfaces and of model diamides. *J. Appl. Polym. Sci.* **1986**, *31*, 1041-1059.

13. Benrashid, R.; Tesoro, G. C., Effect of Surface-Limited Reactions on the Properties of Kevlar® Fibers. *Text. Res. J.* **1990**, *60*, 334-344.

14. Luo, J.; Sun, Y., Acyclic N-Halamine Coated Kevlar Fabric Materials: Preparation and Biocidal Functions. *Industrial & Engineering Chemistry Research* **2008**, *47*, 5291-5297.

15. Yatvin, J.; Sherman, S. A.; Filocamo, S. F.; Locklin, J., Direct functionalization of Kevlar® with copolymers containing sulfonyl nitrenes. *Polymer Chemistry* **2015**, *6*, 3090-3097.

16. Prucker, O.; Rühe, J., Synthesis of Poly(styrene) Monolayers Attached to High Surface Area Silica Gels through Self-Assembled Monolayers of Azo Initiators. *Macromolecules* **1998**, *31*, 592-601.

17. Pyun, J.; Kowalewski, T.; Matyjaszewski, K., Synthesis of Polymer Brushes Using Atom Transfer Radical Polymerization. *Macromol. Rapid Commun.* **2003**, *24*, 1043-1059.

18. Voccia, S.; Jérôme, C.; Detrembleur, C.; Leclère, P.; Gouttebaron, R.; Hecq, M.; Gilbert, B.; Lazzaroni, R.; Jérôme, R., Controlled Free Radical Polymerization of Styrene Initiated from Alkoxyamine Attached to Polyacrylate Chemisorbed onto Conducting Surfaces. *Chem. Mater.* **2003**, *15*, 923-927.

19. Tsujii, Y.; Ejaz, M.; Sato, K.; Goto, A.; Fukuda, T., Mechanism and Kinetics of RAFT-Mediated Graft Polymerization of Styrene on a Solid Surface. 1. Experimental Evidence of Surface Radical Migration. *Macromolecules* **2001**, *34*, 8872-8878.

20. Husemann, M.; Mecerreyes, D.; Hawker, C. J.; Hedrick, J. L.; Shah, R.; Abbott, N. L., Surface-Initiated Polymerization for Amplification of Self-Assembled Monolayers Patterned by Microcontact Printing. *Angew. Chem. Int. Ed.* **1999**, *38*, 647-649.

21. Kim, N. Y.; Jeon, N. L.; Choi, I. S.; Takami, S.; Harada, Y.; Finnie, K. R.; Girolami, G. S.; Nuzzo, R. G.; Whitesides, G. M.; Laibinis, P. E., Surface-Initiated Ring-Opening Metathesis Polymerization on Si/SiO₂. *Macromolecules* **2000**, *33*, 2793-2795.

22. Edmondson, S.; Osborne, V. L.; Huck, W. T. S., Polymer brushes via surface-initiated polymerizations. *Chem. Soc. Rev.* **2004**, *33*, 14-22.

23. Barner-Kowollik, C.; Du Prez, F. E.; Espeel, P.; Hawker, C. J.; Junkers, T.; Schlaad, H.; Van Camp, W., “Clicking” Polymers or Just Efficient Linking: What Is the Difference? *Angew. Chem. Int. Ed.* **2011**, *50*, 60-62.

24. Kolb, H. C.; Finn, M. G.; Sharpless, K. B., Click Chemistry: Diverse Chemical Function from a Few Good Reactions. *Angew. Chem. Int. Ed.* **2001**, *40*, 2004-2021.

25. Rostovtsev, V. V.; Green, L. G.; Fokin, V. V.; Sharpless, K. B., A Stepwise Huisgen Cycloaddition Process: Copper(I)-Catalyzed Regioselective “Ligation” of Azides and Terminal Alkynes. *Angew. Chem. Int. Ed.* **2002**, *41*, 2596-2599.

26. Tornøe, C. W.; Christensen, C.; Meldal, M., Peptidotriazoles on Solid Phase: [1,2,3]-Triazoles by Regiospecific Copper(I)-Catalyzed 1,3-Dipolar Cycloadditions of Terminal Alkynes to Azides. *The Journal of Organic Chemistry* **2002**, *67*, 3057-3064.

27. Arnold, R. M.; McNitt, C. D.; Popik, V. V.; Locklin, J., Direct grafting of poly(pentafluorophenyl acrylate) onto oxides: versatile substrates for reactive microcapillary printing and self-sorting modification. *Chem. Commun.* **2014**, *50*, 5307-5309.

28. Orski, S. V.; Sheppard, G. R.; Arumugam, S.; Arnold, R. M.; Popik, V. V.; Locklin, J., Rate Determination of Azide Click Reactions onto Alkyne Polymer Brush Scaffolds: A Comparison of Conventional and Catalyst-Free Cycloadditions for Tunable Surface Modification. *Langmuir* **2012**, *28*, 14693-14702.

29. Arnold, R. M.; Patton, D. L.; Popik, V. V.; Locklin, J., A Dynamic Duo: Pairing Click Chemistry and Postpolymerization Modification To Design Complex Surfaces. *Acc. Chem. Res.* **2014**, *47*, 2999-3008.

30. Arnold, R. M.; Sheppard, G. R.; Locklin, J., Comparative Aminolysis Kinetics of Different Active Ester Polymer Brush Platforms in Postpolymerization Modification with Primary and Aromatic Amines. *Macromolecules* **2012**, *45*, 5444-5450.

31. Gevrek, T. N.; Bilgic, T.; Klok, H.-A.; Sanyal, A., Maleimide-Functionalized Thiol Reactive Copolymer Brushes: Fabrication and Post-Polymerization Modification. *Macromolecules* **2014**, *47*, 7842-7851.

32. Dübner, M.; Gevrek, T. N.; Sanyal, A.; Spencer, N. D.; Padeste, C., Fabrication of Thiol-Ene “Clickable” Copolymer-Brush Nanostructures on Polymeric Substrates via Extreme Ultraviolet Interference Lithography. *ACS Appl. Mater. Interfaces* **2015**, *7*, 11337-11345.

33. Hensarling, R. M.; Doughty, V. A.; Chan, J. W.; Patton, D. L., “Clicking” Polymer Brushes with Thiol-yne Chemistry: Indoors and Out. *J. Am. Chem. Soc.* **2009**, *131*, 14673-14675.

34. Rahane, S. B.; Hensarling, R. M.; Sparks, B. J.; Stafford, C. M.; Patton, D. L., Synthesis of multifunctional polymer brush surfaces via sequential and orthogonal thiol-click reactions. *J. Mater. Chem.* **2012**, *22*, 932-943.

35. Arumugam, S.; Orski, S. V.; Locklin, J.; Popik, V. V., Photoreactive Polymer Brushes for High-Density Patterned Surface Derivatization Using a Diels–Alder Photoclick Reaction. *J. Am. Chem. Soc.* **2012**, *134*, 179-182.

36. Yameen, B.; Rodriguez-Emmenegger, C.; Preuss, C. M.; Pop-Georgievski, O.; Verveniotis, E.; Trouillet, V.; Rezek, B.; Barner-Kowollik, C., A facile avenue to conductive polymer brushes via cyclopentadiene-maleimide Diels-Alder ligation. *Chem. Commun.* **2013**, *49*, 8623-8625.

37. Yatvin, J.; Brooks, K.; Locklin, J., SuFEx on the Surface: A Flexible Platform for Postpolymerization Modification of Polymer Brushes. *Angew. Chem. Int. Ed.* **2015**, *54*, 13370-13373.

38. Mrksich, M.; Whitesides, G. M., Using self-assembled monolayers to understand the interactions of man-made surfaces with proteins and cells. *Annu. Rev. Biophys. Biomol. Struct.* **1996**, *25*, 55-78.

39. Yamato, M.; Konno, C.; Utsumi, M.; Kikuchi, A.; Okano, T., Thermally responsive polymer-grafted surfaces facilitate patterned cell seeding and co-culture. *Biomaterials* **2002**, *23*, 561-567.

40. Ito, Y., Surface micropatterning to regulate cell functions. *Biomaterials* **1999**, *20*, 2333-2342.

41. Thomas, C. H.; McFarland, C. D.; Jenkins, M. L.; Rezania, A.; Steele, J. G.; Healy, K. E., The role of vitronectin in the attachment and spatial distribution of bone-derived cells on materials with patterned surface chemistry. *J. Biomed. Mater. Res.* **1997**, *37*, 81-93.

42. Saneinejad, S.; Shoichet, M. S., Patterned glass surfaces direct cell adhesion and process outgrowth of primary neurons of the central nervous system. *Journal of Biomedical Materials Research* **1998**, *42*, 13-19.

43. Im, S. G.; Bong, K. W.; Kim, B.-S.; Baxamusa, S. H.; Hammond, P. T.; Doyle, P. S.; Gleason, K. K., Patterning Nanodomains with Orthogonal Functionalities: Solventless Synthesis of Self-Sorting Surfaces. *J. Am. Chem. Soc.* **2008**, *130*, 14424-14425.

44. Discher, D. E.; Janmey, P.; Wang, Y.-l., Tissue Cells Feel and Respond to the Stiffness of Their Substrate. *Science* **2005**, *310*, 1139-1143.

45. Boyan, B. D.; Hummert, T. W.; Dean, D. D.; Schwartz, Z., Role of material surfaces in regulating bone and cartilage cell response. *Biomaterials* **1996**, *17*, 137-146.

46. Huang, L.; Cao, Z.; Meyer, H. M.; Liaw, P. K.; Garlea, E.; Dunlap, J. R.; Zhang, T.; He, W., Responses of bone-forming cells on pre-immersed Zr-based bulk metallic glasses: Effects of composition and roughness. *Acta Biomater.* **2011**, *7*, 395-405.

47. Broyer, R. M.; Schopf, E.; Kolodziej, C. M.; Chen, Y.; Maynard, H. D., Dual Click reactions to micropattern proteins. *Soft Matter* **2011**, *7*, 9972-9977.

48. Hensarling, R. M.; Hoff, E. A.; LeBlanc, A. P.; Guo, W.; Rahane, S. B.; Patton, D. L., Photocaged pendent thiol polymer brush surfaces for postpolymerization modifications via thiol-click chemistry. *Journal of Polymer Science Part A: Polymer Chemistry* **2013**, *51*, 1079-1090.

49. Spruell, J. M.; Wolffs, M.; Leibfarth, F. A.; Stahl, B. C.; Heo, J.; Connal, L. A.; Hu, J.; Hawker, C. J., Reactive, Multifunctional Polymer Films through Thermal Cross-linking of Orthogonal Click Groups. *J. Am. Chem. Soc.* **2011**, *133*, 16698-16706.

50. Brooks, K.; Yatvin, J.; McNitt, C. D.; Reese, R. A.; Jung, C.; Popik, V. V.; Locklin, J., Multifunctional surface manipulation using orthogonal click chemistry. *Langmuir* **2016**.

51. Körner, M.; Prucker, O.; Rühe, J., Kinetics of the Generation of Surface-Attached Polymer Networks through C, H-Insertion Reactions. *Macromolecules* **2016**.

52. Lin, J.; Qiu, S.; Lewis, K.; Klibanov, A., Bactericidal properties of flat surfaces and nanoparticles derivatized with alkylated polyethylenimines. *Biotechnology progress* **2002**, *18*, 1082-1086.

53. Tiller, J.; Liao, C.; Lewis, K.; Klibanov, A., Designing surfaces that kill bacteria on contact. *Proceedings of the National Academy of Sciences of the United States of America* **2001**, *98*, 5981-5985.

54. Kügler, R.; Bouloussa, O.; Rondelez, F., Evidence of a charge-density threshold for optimum efficiency of biocidal cationic surfaces. *Microbiology* **2005**, *151*, 1341-1348.

55. A. Tabata, H. N., T. Maeda, K. Murakami, Y. Miyake, and H. Koura, Correlation between Resistance of *Pseudomonas aeruginosa* to Quaternary Ammonium Compounds and Expression of Outer Membrane Protein OprR. *Antimicrob Agents Chemother* **2003**, *47*, 20933-2099.

56. Nebojsa M. Milovic, J. W., Kim Lewis, Alexander M. Klibanov, Immobilized N-Alkylated Polyethylenimine Avidly Kills Bacteria by Rupturing Cell Membranes With No Resistance Developed. *Biotechnol. Bioeng* **2005**, *90*, 715-722.

57. Li, P.; Poon, Y. F.; Li, W.; Zhu, H.-Y.; Yeap, S. H.; Cao, Y.; Qi, X.; Zhou, C.; Lamrani, M.; Beuerman, R. W.; Kang, E.-T.; Mu, Y.; Li, C. M.; Chang, M. W.; Jan Leong, S. S.; Chan-

Park, M. B., A polycationic antimicrobial and biocompatible hydrogel with microbe membrane suctioning ability. *Nat Mater* **2011**, *10*, 149-156.

58. Yatvin, J.; Gao, J.; Locklin, J., Durable defense: robust and varied attachment of non-leaching poly “-onium” bactericidal coatings to reactive and inert surfaces. *Chem. Commun.* **2014**, *50*, 9433-9442.

CHAPTER 2
DIRECT FUNCTIONALIZATION OF KEVLAR WITH SULFONYL COPOLYMERS
CONTAINING SULFONYL NITRENES ¹

¹ Yatvin, J.; Sherman, S. A.; Filocamo, S. F. and Locklin, J. 2015. *Polymer Chemistry*. 6:3090-3097.

Reprinted here with permission of publisher.

Abstract

Generating innovative methods to functionalize fibers and interfaces are important strategies for developing coatings that impart new or improved properties to a given material. In this work, we present a method for functionalizing highly inert poly(p-phenylene terephthalamide) (Kevlar®) fibers via thermal generation of an electrophilic nitrene, while preserving the mechanical properties of the aramid. Because of the high affinity of the sulfonyl nitrene singlet state for aromatic rings, the use of a sulfonyl azide-based copolymer allows the covalent grafting of a wide variety of common commercial polymers to Kevlar. Also, by using reactive ester copolymers, an avenue for the attachment of more exotic or delicate functionalities like small molecules, dyes, and biomolecules through postpolymerization modification is described.

Introduction

Since the development of poly(*p*-phenylene terephthalamide) fibers by Stephanie Kwolek at DuPont in 1965,¹ Kevlar[®] and other polyaramids have found utility in hundreds of different applications due to their remarkable chemical and mechanical properties. Pristine Kevlar fibers display high tensile strength,² thermal stability,^{3, 4} and resistance to mechanical degradation.⁵ These superior properties are primarily derived from the highly conjugated and extensively hydrogen bonded nature of the aramid backbone. This same high degree of conjugation, along with the deactivated nature of the aryl backbone and lack of reactive functional groups, also makes Kevlar and other aramids difficult to process and derivatize using reactive coating methods, which are effective strategies used to impart new properties onto textiles such as anti-wrinkle technology,⁶ hydrophobic,⁷ or antimicrobial coatings.⁸⁻¹⁰

Current methods that have been used to functionalize Kevlar include epoxy resins,¹¹⁻¹³ electrochemical deposition,¹⁴ impregnation,¹⁵ isocyanates,¹⁶ radiation, plasma, or chemical radical generation,¹⁷⁻²⁰ conventional solution-based electrophilic aromatic substitution,²¹⁻²³ silanation,^{24, 25} or hydrolysis with strong acids to generate reactive end groups.²⁶ Each of these approaches has critical issues that limit their widespread utility. Most employ harsh chemistry that leads to degradation of the fibers or a functionalizing moiety, while others involve exotic strategies and unstable compounds. Among these approaches are techniques that do not generate covalent bonds between the coating and the aramid fibers, and therefore produce coatings that are subject to dewetting, delamination, and leaching. It is also important to note that several of these techniques depend on exposure to chloride ions, which are known to damage Kevlar.²⁷

In order to circumvent these issues, we have developed a simple strategy that utilizes a *p*-

styrene sulfonyl azide (SSAz) monomer²⁸ to generate covalent graft points between a copolymer coating and Kevlar fabric. SSAzs can form covalent bonds via an excited nitrene,²⁹ which is generated through the decomposition and subsequent elimination of nitrogen gas from the azide. The elimination occurs in the presence of UV light or heat.^{30,31} This reactive nitrene can perform several chemistries: C-H or O-H insertions, addition across double bonds to form aziridines, trigger homolytic cleavage of C-H bonds followed by recombination, or electrophilic addition to aromatic rings.³² There are two mechanisms of nitrene C-H insertion: either a direct insertion from the singlet state into a double bond, or hydrogen atom extraction by a triplet state nitrene

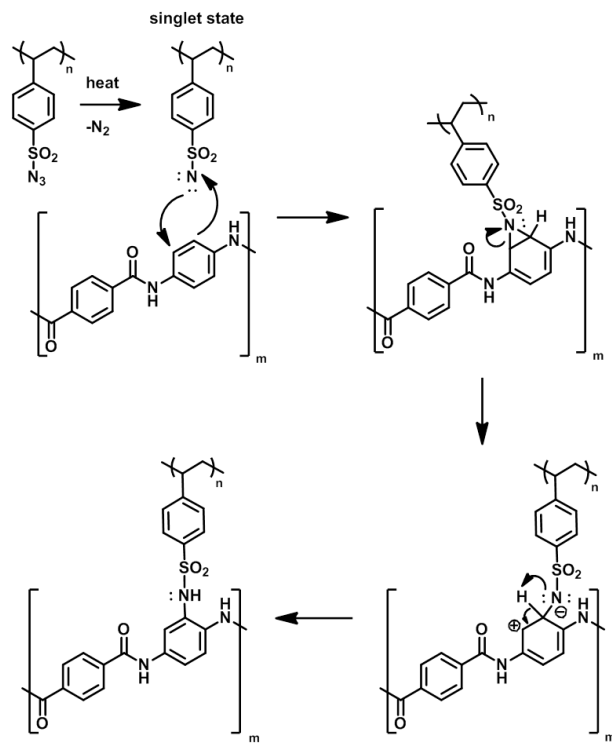


Figure 2.1. Arrow pushing mechanism of the grafting of a styrene sulfonyl azide containing copolymer onto a Kevlar substrate.

and subsequent radical-radical recombination between the radical center and the sulfonyl nitrogen radical, both of which lead to covalent bond formation.

SSAzs differ from other C-H grafting chemistries like diradicaloid benzophenone,^{8, 33, 34} or carbenes derived from diaryldiazonium salts,³⁵⁻³⁷ α -diazoesters,³⁸ or diazirines³⁹ in several important ways. First, polymers incorporating SSAz as a comonomer afford the unique combination of long-term stability under ambient conditions, easy synthetic accessibility, a choice of either photochemical or thermal activation, and the high affinity of the sulfonyl nitrene singlet state for aromatic rings. Perfluorophenylazide based grafting chemistry, which has been used extensively by the Yan group,^{40, 41} has a similar reactivity as SSAzs; however the high fluorine content of perfluorophenylazides leads to incompatible wetting on different polymer interfaces, which prevents thin coatings with consistent thickness and uniformity. SSAzs on the other hand are generally more compatible with respect to wetting and do not suffer from this issue. The SSAz copolymers described in this work were all synthesized from low-cost, commercially available starting materials and are stable indefinitely under ambient conditions.

The SSAz monomer starts to undergo thermal decomposition and nitrene generation at approximately 120 °C, with maximum nitrene generation kinetics occurring at 180 °C.²⁸ The most important aspect of these materials for this work is that while sulfonyl nitrenes facilely insert into *alkyl* C-H bonds, this functionality is even more reactive towards *aryl* groups,³¹ which is critical in covalent grafting to substrates like Kevlar with high aryl content. One recent example that demonstrates the reactivity of nitrenes with a polyaramid substrate is work by McVerry *et al.* in which a perfluorophenyl azide-terminated polyethyleneglycol was grafted onto a polyaramid reverse-osmosis filter using photochemical activation.⁴²

The copolymerization of SSAz with other monomers allows for the grafting of a large variety of heat or UV stable polymeric functionalities to the surface of Kevlar via the mechanism in Figure 2.1. Since Kevlar and other polyaramids are known to have high thermal stability but are susceptible to UV-catalyzed degradation,⁴³⁻⁴⁵ we have used thermal grafting in this work. Thermal grafting also provides access to the entire geometry of the fibers, rather than just the immediate surface where UV light is limited by substrate transparency and penetration depth. To demonstrate the versatility of thermal grafting onto aramid substrates, we have synthesized several different SSAz containing copolymers. Common monomers such as acrylonitrile and 4-vinyl benzyl chloride were copolymerized with SSAz to display the effectiveness of covalent grafting despite highly variable polymer wettability and solubility conditions. Poly-4-vinyl-N-benzyl-N-methylbutan-1-amine and polymethacrylic acid copolymers were also synthesized as suitable cationic and anionic base polymers for layer-by-layer (LBL) deposition on the surface of Kevlar. This was followed with precipitation of TiO₂ in order to directly observe the coating via EDS (energy-dispersive X-ray spectroscopy), WDS (wavelength-dispersive X-ray spectroscopy) and SEM (scanning electron microscopy). We also copolymerized SSAz with the pentafluorophenol acrylate (PFPA) monomer, an activated ester with superior utility for post-polymerization modification of surfaces.⁴⁶ The use of PFPA allows the attachment of more delicate or complex functionality that would not survive the initial polymerization or grafting procedures, or would be difficult to synthesize as a copolymer. Most of the previous work for functionalizing Kevlar surfaces focused on small molecule derivatization; however by using SSAz we can take advantage of the fact that polymeric materials are easier to process and have superior coating properties.

Materials and Procedure

Materials: All compounds were purchased from Alpha-Aesar, TCI, or Sigma-Aldrich and unless otherwise noted were used as received. Methylmethacrylate and 4-vinylbenzyl chloride were purified by flashing through basic alumina plugs. Acrylonitrile was purified by flashing through a neutral alumina plug. Methacrylic acid was purified by vacuum distillation. Pentafluorophenol acrylate was synthesized according to a previously published procedure.⁴⁷ 850 Denier Kevlar KM2 was obtained from Barrday, and was cleaned by sonicating in acetone for 30 minutes, sonicating in hexane for 30 minutes, stirring in 2% w/w sodium borate solution for 1 hr at 85 °C, and then stirring in water at 75 °C for 1 hr, followed by drying in a vacuum oven at room temperature.

Equipment: ¹H NMR and ¹³C NMR of small molecules were taken on a Varian Mercury 300 MHz NMR. Polymer spectra were taken on a Varian Inova 500 MHz NMR. FTIR studies were done using a Thermo-Nicolet model 6700 spectrometer equipped with a variable angle grazing angle attenuated total reflection (GATR-ATR) accessory (Harrick Scientific) at 64 scans with 4 cm⁻¹ resolution. Electron dispersive spectroscopy and wavelength dispersive spectroscopy were taken on a JEOL JXA-8600 Electron Microprobe at 20 kV. Scanning electron microscopy was taken on a FEI Inspec F FEG SEM at 20 kV. Fluorescence microscopy pictures were taken using an 8 megapixel digital camera on a Zeiss AX10 Observer inverted microscope with an X-cite Series 120 fluorescent light source and Chroma Technology filter model 11000 FITC UV filter (350 nm excitation, >430 nm emission). Tensile testing was done on an Instron 5500R Series Model 4302 with reported values being the average of 15 pulled yarns from the warp direction of the Kevlar sample. The tensile testing procedure from ASTM D279/D7269M was used, with a 1 kN load cell, and 10 inch yarns with 2.8 twists/inch in the Z direction. A Mettler Toledo TGA/SDTA851 was used to perform thermogravimetric analysis on samples at a heating rate of 10 °C/min. Nitrogen at

50 mL/min was used as the carrier gas.

Styrene sulfonyl chloride: Synthesized using the procedure developed by Schuh *et al.*²⁸ The crude product was passed through a silica plug in 1:1 ethyl acetate:hexane (78% yield) and stored in the freezer at -20 °C. ¹H NMR (300 MHz, CDCl₃) δ= 7.99 (td, *J* = 8.4 Hz, 2.4 Hz, 2H, *H*-C=C-SO₂) 7.60 (td, *J* = 6.9 Hz, 1.5 Hz, 2H, *H*-C=C-CH₂) 6.78 (dd *J* = 17.7 Hz, 10.8 Hz, *H*-C=CH₂) 5.97 (d, *J* = 17.7 Hz, *H_{cis}*CH-C=CH₂) 5.54 (d, *J* = 10.8 Hz, *H_{trans}*CH-C=CH₂). ¹³C NMR (75 MHz, CDCl₃) δ=144.4 (Car-SO₂N₃), 142.9 (Car-CH), 134.7 (CH=CH₂), 127.4 (2 × Car), 1 27.1 (2 × Car), 119.3 (-CH₂=CH).

Styrene sulfonyl azide (1): Synthesized according to Schuh *et al.* (74% yield).²⁸ When handling the SSAz monomer, it is important to note that it is stable under cold (-20 °C) storage, but will form an insoluble solid if stored neat at room temperature after 24 hours in the presence of light. It should also not be subjected to temperatures above ~30 °C in a concentrated form, as this can also result in an insoluble mass. ¹H NMR (300 MHz, CDCl₃) δ= 7.91 (d, 8.4 Hz, *H*-C=C-SO₂) 7.61 (d, 8.4 Hz, *H*-C=C-CH₂) 6.78 (dd, 17.1 Hz, 11.1 Hz, *H*-C=CH₂) 5.95 (d, 17.7 Hz, *H_{cis}*CH-C=CH₂) 5.52 (d, 10.8 Hz, *H_{trans}*CH-C=CH₂). ¹³C NMR (75 MHz, CDCl₃) δ= 143.7 (Car-SO₂N₃), 136.7 (C-CH_{ar}), 134.6 (CH=CH₂), 127.6 (2 × Car), 126.9 (2 × Car), 118.6 (CH₂=CH). IR (neat cm⁻¹): 3094, 3069 2128, 1593, 1400, 1372, 1190, 1169, 1088, 989, 927, 844, 759, 748, 650, 597.

Polymethylmethacrylate-co-styrene sulfonyl azide (pMMA-co-SSAz) (2): 1.0 g (9.98 mmol) methylmethacrylate, 140 mg (0.5 mmol) styrene sulfonyl azide, and 18 mg (0.11 mmol) of AIBN were added to an oven dried Shlenk flask with 10 mL dry toluene. The solution was degassed for 30 minutes with argon, before placing on a Shlenk line under nitrogen for reaction, and the headspace purged. The reaction was conducted at 65 °C for 24 hours, then precipitated into cold

methanol and suction filtered to obtain 270 mg of off-white solid (23% yield). ^1H NMR (500 MHz, CDCl_3) δ = 7.87 (bd, 2H) 7.20 (bd, 2H) 3.60 (bs, 27H) 3.01 (bm, 2H) 0.5-2.1 (bm, 46H).

Poly-4-vinylbenzylchloride-co-styrene sulfonyl azide (p4VBC-co-SSAz) (3): 2 g (13.1 mmol) of 4-vinylbenzyl chloride, 144 mg (0.69 mmol) styrene sulfonyl azide, and 47 mg (0.28 mmol) of AIBN were added to an oven dried Shlenk flask with 10 mL dry toluene. The solution was degassed for 30 minutes with argon, before placing on a Shlenk line under nitrogen for reaction, and the headspace purged. The reaction was conducted at 65 °C for 54 hours, then precipitated into cold methanol and suction filtered to obtain 1.95 g of off-white solid (91% yield). ^1H NMR (500 MHz, DMSO-d_6) δ = 7.5-7.6 (bm, 4H) 6.9-7.5 (bm, 20H) 6.3-6.9 (bm, 20H) 4.6-4.9 (bs, 20H) 1.0-2.3 (bm, 30H).

Poly-4-vinyl-N-benzyl-N-methylbutan-1-amine-co-styrene sulfonyl azide (p4VBA-co-SSAz) (4): 0.94g of P4VBC-co-SSAz was dissolved in 18 mL dry THF, and 1.17 g (13.4 mmol) of 4-methylbutan-1-amine which had been dried over molecular sieves for 24 hours was added and the reaction conducted on a Shlenk line under nitrogen at room temperature. After 72 hours the developed amine salt was vacuum filtered off, the solvent removed by evaporation, and the crude product redissolved in boiling acetone. The polymer was precipitated by quickly adding this solution to water and suction filtering the solid to obtain 1.25 g of off-white solid. (95% yield) *Note: this polymer should be stored as a stock solution in chloroform.* ^1H NMR (500 MHz, CDCl_3) δ = 6.4-8.0 (bd, 5H) 3.2-3.7 (bs, 2H) 0.7-2.9 (bm, 16 H).

Polyacrylonitrile-co-styrene sulfonyl azide (pAN-co-SSAz) (5): 1 g (18.8 mmol) of acrylonitrile, 210 mg (1 mmol) styrene sulfonyl azide, and 68 mg (0.4 mmol) of AIBN was added to an oven dried Shlenk flask with 10 mL dry toluene. The solution was degassed for 30 minutes with argon, before placing on a Shlenk line under nitrogen for reaction, and the headspace purged. The

reaction was conducted at 65 °C for 24 hours. Toluene was evaporated off, and the solid was redissolved in DMF and precipitated into ethyl acetate twice. The solid polymer was suction filtered to obtain 0.40 g of yellow solid (33% yield). ^1H NMR (500 MHz, DMSO-d₆) δ = 7.4-8.2 (bm 4H) 3.0-3.3 (bm, 11H) 1.6-2.3 (bm 28H).

Polymethacrylic acid-co-styrene sulfonyl azide (pMAA-co-SSAz) (6): 1 g (11.6 mmol) of methacrylic acid, 130 mg styrene sulfonyl azide, and 42 mg of AIBN was added an oven dried Shlenk flask with 10 mL acetonitrile. The solution was degassed for 30 minutes with argon, before placing on a Shlenk line under nitrogen, and the headspace purged. The reaction was conducted at 65 °C for 24 hours, then 10 mL of methanol was then added to the reaction to fully solubilize the crude polymer. The solution was then precipitated into ethyl acetate and suction filtered to obtain 0.67 g of off-white solid (59% yield). ^1H NMR (500 MHz, DMSO-d₆) δ = 12.1-12.5 (bs, 20H) 7.9-8.0 (bm, 2H) 7.6-7.7 (bm, 2H) 1.3-2.1 (bm, 40H) 0.5-1.3, 60H).

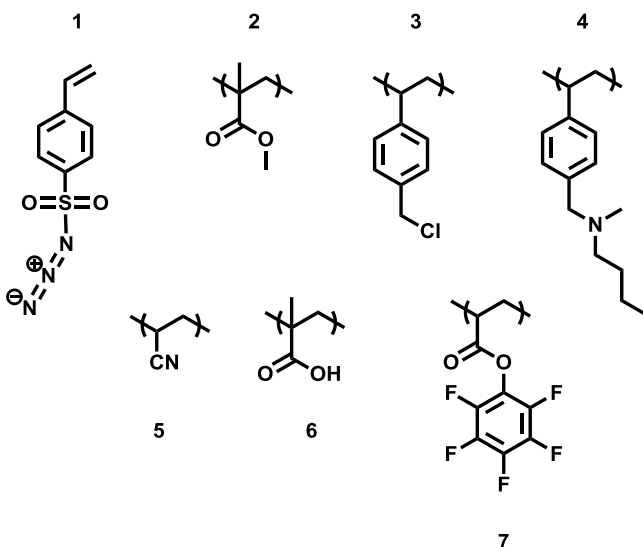


Figure 2.2. Styrene sulfonyl azide monomer (1) and copolymer structures used in this work: polymethylmethacrylate (2), polyvinylbenzyl chloride (3), Poly-4-vinyl-N-benzyl-N-methylbutan-1-amine (4), polyacrylonitrile (5), polymethacrylic acid (6), and polypentafluorophenol acrylate (7).

Polypentafluorophenolacrylate-co-styrene sulfonyl azide (pPFPA-co-SSAz) (7): 1.0 g (4.2 mmol) of pentafluorophenol acrylate, 46 mg (0.22 mmol) styrene sulfonyl azide, and 15 mg AIBN were added to an oven dried Shlenk flask with 10 mL benzene. The solution was degassed for 1 hour, before placing on nitrogen line for reaction, and the headspace purged. The reaction was conducted at 65 °C for 24 hours, then the solvent was removed by rotary evaporation. The clear viscous liquid remaining was redissolved in THF, precipitated into cold methanol, and suction filtered to obtain 0.42 g of white solid (26% yield). ^1H NMR (500 MHz, CDCl_3) δ = 7.87 (bd, 2H) 7.41 (bd, 2H) 1.5-3.1 (bm, 65H).

Kevlar coating: A clean 2.54 cm x 2.54 cm swatch of Kevlar was dipcoated in a 10 mg/mL solution of polymer in a favorable solvent, then dried in a vacuum oven at room temperature. The swatch

was then placed on a hotplate held at 180 °C in a nitrogen atmosphere under a piece of stainless steel that had been previously heated to the same temperature. After 1 hour, the swatch was removed, heavily sonicated in the original coating solvent and dried in a vacuum oven at room temperature.

Layer-by-layer (LbL) deposition and titania precipitation: A coated swatch of Kevlar was soaked for 2 minutes in 0.1 mM HCl solution (pH=4). Dipcoating was done by alternating between 0.1% w/w polystyrene sulfonate and 0.1% w/w branched polyethyleneimine solutions, with a deionized water washing step between each dip. This process was repeated to form 5 layers. After LbL, the swatch was dried in a vacuum oven at room temperature. TiO₂ was precipitated by placing the coated swatch in 25 mL of a 25 mM (0.076 g/25 mL) Tris buffer solution, then adding 0.5 mL of 50% w/w aqueous dihydroxybis(ammoniumlactato)titanium(IV) and placing on a shaker at 250 rpm for 6 hours.⁴⁸ The swatch was removed, rinsed with deionized water, and dried in a vacuum oven at room temperature.

Attachment of 1-pyrenemethylamine: A Kevlar swatch was dipped in 50 mg/mL PPFPA-co-SSAz THF solution, dried at room temperature in a vacuum oven, then cured for 1 hr at 180 °C. After curing, the swatch was sonicated in THF to remove any physisorbed polymer. The swatch was then placed in an oven dried Shlenk flask under inert atmosphere. Solutions of 40 mM 1-pyrenemethylamine hydrochloride and 80 mM triethylamine were prepared in DMF and added to the flask, and the mixture was stirred for 1 hour at room temperature under nitrogen. The swatch was Soxlet extracted with acetone overnight in the dark to wash away excess 1-pyrenemethylamine and dried in a vacuum oven at room temperature.

Results and Discussion

Scheme 2.2 shows the variety of monomers that were copolymerized with SSAz (1) in this work, including: methyl methacrylate (2), 4-vinylbenzyl chloride (3), poly-4-vinyl-N-benzyl-N-methylbutan-1-amine (4), acrylonitrile (5), methacrylic acid (6), and pentafluorophenol acrylate (7), a monomer easily synthesized in one step from methacryloyl chloride and pentafluorophenol.⁴⁶ All of these polymerizations were successful, provided the reaction was conducted under suitably dilute conditions. It is of importance to note that all SSAz free radical polymerizations should be performed at concentrations of no more than ~10-20% v/v monomer, as more concentrated reactions gel after several hours at polymerization temperature. Regardless of feed monomer, this gel was insoluble in common solvents, likely indicating a crosslinked polymer network. Nitrene formation at 65 °C is negligible, however Breslow *et al.* found that in the presence of a hydroperoxide radical initiator, benzene sulfonyl azide showed evidence of decomposition to a benzene sulfonyl radical.³¹ It follows that in this system, AIBN can initiate the radical decomposition of SSAz, creating free radicals along the polymer backbone, leading to premature crosslinking. By avoiding more concentrated or neat polymerizations, this side reaction can be circumvented.

All the polymers synthesized in this work contained the SSAz crosslinker at 5 mol%, which was chosen to provide a balance between sufficient crosslinking points for grafting while still preserving the properties of a homopolymer prepared from the primary monomer. The resulting polymers were stable for months under ambient conditions with one exception. To produce an amine functionalized polymer, poly-4-vinylbenzylchloride-co-styrene sulfonyl azide (p4VBC-co-SSAz) was post-polymerization modified with N-butylmethylamine to yield poly-4-vinyl-N-benzyl-N-methylbutan-1-amine-co-styrene sulfonyl azide (**p4VBA-co-SSAz**). After purification,

if left in the dry state, pVBA-co-SSAz becomes completely insoluble after several hours. This is surprising because the precursor, p4VBC-co-SSAz, is stable under ambient conditions. Because water is used to precipitate the polymer and remove leftover N-methylbutylamine, we hypothesize that a small proportion of the benzyl chloride groups may remain after post-polymerization modification, which can result in the amine catalyzed formation of dibenzyl ether

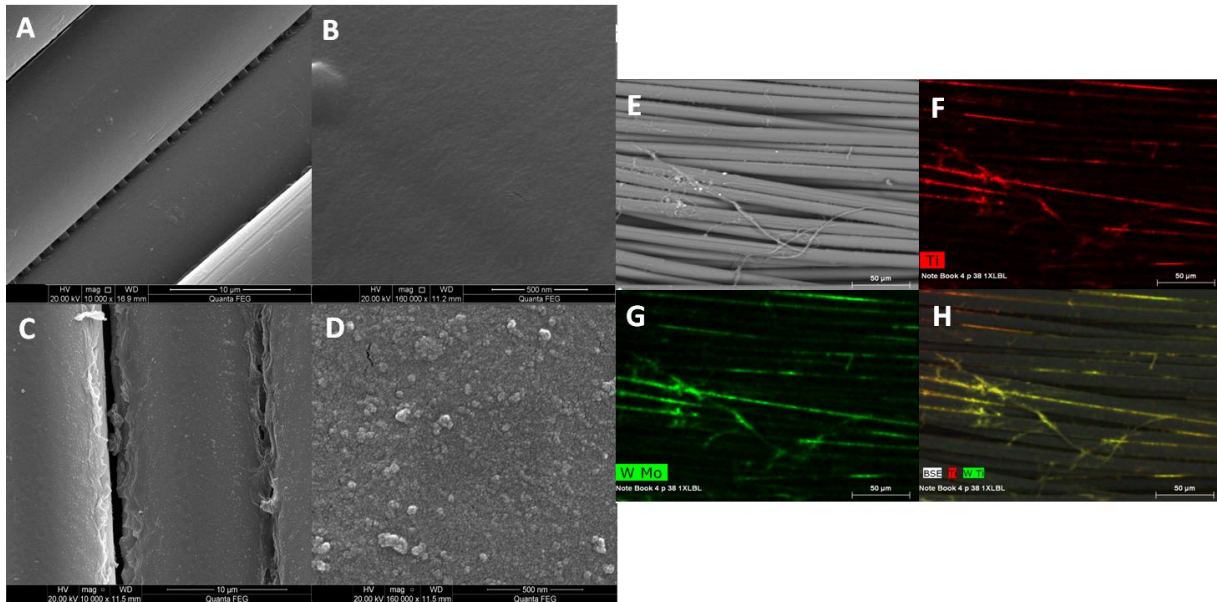


Figure 2.3 (A-D) Scanning electron microscope images of (A) SSAz copolymer coated Kevlar with SSAz copolymer cross-bridges; (B) high magnification image of the coated Kevlar fibers which shows the smooth morphology; (C) LBL coated Kevlar with precipitated TiO_2 ; (D) high magnification image of TiO_2 nanoparticles precipitated on coated Kevlar. (E-H) SSAZ copolymer coated Kevlar elemental mapped at 4.511 keV (Ti $\text{K}\alpha$ line) using (E) backscattered electrons (F) EDS, (G) WDS, and (H) overlaid EDS and WDS data.

crosslinks. Sufficient crosslinking renders the polymer insoluble. However, p4VBA-co-SSAz is stable for months if immediately dissolved and kept in an anhydrous chloroform solution.

The polymers produced in this study were cured onto Kevlar swatches at 180 °C for 1 hour, and produced coatings such as those seen in the SEM images in Figure 2.3A and B. These images of polymer coated Kevlar demonstrate the nature of the attachment chemistry. The clearest features are the crosslinked polymer bridges that extend between Kevlar strands (Figure 2.3A), and the highly smooth coating on the yarn surface (Figure 2.3B). The coating is homogeneous across all the strands in a given sample, which indicates uniform distribution and wetting. There were few, if any, defects or voids observed via SEM.

By using SSAzs to attach a base polymer like pVBA-co-SSAz or poly(methacrylic acid-co-styrene sulfonyl azide) (pMAA-co-SSAz), a surface was prepared that was conducive to LbL deposition of anionic poly(styrenesulfonate) and cationic poly(ethyleneimine). After 5 dipping cycles, a coating of titania nanoparticles were precipitated on the Kevlar substrate using previously described methods.⁴⁸ The titania nanoparticles were observable by SEM, EDS, and WDS. Figure 2.3C shows an increased surface roughness along with a morphological change due to the precipitated TiO₂, and under high magnification (Figure 2.3D), TiO₂ nanoparticles are evident. The presence of titanium on the surface is also apparent in the elemental maps (Figure 2.3 F-H) generated from EDS and WDS from the Ti K α peak at 4.511 keV.

To determine whether the mechanical properties were damaged during the curing process or by the presence of the polymer coating, Kevlar yarns were subjected to tensile testing on an Instron, the results of which are shown in Table 2.1. p4VBA-co-SSAz coated and cured (PCC) Kevlar was compared to Kevlar that had been thermally cured without any coating (TC), and to virgin Kevlar. The results indicated that there was minimal difference in the mechanical properties between all

three samples. With respect to the virgin Kevlar and the TC Kevlar, there was a slight decrease in tensile stress at max load and energy at break, and a slight increase in Young's modulus. There is essentially no statistical difference in these properties between the PCC Kevlar and the TC Kevlar. The net difference between the virgin Kevlar and the PC Kevlar across the properties measured is 6-14%, which borders the standard deviation (4-7%) of the measurements. The close values of the TC and PCC Kevlar tensile results also indicated that the small change in mechanical properties is unrelated to the polymer coating. The thermal curing is done under nitrogen atmosphere to avoid oxidative damage, and it is likely that some molecular rearrangement of water between the amorphous and crystalline regions in the Kevlar is the source of slight mechanical losses.^{49, 50} There was, however, a greater tensile strength loss when curing with pMAA-co-SSAz (Supporting information). Curing with this polymer derivative caused a 14% loss in tensile stress at max load and modulus, and a 25% loss of energy at break. We originally hypothesized that acid-catalyzed hydrolysis at the curing temperature is caused some chain-scission in Kevlar, resulting in more significant deterioration of the mechanical properties with this acid containing coating. However, after presenting this data at the American Chemical Society meeting in Philadelphia in 2015, a DuPont scientist informed us that molecular rearrangement of the Kevlar chains occurs at raised temperatures, and causes slight changes in the mechanical properties.

Table 2.1 Tensile data for untreated Kevlar, thermally cured Kevlar, and Kevlar cured in the presence of p4VBA-co-SSAz.

	Tensile stress at max load (MPa)	Young's modulus (gf/den)	Energy at break (J)
Virgin Kevlar	20.158 +/- 0.818	726.985 +/- 7.531	0.923 +/- 0.070
Thermal Control (TC)	19.281 +/- 0.757	743.618 +/- 6.991	0.837 +/- 0.055
p4VBA-co-SSAZ (PCC)	18.930 +/- 0.783	744.818 +/- 10.376	0.808 +/- 0.062

Thermal gravimetric analysis of a PMMA-co-SSA coated Kevlar sample showed little change

in the thermal properties of the material as compared to the control sample (Figure 2.4). The coated sample had a ~5% weight loss between 250-550 °C, before the decomposition temperature of Kevlar that occurs around 550 °C, which likely corresponds to the degradation of the PMMA-co-SSA coating.

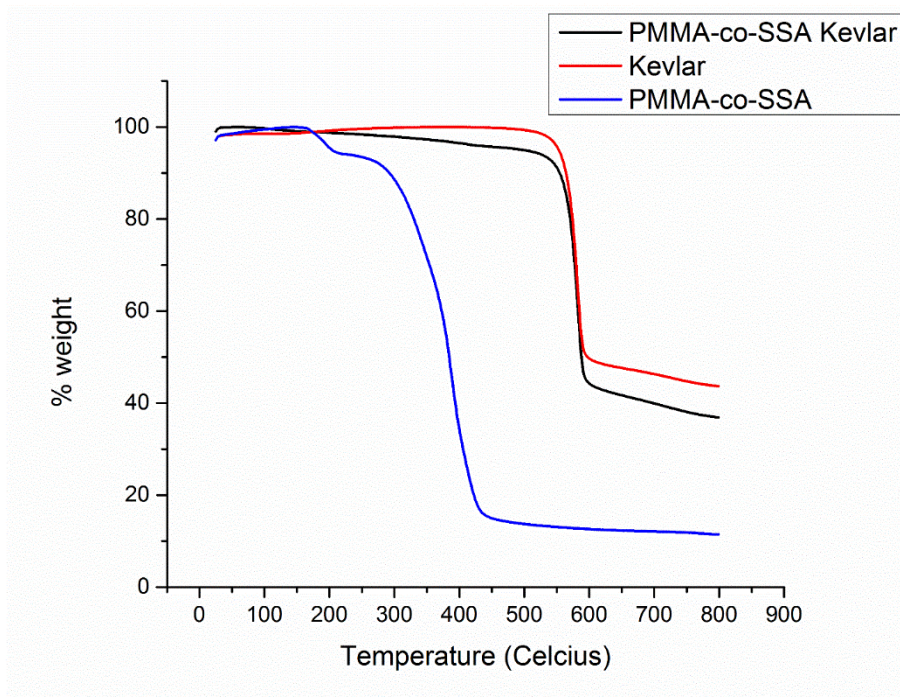


Figure 2.4. Thermal gravimetric analysis data of Kevlar coated in PMMA-co-SSA (black), virgin Kevlar (red), and PMMA-co-SSA (blue).

The pMMA-co-SSAz copolymer was also used to provide direct spectroscopic evidence of the incorporation of a PSAz containing polymer onto Kevlar. Poly(methylmethacrylate) has two distinct IR peaks at 1728 cm^{-1} and 1149 cm^{-1} (attributed to the ester C=O and C-O stretches) that can be differentiated from bulk Kevlar. Both pMMA-co-SSAz and commercial pMMA were applied to and cured at 180°C on Kevlar swatches, and the FTIR spectra recorded. Kevlar has a primarily C=O amide I (1645 cm^{-1}), an amide II primarily N-H mode, a C=C_{aromatic} band (1515,

cm^{-1}), an amide III with complex contributions (1319 cm^{-1}), a $\text{C}-\text{O}_{\text{aromatic}}$ stretch (1262 cm^{-1}), and a $\text{C}-\text{H}_{\text{aromatic}}$ in-plane vibration peak (1018 cm^{-1}). Figure 2.4 shows that after curing and prior to rinsing, both pMMA and pMMA-co-SSAz coated Kevlar contain the pMMA ester carbonyl peak at 1728 cm^{-1} and the $\text{C}-\text{O}$ peak at 1149 cm^{-1} . However after sonication in dichloromethane, only the Kevlar cured with the pMMA-co-SSAz retains the ester $\text{C}=\text{O}$ and $\text{C}-\text{O}$ peaks, indicating that the polymer is still covalently attached. Finally, in order to demonstrate the flexibility and modularity of this thermal grafting approach, the activated ester monomer PFPA was

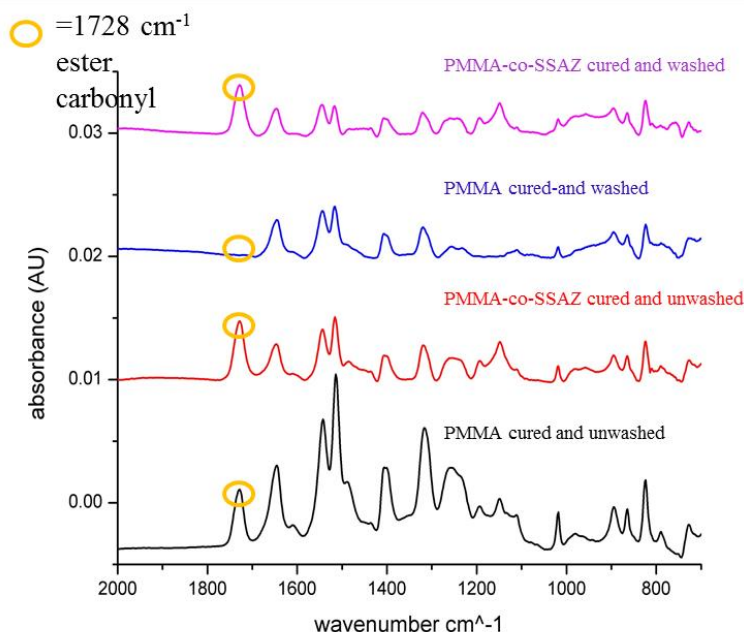


Figure 2.5. FTIR spectra demonstrating the robust attachment of PMMA-co-SSAz copolymer to Kevlar. After coating with PMMA or PMMA-co-SSAz the Kevlar swatches display the methacrylic 1728 cm^{-1} ester peak. After rinsing, it is evident that the coating is retained only on the swatch that underwent thermal grafting PMMA-co-SSAz.

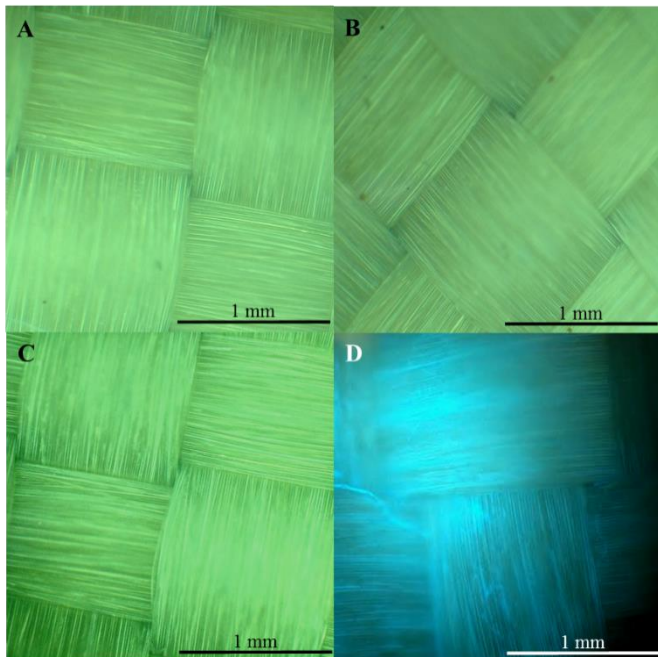


Figure 2.6. Fluorescence micrographs of (a) Virgin Kevlar, (b) Kevlar coated with PPFPA- co-SSAz; (c) Plain Kevlar immersed in 1-pyrenemethylamine solution; (d). Kevlar coated with pPFPA-co-SSAz that has undergone post-polymerization modification with 1- pyrenemethylamine.

copolymerized with SSAz. PFPA is notable for its fast and selective reactions with amines (pseudo-first order rate constant of 0.246 s^{-1} with primary alkyl amines), and reduced susceptibility to hydrolysis.⁴⁶ pPFPA-co-SSAz allows the functionalization of Kevlar with moieties not amenable to high temperature curing or inclusion directly as a monomer by acting as an excellent substrate for post-polymerization modification. To demonstrate that the PFPA functionality remains reactive after grafting to Kevlar, 1-pyrenemethylamine was reacted with the coated surface to produce a copolymer containing pendant pyrene moieties. Figure 3 shows fluorescence microscopy images of the pPFPA-co-SSAz functionalized Kevlar after post-polymerization modification with 1-pyrenemethylamine. The polymer containing pendant pyrene moieties shows

a strong blue fluorescence (Figure 2.6), whereas the controls (plain Kevlar, plain Kevlar exposed to 1-pyrenemethyl amine, and Kevlar cured with pPFPA-co-SSAz) only exhibit the inherent green fluorescence of Kevlar (Figure 2.6A-C).

Conclusion

In this work, we have adapted a versatile monomer, *p*-styrene sulfonyl azide, for use in the robust coating of inert aramid textiles. Using this approach, a variety of free radical compatible monomers are amenable to covalent grafting, along with the postpolymerization or post-grafting modification of reactive ester containing copolymers with nucleophilic substrates. The copolymers in this study were cured for 1 hour at 180 °C to ensure full crosslinking, however this curing time and high temperature are likely not necessary in all cases. All the polymers synthesized in this study except the unique case of pVBA-co-SSAz did not display any change in properties over several months of experimentation, demonstrating that the SSAz functionality in these polymers is highly stable and can be stored under ambient conditions. It has also been demonstrated that the curing process does not significantly damage the mechanical integrity of Kevlar.

References

1. Mera, H.; Takata, T., High-Performance Fibers. In *Ullmann's Encyclopedia of Industrial Chemistry*, Wiley-VCH Verlag GmbH & Co. KGaA2000.
2. Zhu, D.; Mobasher, B.; Rajan, S., Dynamic Tensile Testing of Kevlar 49 Fabrics. *J. Mater. Civ. Eng.* **2011**, 23, 230-239.
3. Li, X.-G.; Huang, M.-R., Thermal degradation of Kevlar fiber by high-resolution thermogravimetry. *J. Appl. Polym. Sci.* **1999**, 71, 565-571.
4. Brown, J.; Ennis, B., Thermal Analysis of Nomex® and Kevlar® Fibers. *Text. Res. J.* **1977**, 47, 62-66.
5. Pinto, R.; Carr, D.; Helliker, M.; Girvan, L.; Gridley, N., Degradation of military body armor due to wear: Laboratory testing. *Text. Res. J.* **2012**, 82, 1157-1163.
6. Welch, C. M., Tetracarboxylic Acids as Formaldehyde-Free Durable Press Finishing Agents: Part I: Catalyst, Additive, and Durability Studies. *Text. Res. J.* **1988**, 58, 480-486.
7. Zimmermann, J.; Reifler, F. A.; Fortunato, G.; Gerhardt, L.-C.; Seeger, S., A Simple, One-Step Approach to Durable and Robust Superhydrophobic Textiles. *Adv. Funct. Mater.* **2008**, 18, 3662-3669.
8. Dhende, V. P.; Samanta, S.; Jones, D. M.; Hardin, I. R.; Locklin, J., One-Step Photochemical Synthesis of Permanent, Nonleaching, Ultrathin Antimicrobial Coatings for Textiles and Plastics. *ACS Appl. Mater. Interfaces* **2011**, 3, 2830-2837.
9. Hsu, B. B.; Klibanov, A. M., Light-Activated Covalent Coating of Cotton with Bactericidal Hydrophobic Polycations. *Biomacromolecules* **2010**, 12, 6-9.

10. Kim, Y. H.; Nam, C. W.; Choi, J. W.; Jang, J., Durable antimicrobial treatment of cotton fabrics using N-(2-hydroxy)propyl-3-trimethylammonium chitosan chloride and polycarboxylic acids. *J. Appl. Polym. Sci.* **2003**, *88*, 1567-1572.
11. Yeh, J. R.; Teply, J. L., Compressive Response of Kevlar/Epoxy Composites. *J. Compos. Mater.* **1988**, *22*, 245-257.
12. Strife, J. R.; Prewo, K. M., The Thermal Expansion Behavior of Unidirectional and Bidirectional Kevlar/Epoxy Composites. *J. Compos. Mater.* **1979**, *13*, 264-277.
13. Mittelman, A.; Roman, I., Tensile properties of real unidirectional Kevlar/epoxy composites. *Composites* **1990**, *21*, 63-69.
14. Little, B. K.; Li, Y.; Cammarata, V.; Broughton, R.; Mills, G., Metallization of Kevlar Fibers with Gold. *ACS Appl. Mater. Interfaces* **2011**, *3*, 1965-1973.
15. Mahfuz, H.; Clements, F.; Rangari, V.; Dhanak, V.; Beamson, G., Enhanced stab resistance of armor composites with functionalized silica nanoparticles. *J. Appl. Phys.* **2009**, *105*, -.
16. Chen, W.; Qian, X.-M.; He, X.-Q.; Liu, Z.-Y.; Liu, J.-P., Surface modification of Kevlar by grafting carbon nanotubes. *J. Appl. Polym. Sci.* **2012**, *123*, 1983-1990.
17. Zhang, Y.; Jiang, Z.; Huang, Y.; Li, Q., The modification of Kevlar fibers in coupling agents by γ -ray co-irradiation. *Fibers Polym* **2011**, *12*, 1014-1020.
18. Luo, J.; Sun, Y., Acyclic N-Halamine Coated Kevlar Fabric Materials: Preparation and Biocidal Functions. *Industrial & Engineering Chemistry Research* **2008**, *47*, 5291-5297.
19. Fan, G.; Zhao, J.; Zhang, Y.; Guo, Z., Grafting modification of Kevlar fiber using horseradish peroxidase. *Polym. Bull.* **2006**, *56*, 507-515.
20. Sheu, G. S.; Shyu, S. S., Surface modification of Kevlar 149 fibers by gas plasma treatment. *J. Adhes. Sci. Technol.* **1994**, *8*, 531-542.

21. Wu, Y.; Tesoro, G. C., Chemical modification of Kevlar fiber surfaces and of model diamides. *J. Appl. Polym. Sci.* **1986**, *31*, 1041-1059.

22. Benrashid, R.; Tesoro, G. C., Effect of Surface-Limited Reactions on the Properties of Kevlar® Fibers. *Text. Res. J.* **1990**, *60*, 334-344.

23. Lin, T. K.; Kuo, B. H.; Shyu, S. S.; Hsiao, S. H., Improvement of the adhesion of Kevlar fiber to bismaleimide resin by surface chemical modification. *J. Adhes. Sci. Technol.* **1999**, *13*, 545-560.

24. Li, J.; Ye, F. B., Effect of surface modification of Kevlar fibre on friction and wear properties of UHMWPE composites. *Plast., Rubber Compos.* **2010**, *39*, 264-267.

25. Ai, T.; Wang, R.; Zhou, W., Effect of grafting alkoxy silane on the surface properties of Kevlar fiber. *Polym. Compos.* **2007**, *28*, 412-416.

26. Li, G.; Zhang, C.; Wang, Y.; Li, P.; Yu, Y.; Jia, X.; Liu, H.; Yang, X.; Xue, Z.; Ryu, S., Interface correlation and toughness matching of phosphoric acid functionalized Kevlar fiber and epoxy matrix for filament winding composites. *Compos. Sci. Technol.* **2008**, *68*, 3208-3214.

27. Akdag, A.; Kocer, H. B.; Worley, S. D.; Broughton, R. M.; Webb, T. R.; Bray, T. H., Why Does Kevlar Decompose, while Nomex Does Not, When Treated with Aqueous Chlorine Solutions? *J. Phys. Chem. B* **2007**, *111*, 5581-5586.

28. Schuh, K.; Prucker, O.; Rühe, J., Surface Attached Polymer Networks through Thermally Induced Cross-Linking of Sulfonyl Azide Group Containing Polymers. *Macromolecules* **2008**, *41*, 9284-9289.

29. Raghuraman, G. K.; Schuh, K.; Prucker, O.; Rühe, J., Attachment of Polymer Films to Solid Surfaces via Thermal Activation of Self-assembled Monolayers Containing Sulphonyl Azide Group. *Langmuir* **2009**, *26*, 769-774.

30. Sloan, M. F.; Renfrow, W. B.; Breslow, D. S., Thermal reactions of sulfonyl azides with aliphatic hydrocarbons. *Tetrahedron Lett.* **1964**, *5*, 2905-2909.

31. Breslow, D. S.; Sloan, M. F.; Newburg, N. R.; Renfrow, W. B., Thermal reactions of sulfonyl azides. *J. Am. Chem. Soc.* **1969**, *91*, 2273-2279.

32. Scriven, E. F. V., *Azides and Nitrenes: Reactivity and Utility*. Academic Press: Orlando, **1984**.

33. Christensen, S. K.; Chiappelli, M. C.; Hayward, R. C., Gelation of Copolymers with Pendent Benzophenone Photo-Cross-Linkers. *Macromolecules* **2012**, *45*, 5237-5246.

34. Prucker, O.; Naumann, C. A.; Rühe, J.; Knoll, W.; Frank, C. W., Photochemical Attachment of Polymer Films to Solid Surfaces via Monolayers of Benzophenone Derivatives. *J. Am. Chem. Soc.* **1999**, *121*, 8766-8770.

35. Moloney, M. G.; Ebenezer, W.; Awenat, K. Process for surface functionalization of polymeric substrates using diaryl carbenes as reactive intermediates. US6699527 B1, 2004.

36. Awenat, K. M.; Davis, P. J.; Moloney, M. G.; Ebenezer, W., A chemical method for the convenient surface functionalisation of polymers. *Chem. Commun.* **2005**, 990-992.

37. Wang, H.; Griffiths, J.-P.; Egddell, R. G.; Moloney, M. G.; Foord, J. S., Chemical Functionalization of Diamond Surfaces by Reaction with Diaryl Carbenes. *Langmuir* **2008**, *24*, 862-868.

38. Navarro, R.; Pérez Perrino, M.; Prucker, O.; Rühe, J., Preparation of surface-attached polymer layers by thermal or photochemical activation of α -diazoester moieties. *Langmuir* **2013**, *29*, 10932-10939.

39. Blencowe, A.; Hayes, W., Development and application of diazirines in biological and synthetic macromolecular systems. *Soft Matter* **2005**, *1*, 178-205.

40. Liu, L.; Yan, M., A General Approach to the Covalent Immobilization of Single Polymers. *Angew. Chem. Int. Ed.* **2006**, *45*, 6207-6210.

41. Liu, L.-H.; Yan, M., Perfluorophenyl Azides: New Applications in Surface Functionalization and Nanomaterial Synthesis. *Acc. Chem. Res.* **2010**, *43*, 1434-1443.

42. McVerry, B. T.; Wong, M. C. Y.; Marsh, K. L.; Temple, J. A. T.; Marambio-Jones, C.; Hoek, E. M. V.; Kaner, R. B., Scalable Antifouling Reverse Osmosis Membranes Utilizing Perfluorophenyl Azide Photochemistry. *Macromol. Rapid Commun.* **2014**, *35*, 1528-1533.

43. DuPont, Kevlar Aramid Fiber: Technical Guide. **1992**.

44. R. Davis, S. N., and J.W. Chin, Accelerated Weathering of Firefighter Protective Clothing: Delineating the Impact of Thermal, Moisture, and Ultraviolet Light Exposures. In *NIST Technical Note 1746* 2012.

45. Wei, C.; Ximming, Q.; Xueqiu, H.; Jiping, L. In *Enhanced ultraviolet resistance of Kevlar fibers with TiO₂ films*, Reliability, Maintainability and Safety (ICRMS), 2011 9th International Conference on, 12-15 June 2011, 2011; pp 1267-1272.

46. Arnold, R. M.; Sheppard, G. R.; Locklin, J., Comparative Aminolysis Kinetics of Different Active Ester Polymer Brush Platforms in Postpolymerization Modification with Primary and Aromatic Amines. *Macromolecules* **2012**, *45*, 5444-5450.

47. Eberhardt, M.; Mruk, R.; Zentel, R.; Théato, P., Synthesis of pentafluorophenyl(meth)acrylate polymers: New precursor polymers for the synthesis of multifunctional materials. *Eur. Polym. J.* **2005**, *41*, 1569-1575.

48. Filocamo, S.; Stote, R.; Ziegler, D.; Gibson, H., Entrapment of DFPase in titania coatings from a biomimetically derived method. *J. Mater. Res.* **2011**, *26*, 1042-1051.

49. Abu Obaid, A.; Deitzel, J. M.; Gillespie, J. W.; Zheng, J. Q., The effects of environmental conditioning on tensile properties of high performance aramid fibers at near-ambient temperatures. *J. Compos. Mater.* **2011**, *45*, 1217-1231.

50. Fukuda, M.; Kawai, H., Effect of Water on the Crystal Structure of Regular Kevlar. *Sen'i Gakkaishi* **1996**, *52*, 582-590.

CHAPTER 3:
SUFEX ON THE SURFACE: A FLEXIBLE PLATFORM FOR POSTPOLYMERIZATION
MODIFICATION OF POLYMER BRUSHES ¹

¹ Yatvin, J.; Brooks, K; and Locklin, J. 2015. *Angew. Chem. Int. Ed.* 54:13370-13373.

Reprinted with permission from publisher.

Abstract

Polymer brushes present a unique architecture for tailoring surface functionalities due to their distinctive physicochemical properties. However, the polymerization chemistries used to grow brushes place limitations on the monomers that can be grown directly from the surface. Several forms of click chemistry have previously been used to modify polymer brushes via postpolymerization modification with high efficiency, however it is usually difficult to include the unprotected moieties in the original monomer. We present the use a new form of click chemistry known as SuFEx (sulfur(VI) fluoride exchange), which allows a silyl ether to be rapidly and quantitatively clicked to a polymer brush containing native $-\text{SO}_2\text{F}$ groups with rapid pseudofirst order rates as high as 0.04 s^{-1} . Furthermore, we demonstrate the use of SuFEx to facilely add a variety of other chemical functional groups to brush substrates that have highly useful and orthogonal reactivity, including alkynes, thiols, and dienes.

Introduction

Over the past decade, click chemistries have become essentially a standard coupling strategy used to covalently immobilize or conjugate a variety of simple and complex molecules in the chemical and biological sciences.¹⁻³ These chemistries have also had an equally important impact on surface science, as they allow the attachment of complex or delicate molecules with high fidelity, speed, and conversion to solid or particle supports.³⁻⁷ Conversely, click chemistries can be used to attach polymers to substrates, one another, or add functionality along the backbone in an efficient and orthogonal manner.⁸⁻¹⁰ Polymer brushes have emerged at the forefront of surface functionalization due to the unique physicochemical properties of stretched polymer chains and the ability to have a high density of functional groups in a given area. Also, the functionalization of reactive polymer brushes via highly efficient forms of postpolymerization modification (PPM) reactions has emerged as an expanding field.¹¹⁻¹⁷ By combining the unique properties of polymer brushes and click chemistry PPM, surfaces with desirable and unique properties can be quickly generated

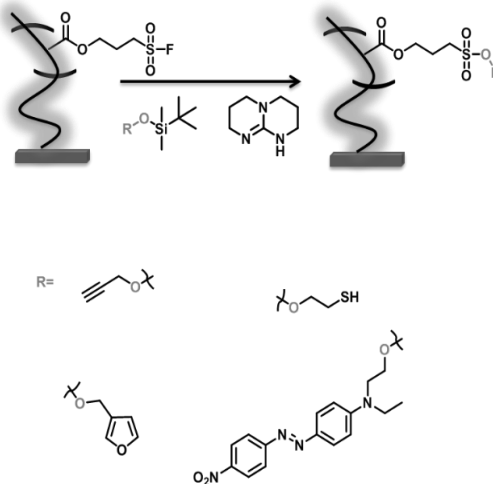


Figure 3.1. Synthetic scheme for SuFEx brushes. (bottom) Selection of reactive functionalities for PPM of p(FSPMA) brushes.

without laborious monomer or polymer synthesis. The ability to use a variety of coupling

strategies, especially highly robust and efficient click chemistries, is particularly important for decorating surfaces with multiple functionalities.¹⁸⁻²¹ However, some click reactions have inherent drawbacks such as oxygen sensitivity or difficult synthetic access. Our lab has already demonstrated several uses of PPM click chemistry on polymer brushes to design complex interfaces.²¹ Herein, we demonstrate the application of a new form of click chemistry, sulfur(VI) fluoride exchange (SuFEx), for the efficient functionalization of polymer brushes, with the aim towards increasing the ability to functionalize surfaces in an orthogonal fashion. We also believe that SuFEx provides a simple platform to graft other challenging functional groups that are intolerant of the required polymerization conditions, such as other click motifs, to brush surfaces. The sulfur-fluoride exchange reaction, which was recently revived from an unrecognized state by the Sharpless group,²² is based on the unique reactivity of sulfonyl fluorides. Unlike electrophilic sulfonyl chlorides, sulfonyl fluorides are generally unreactive under a wide variety of harsh reaction conditions.²² However, in the presence of certain non-nucleophilic bases, such as diazabicycloundec-7-ene (DBU), or 2-tert-butyl-imino-2-diethylamino-1,3-dimethylperhydro-1,3,2-diaza-phosphorine (BEMP), it has been previously demonstrated that sulfonyl fluorides will undergo exchange with silyl ethers in a highly selective fashion to form a new S-O bond (Scheme 1). This reaction is driven by the thermodynamically favorable formation of a Si-F bond (bond dissociation energy = 565 kJ·mol⁻¹).²³ Other sulfonyl halides are much less suitable for this reaction due to their higher degree of SO₂-X bond hydrolyzability and the lower Si-X bond formation energy (Si-Cl = 456 kJ·mol⁻¹, Si-Br = 343 kJ·mol⁻¹, Si-I=399 kJ·mol⁻¹). The exact mechanism of the exchange has not been completely elucidated, but Gembus *et al.* hypothesized that a sulfonyl ammonium fluoride salt is formed by the reaction of an amine with the sulfonyl fluoride, which can then react with the silyl ether to form a sulfonate ester plus inert silyl fluoride.²⁴

Equipment and Materials

All compounds were purchased from Alpha-Aesar, TCI, or Sigma-Aldrich and unless otherwise noted used as received. DMF and DCM were obtained dry after passing through an MBraun MB-SPS. Imidazole was recrystallized in DCM. Acetonitrile, triethylamine, DBU, propargyl alcohol, furfuryl alcohol, and mercaptoethanol were dried over 4 Å molecular sieves.

FTIR studies were done using a Thermo-Nicolet model 6700 spectrometer equipped with a variable angle grazing angle attenuated total reflection (GATR-ATR) accessory (Harrick Scientific) at 64 scans with 4 cm^{-1} resolution. Polymerization was conducted in a Rayonet RPR-600 Mini UV reactor using 350 nm bulbs. Thickness was determined on a J.A. Woollam M-2000 V spectroscopic ellipsometer with a white light source at three angles of incidence (65°, 70°, and 75°) to the silicon wafer normal. A Cauchy model was used to fit the film thickness, extinction coefficient, and refractive index of the polymer brush layer. Static contact angle measurements were taken on a Krüss DSA 100 using a 1 μL drop of 18 $\text{M}\Omega$ water (pH 7). UV-Vis studies were performed on a Varian Cary 50 UV-Vis Spectrophotometer. ^1H and ^{19}F NMR were taken on a Varian Mercury 300 MHz NMR. The number- and weight-average molecular weights of the copolymer were estimated using gel permeation chromatography (Viscotek, Malvern Inc.) with two high-molecular-weight columns (I-MBHMW-3078) and one low-molecular-weight column (I-MBLMW-3078) with THF as the eluent at 40 °C. Triple-point detection, consisting of the refractive index, light scattering, and viscometry, was used. Polystyrene standards were used to determine the molecular weight from the universal calibration. AFM images were taken using Peakforce Quantitative Nanomechanical Mapping on a Bruker Multimode AFM with Scanasyst-AIR, $k=0.4 \text{ N/m}$, resonant frequency (f_0)=50-90 kHz.

Synthesis of p(FSPMA) brushes: In a glovebox, plasma cleaned slides were immersed for 16 hr in a 10 mM dry toluene solution of azo-based silane initiator prepared according to Arnold *et al.* to form an photoinitiator monolayer.²⁵ Slides were removed from the glovebox and sonicated in dry toluene. FSPMA was degassed with Ar for 2 hours. Both the slides and degassed FSPMA were then brought into the glovebox. Slides were placed in glass vials with 0.3 mL FSPMA and tightly sealed using Teflon tape. Vials were removed from the glovebox and irradiated with 350 nm light (1.25 mW/cm²) in a UV reactor for 2 hours. Slides were removed from the vials and sonicated with THF to remove any physisorbed polymer.

Postpolymerization modification of brushes: 0.1 mmol of a silyl ether protected molecule was dissolved in 2 mL of MeCN, and the substrate was added along with a small stir bar. 0.02 mmol of either DBU or TBD was added, and the p(FSPMA) substrate immersed in the solution for 2 hours at room temperature for DBU or 3 minutes for TBD. The substrate was then washed with CH₂Cl₂ and isopropanol.

Synthesis

3-(chlorosulfonyl)propyl methacrylate: 10.00 g (48.3 mmol) of sodium 3-(methacryloyloxy)propane-1-sulfonate was added to a round bottom flask followed by 16 mL (82 mmol) of thionyl chloride and 2 drops of catalytic DMF. The reaction was refluxed overnight and then quenched by slowly adding the reaction mixture to ice. The water layer was extracted 2x with ether. The ether layer was then extracted 2x with water and dried over MgSO₄. Solvent was removed under reduced pressure to yield 6.2g (73% yield) of a pale yellow oil, which was stored at -20 °C. ¹H NMR (300 MHz, CDCl₃) δ= 6.12 (s, 1H) 5.63 (s, 1H) 4.33 (t, *J* = 6.0 Hz, 2H) 3.78 (t, *J* = 9.0 Hz, 2H) 2.43 (quintet, *J* = 6 Hz, 2H) 1.95 (s, 3H).

3-(fluorosulfonyl)propyl methacrylate: 6.20 g of 3-chlorosulfonylpropyl methacrylate was dissolved in 10 mL of MeCN, and the solution was added to 10.6 g of KFHF dissolved in 33 mL of water in a polyethylene container. The solution was stirred vigorously at room temperature to elicit an unstable emulsion for 7 hours and then extracted with ether. The ether layer was washed 2x with saturated sodium bicarbonate solution, dried over MgSO₄, and then flashed through a neutral alumina plug. Solvent was removed under reduced pressure, and the monomer was further purified by vacuum distillation to yield 4.67 g (81% yield) of clear oil which was stored at -20 °C. *Caution KFHF etches glass, and spills should be treated similarly to HF solution spills. ¹H NMR (300 MHz, CDCl₃) δ= 6.12 (s, 1H) 5.63 (s, 1H) 4.30 (t, *J* = 6.0 Hz, 2H) 3.49 (m, 2H) 2.34 (m, 2H) 1.95 (s, 3H). ¹⁹F NMR (282 MHz, MeCN-d₃) δ= 52.03 (t, *J* = 0.56, 1 F).

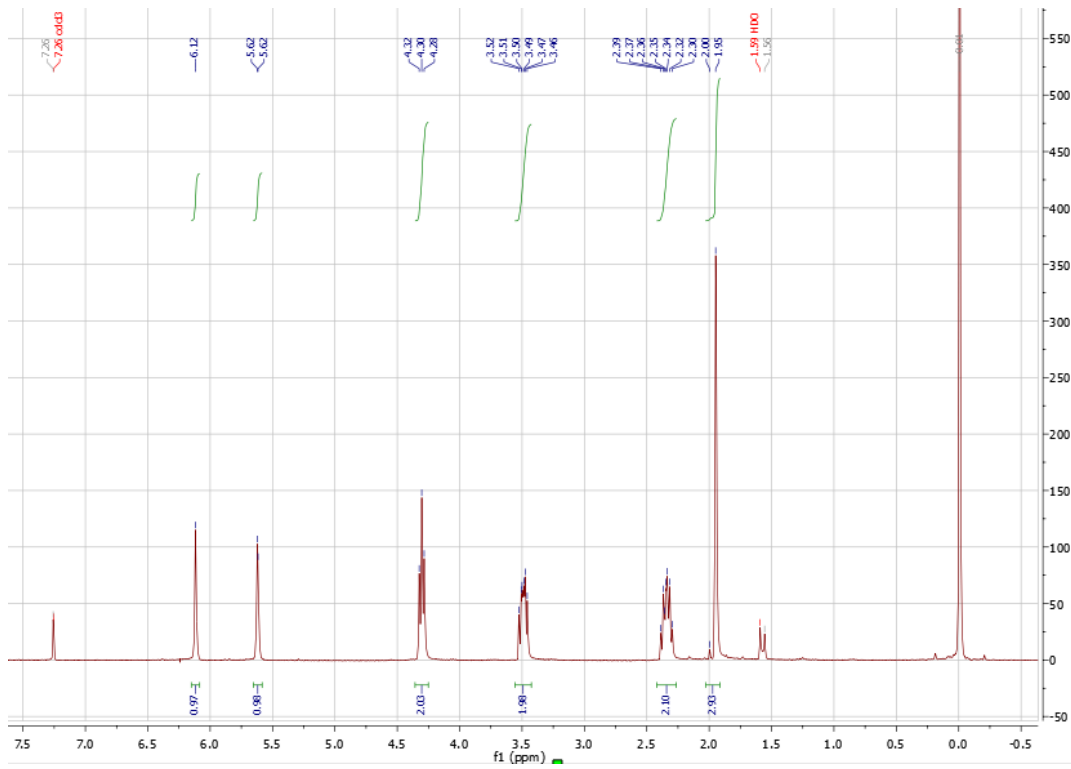


Figure 3.2. ¹H NMR of 3-(fluorosulfonyl)propyl methacrylate.

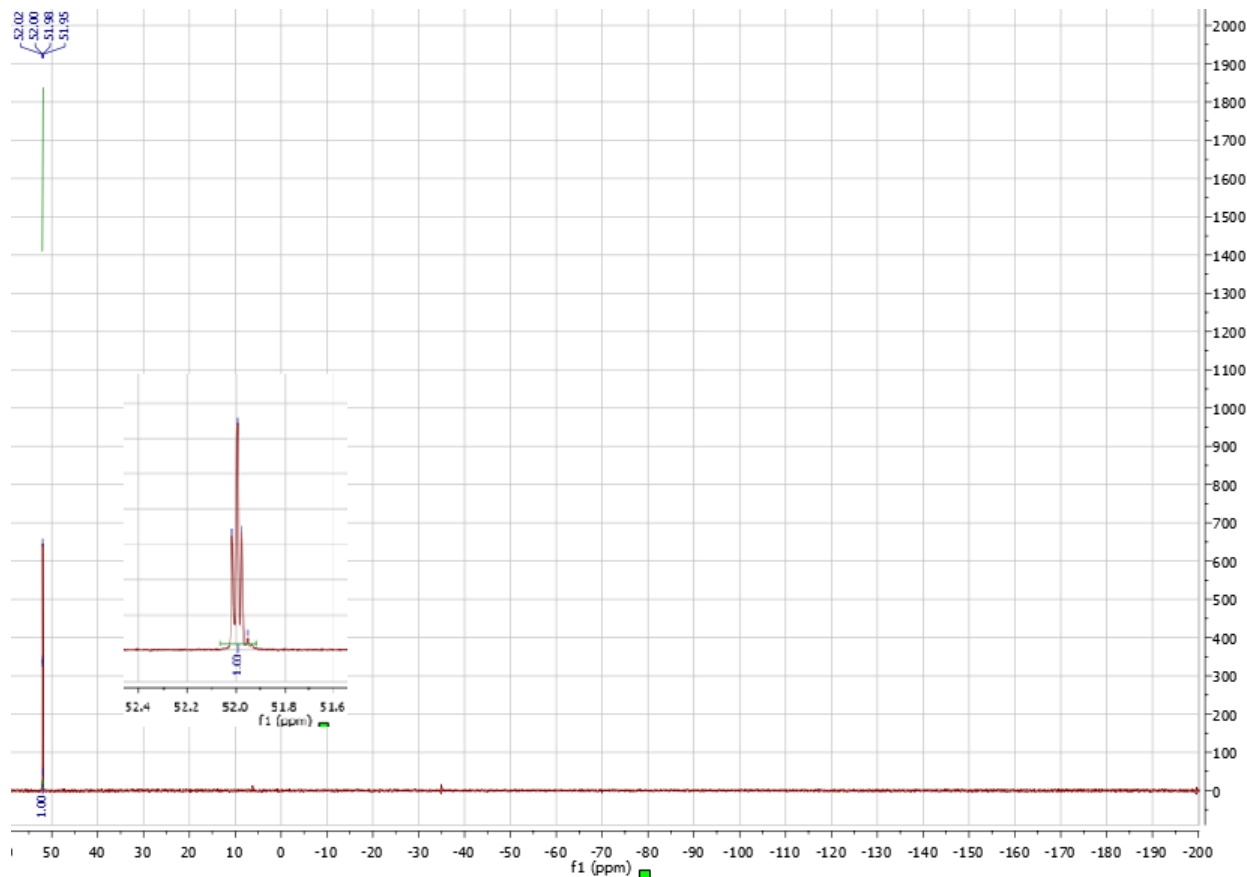


Figure 3.3. ^{19}F NMR of 3-(fluorosulfonyl)propyl methacrylate.

TMS-Disperse Red 1: 3.00 g (9.54 mmol) of Disperse Red 1 and 1.46 mL (10.49 mmol) of triethylamine were dissolved in 50 mL of DCM in a 3-neck round bottom flask. 1.27 mL (10.02 mmol) of trimethylchlorosilane was added to the flask, and the reaction stirred overnight at room temperature. DCM was removed by evaporation under reduced pressure and ether added. The solution flashed through a Celite plug then solvent was removed under vacuum to yield 1.13 g (31% yield) of a dark red solid, which was stored under an inert atmosphere. ^1H NMR (300 MHz, CDCl_3) δ = 8.31 (d, J = 9.0 Hz, 2H) 7.95 (d, J = 9.0 Hz, 4H) 6.79 (d, J = 9.0 Hz, 2H) 3.80 (t, J = 6.0 Hz, 2H) 3.5-3.6 (m, 4H) 1.26 (t, J = 6.0 Hz, 3H).

tert-butyldimethyl(prop-2-yn-1-yloxy)silane(a): 1 g (17.8 mmol) of propargyl alcohol, 2.43 g (35.70 mmol) of imidazole, and 2.70 g (17.90 mmol) of TBDMS-Cl, were dissolved in 7 mL of DCM, and the reaction was stirred overnight at room temperature. The reaction was extracted with 2x with water then the DCM removed by evaporation under reduced pressure. The crude product was distilled under reduced pressure to yield 2.20 g (72% yield) of a clear oil. ^1H NMR (300 MHz, CDCl_3) δ = 4.31 (dd, J = 3.0, 3.0 Hz, 2H) 2.38 (m, 1H) 0.91 (s, 9H) 0.12 (s, 6H).

2-((tert-butyldimethylsilyl)oxy)ethane-1-thiol(b): 1 g (12.80 mmol) of 1-octanol, 1.45 g (13.06 mmol) of imidazole, and 1.56 g (26.88 mmol) of TBDMS-Cl were dissolved in 7 mL of DCM, and the reaction was stirred overnight at room temperature. The reaction was extracted with 2x with water then the DCM removed by evaporation under reduced pressure to yield 1.06 g (49% yield) of a clear oil. ^1H NMR (300 MHz, CDCl_3) δ = 3.75 (t, J = 6 Hz, 2H) 2.63 (m, 2H) 1.53 (t, J = 9 Hz, 1H) 0.88 (s, 9H) 0.07 (s, 6H).

tert-butyl(cyclopenta-1,3-dien-1-ylmethoxy)dimethylsilane: 1 g (10.19 mmol) of furfuryl alcohol, 1.10 g (10.38 mmol) of tert-butyldimethylchlorosilane, and 1.18 g (21.40 mmol) of imidazole were dissolved in 7 mL of DCM, and the reaction was stirred overnight at room temperature. The reaction was extracted with 2x with water then the solvent evaporated under reduced pressure to yield 1.06 g (57% yield) of a yellow oil. ^1H NMR (300 MHz, CDCl_3) δ = 7.37 (dd, J = 0.1 Hz, 1H) 6.31 (m, 1H), 6.22 (dd, J = 3.0, 0.2, Hz 1H) 4.64 (s, 1H) 0.91 (s, 9H) 0.08 (s, 6H).

TBDMS-Disperse Red 1: 1.00 g (2.59 mmol) of Disperse Red 1, 0.42 g (6.22 mmol) of imidazole, and 0.43 g (2.84 mmol) of tert-butyldimethylchlorosilane were dissolved in 20 mL DMF. The reaction was stirred overnight. Water and ether were added, and the organic layer was extracted 3x with water. Ether was removed by evaporation under reduced pressure to yield 0.92 g of a dark red powder (86% yield). ^1H NMR (300 MHz, CDCl_3) δ = 8.32 (d, J = 9.0 Hz, 2H) 7.90 (d, J = 9.0

Hz, 4H) 6.76 (d, J = 9.0 Hz, 2H) 3.83 (t, J = 6.0 Hz, 2H) 3.45-3.60 (m, 4H) 1.24 (t, J = 6.0 Hz, 3H) 0.89 (s, 9H) 0.04 (s, 6H).

Gel permeation chromatography

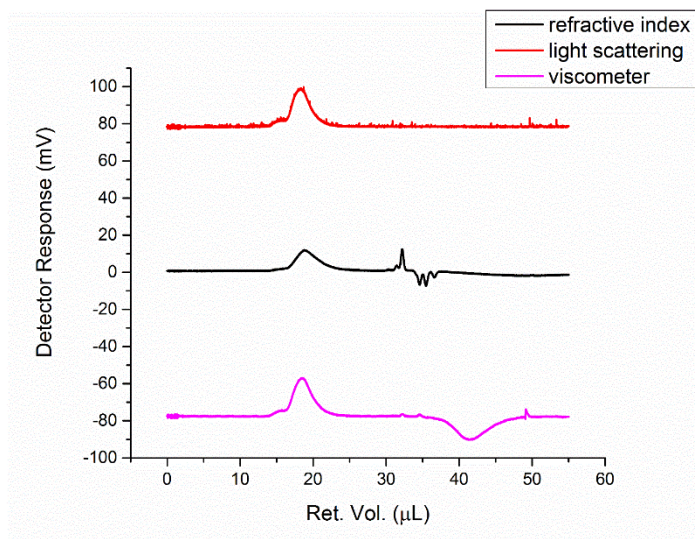


Figure 3.4. Triple detection GPC data for isolated solution polymer generated by surface initiated polymerization of FSPMA.

M_n - (Daltons) 171218

M_w - (Daltons) 283145

M_z - (Daltons) 400284

Dispersity - 1.65

Absorbance data

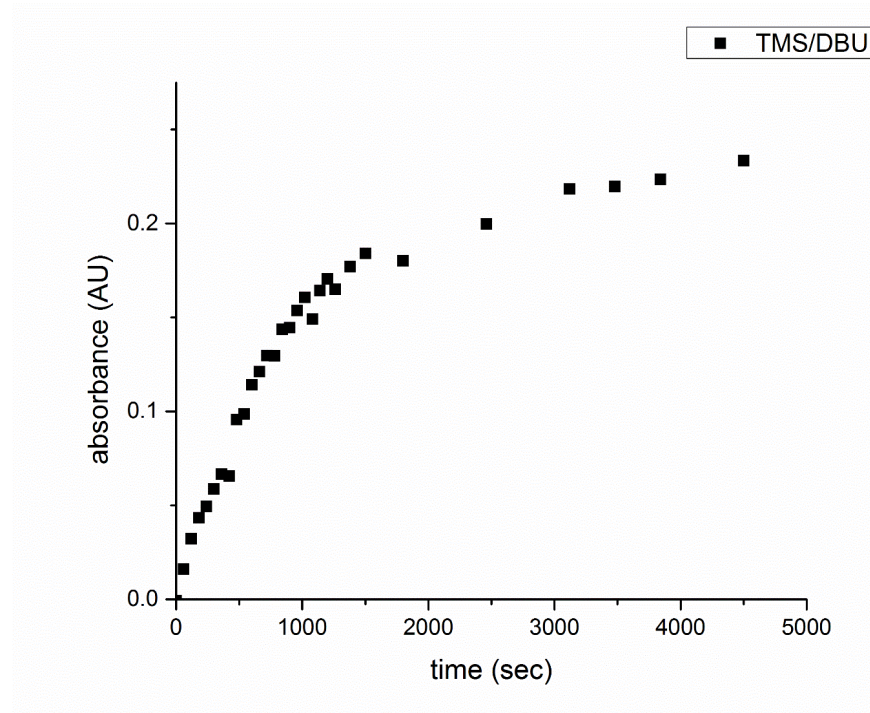


Figure 3.5. Absorbance vs. time of DR1-TMS surface SuFEx catalyzed by DBU.

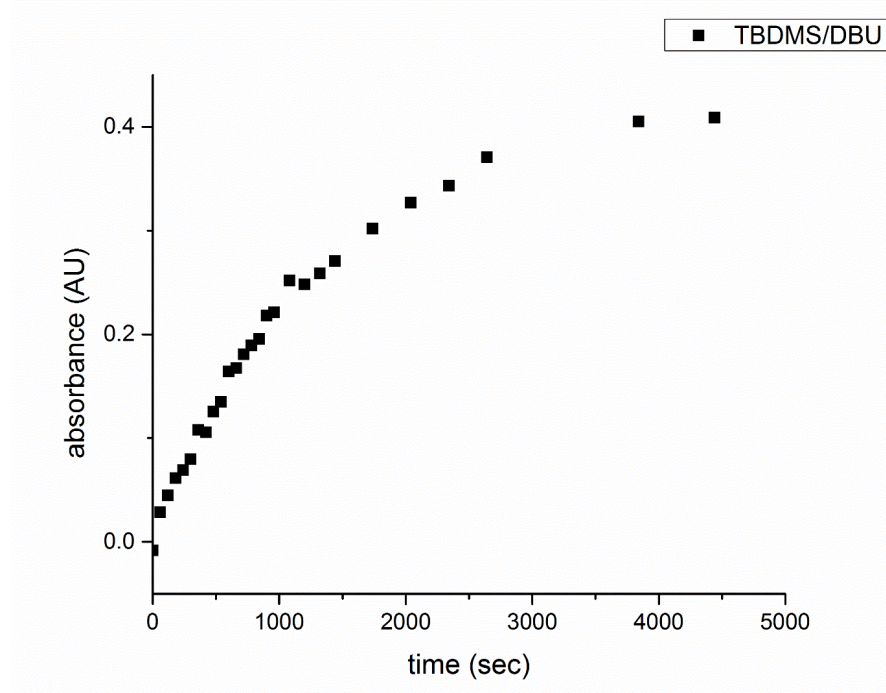


Figure 3.6. Absorbance vs. time of DR1-TBDMS surface SuFEx catalyzed by DBU.

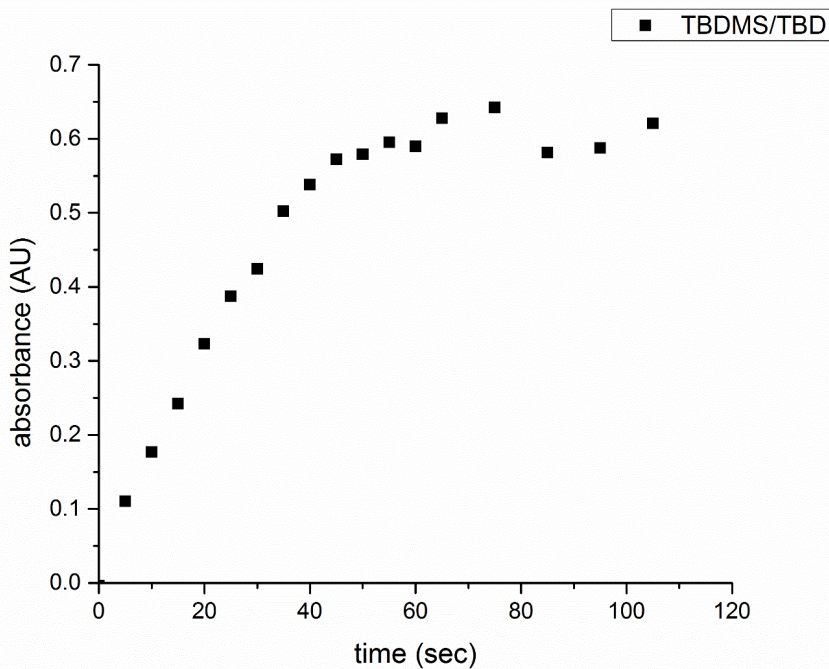


Figure 3.7. Absorbance vs. time of DR1-TBDMS surface SuFEx catalyzed by TBD.

Grafting density calculation

The p(FSPMA) from solution polymer's number-average molecular weight, which was assumed to be similar to the brush polymer's number-average molecular weight, was determined to be 171,218 Da. The density of the polymer was assumed to be close to that of the monomer (1.5). Using these values in Equation (1), where h is the thickness (25 nm), ρ is the bulk density, N_A is Avogadro's number, and M_n is the number-average molecular weight,

Equation 3.1.

$$\sigma = \frac{h\rho N_A}{M_n}$$

the grafting density (σ) of the brushes was determined to be **0.14 chains/nm²**.

Rate constant calculation

Since the number of silyl ether and catalyst molecules in solution is several orders of magnitude more than the number of sulfonyl fluorides on the surface, the reaction kinetics can be considered as pseudo-first order, which can be described by the equation:

Equation 3.2.

$$k't = \ln \left(\frac{A_0 - A_\infty}{A_t - A_\infty} \right)$$

where k' is the pseudo-first-order rate constant, and A_0 , A_∞ , and A_t correlate to the initial absorbance, the final absorbance, and absorbance at time t , respectively. By plotting the absorbance vs time, an area of the graph where there is a linear increase with time with respect to absorbance at the beginning of the reaction is observed. The slope of the line obtained by plotting $\ln((A_0 - A_\infty)/(A_t - A_\infty))$ versus time from this linear area of the graph time gives k' .

Dye functional group density calculation

The number of molecules in a given unit area can be calculated by using a rearrangement of Beer's law

Equation 3.3.

$$d = \frac{A * N_A}{\varepsilon * 1000 \text{ cm}^2}$$

where d is the surface coverage in molecules/cm², A is absorbance, N_A is Avogadro's number, and ε is the extinction coefficient of Disperse Red 1 at 485 nm ($3.6 \times 10^4 \text{ M}^{-1} \text{ L}^{-1}$). $d = 1.02 \times 10^{16}$ molecules/cm² for the substrate, and by taking the thickness of the film into account (30 nm), the functional group density per unit volume is calculated to be **3.62 dye molecules/nm³**.

Electron Dispersive X-Ray Spectroscopy

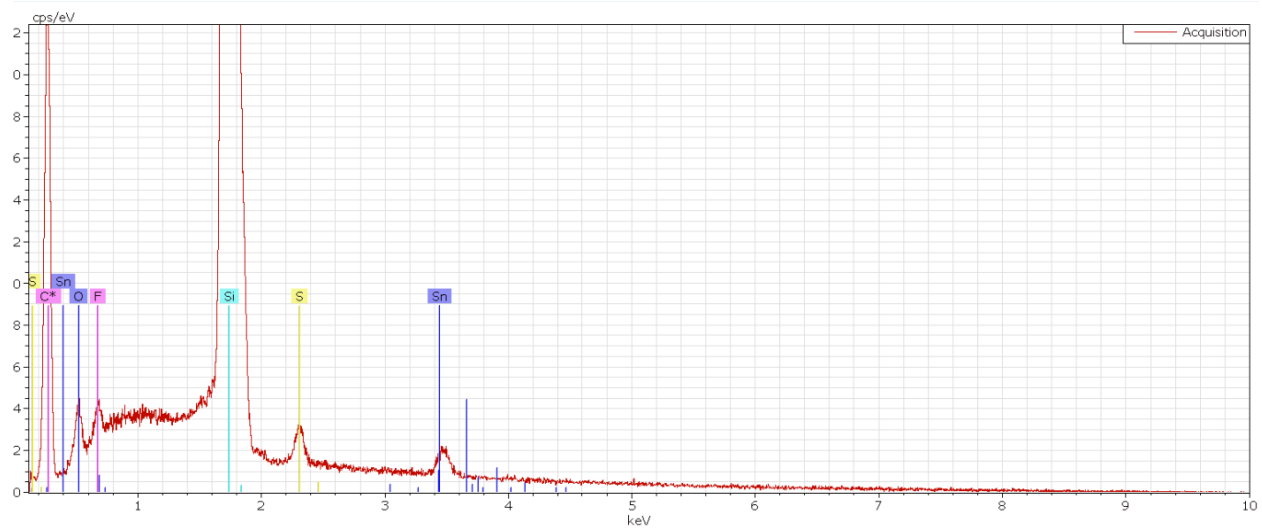


Figure 3.8. pFSPMA brush. The fluorine peak is found at 0.7 keV.

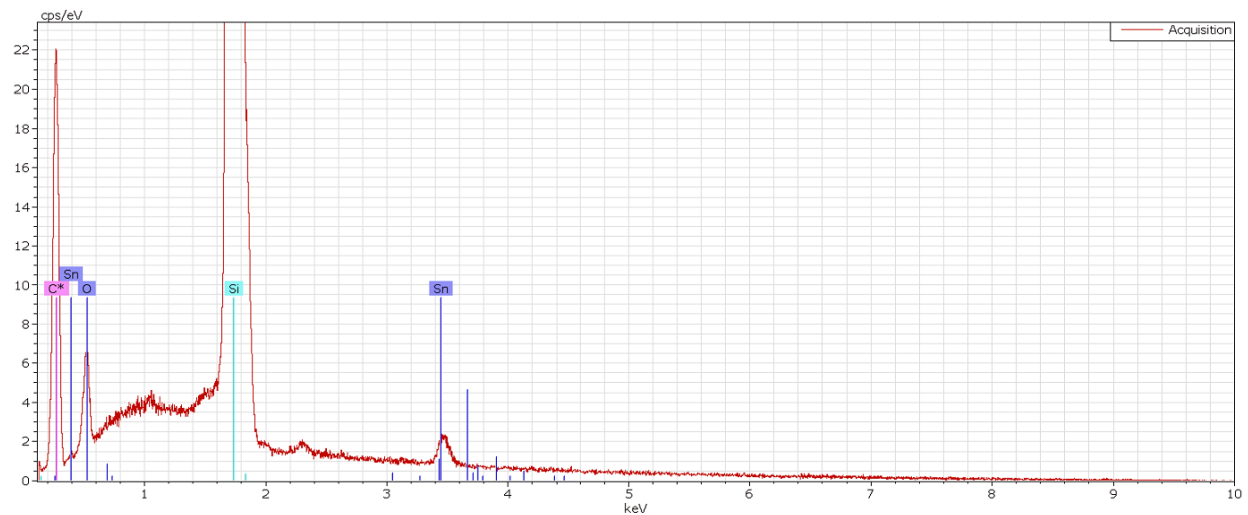


Figure 3.9. pFSPMA brush SuFEx reacted with TBDMS-mercaptopropanol

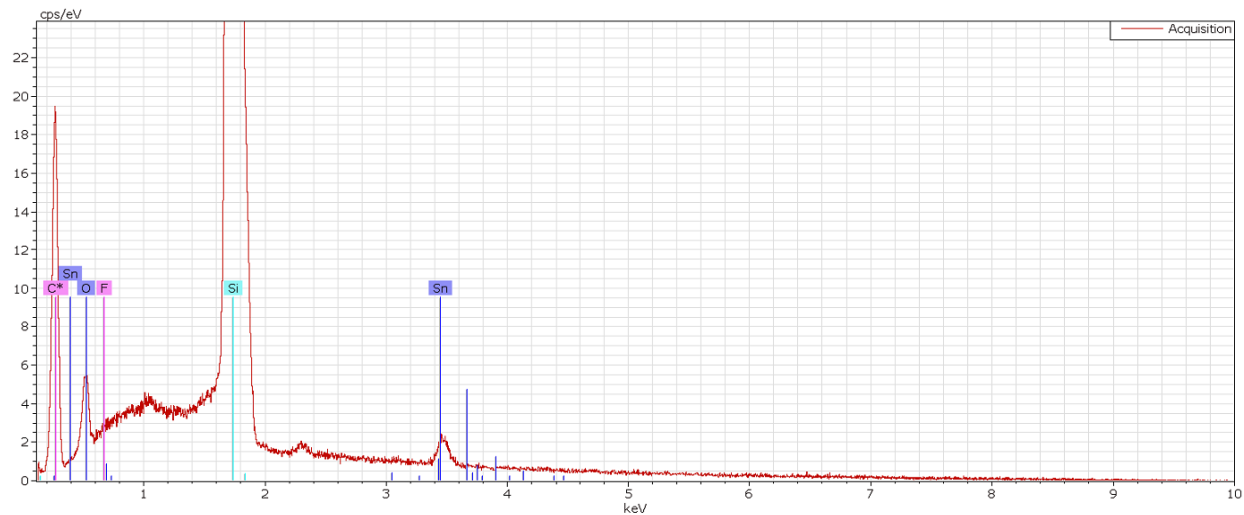


Figure 3.10. pFSPMA brush SuFEx reacted with TBDMS-propargyl alcohol.

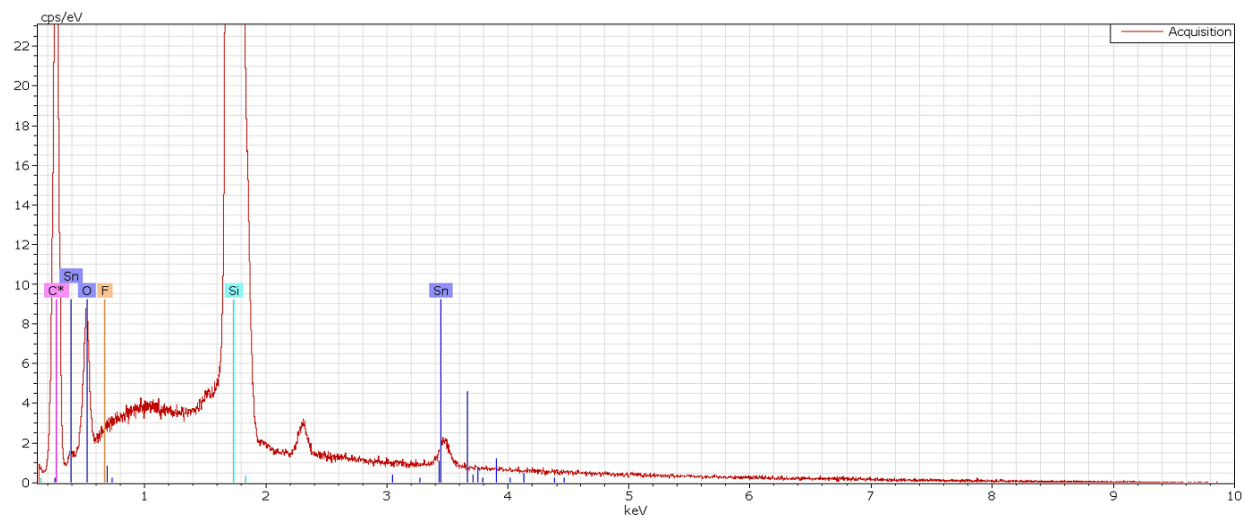


Figure 3.11. pFSPMA brush SuFEx reacted with TBDMS-furfuryl alcohol.

Results and Discussion

In order to explore SuFEx chemistry on surfaces, a sulfonyl fluoride monomer, 3-(fluorosulfonyl)propyl methacrylate (FSPMA) monomer, was synthesized in two steps from sodium 3-(methacryloyloxy)propane-1-sulfonate (Supporting Information). Next, p(FSPMA) brushes were grown from an azo-based silane initiator monolayer using radical polymerization

initiated with UV light.²⁵ Brushes of ~25 nm were grown via this method, and the solution polymer was isolated and analyzed via GPC to obtain molecular weight data in order to estimate the grafting density of the brushes (0.14 chains/nm²). The p(FSPMA) brushes demonstrated excellent reactivity with silyl ethers in the presence of certain non-nucleophilic amines, which is consistent with the SuFEx reaction in solution, albeit with some interesting differences. These brushes were then explored to examine the suitability for efficient and highly specific postpolymerization modification. Triazabicyclodecene (TBD), a new catalyst for this reaction, was also investigated for its suitability for SuFEx.

Many of the chemical functional groups involved in the most widely used click chemistries are poorly compatible with free radical polymerization conditions. These functionalities include unprotected terminal alkynes and azides for CuAAC (Cu(I) catalyzed azide/alkyne cycloaddition), thiols and alkenes for Michael addition, and dienes or dienophiles for Diels-Alder. Thiol-ene/yne chemistry, which, while not strictly a click reaction, shares several important traits such as fast kinetics and modularity, and is also not compatible with radical polymerization to high molecular weight because of chain transfer and/or cross-linking. Sulfonyl fluorides are tolerant of free radical polymerization conditions, and we also illustrate that p(FSPMA) brushes are an excellent platform to add some of these other reactive moieties to surface via easily synthesized tert-butyldimethylsilyl (TBDMS) protected alcohol precursors (Scheme 1).

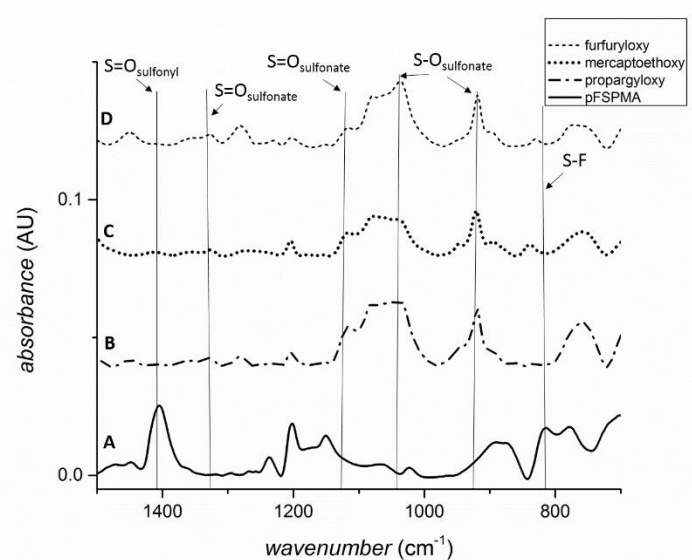


Figure 3.12. GATR-FTIR spectra of p(FSPMA) brush and PPM brushes. (A) p(FSPMA) (B) propargyloxy brush (C) mercaptoethoxy brush (D) furfuryloxy brush.

Figure 3.12 shows the grazing incidence attenuated total reflection infrared spectrum (GATR-IR) of the p(FSPMA) brushes grown via free radical polymerization along with subsequent PPM with the different TBDMS precursors shown in Scheme 1. The p(FSPMA) brushes (Figure 3.12 A) display the spectral features apparent in the monomer, such as C=O ester stretches at 1731 and 1236 cm^{-1} , symmetrical and asymmetrical S=O stretches of the sulfonyl fluoride at 1405 and 1200 cm^{-1} , and an S-F stretch at 816 cm^{-1} . After immersion in acetonitrile (MeCN) with DBU or TBD and a silyl ether protected molecule (propargyloxy-TBDMS, mercaptoethoxy-TBDMS, furfuryloxy-TBDMS, Figure 3.12 (B-D) respectively) at ambient temperature and open to atmosphere, spectral features of sulfonate ester formation appear. The S=O symmetrical stretch completely shifts to 1338 cm^{-1} , while the peaks at 1158 and 1038 cm^{-1} are assigned to the S-O stretches. Also in each case, the S-F stretch at 816 cm^{-1} disappears. We also observed the

disappearance of fluorine on the surface via electron dispersive X-ray spectroscopy (Supplemental Information).

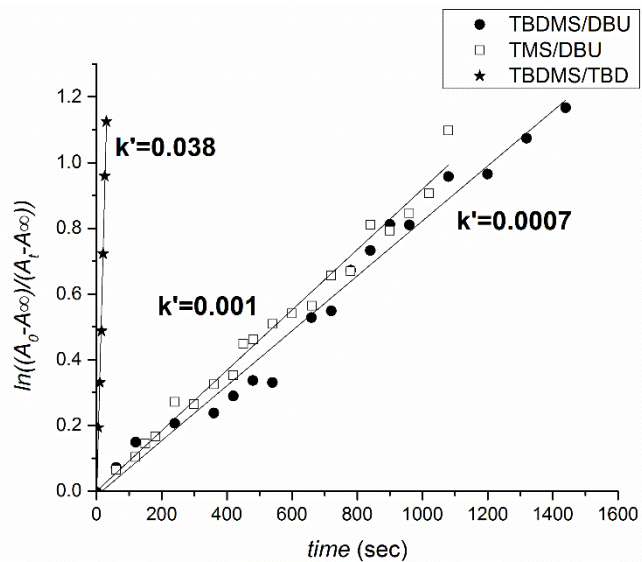


Figure 3.13. Pseudo-first order kinetic plot of the linear region of DR1-silyl ether derivatives undergoing SuFEx with p(FSPMA) brush glass substrates. (●) TMS-DR1 catalyzed by DBU (□) TBDMS-DR1 catalyzed by DBU (*) TBDMS-DR1 catalyzed by TBD.

UV-Vis data was obtained by dipping p(FSPMA) brush functionalized glass slides in solutions containing a catalyst and silyl ether protected Disperse Red 1, rinsing with good solvent, then monitoring the appearance of the Disperse Red 1 dye peak at 486 nm. These studies established that in the brush system, assuming pseudo-first order kinetics, the rates of reaction for the TMS and TBDMS protected Disperse Red 1 (DR1) in the presence of DBU were similar ($k_{TMS} = 0.001$ vs $k_{TBDMS} = 0.0007$) (Figure 2). Rate constants were obtained during the portion of the functionalization reaction where substrate absorbance increased linearly with reaction time, before steric constraints and lowered SO_2F availability changed reaction dynamics (Supporting Information). The similarity of DBU surface reaction rate constants of TMS and TBDMS derivatives contradicts other reports where the reaction is carried out in homogeneous solution,

and it was observed that SuFEx reactions with TBDMS derivatives are generally less favorable and may require heating to start the reaction.^{24,26} Also, we observed when using TBD as a catalyst, the reaction rate increased more than an order of magnitude ($k' = 0.038 \text{ s}^{-1}$) with the same TBDMS-DR1. The fact that TBD exhibits more than an order of magnitude faster SuFEx kinetics than DBU while still using the TBDMS derivative makes it a superior choice as a catalyst for SuFEx. A brush reaction rate constant of $k' = 0.038 \text{ s}^{-1}$ is comparable to the rate constant previously established for CuAAC in polymer brushes ($k' = 0.02$).²⁷ The functional group density of dye molecules on the surface after reaction completion is similar to what was obtained using activated ester brushes (3.62 dye molecules/nm³ for SuFEx vs 3.60 dye molecules/nm³ for pentafluorophenol based activated esters),²⁵ indicating that the reaction has proceeded to very high conversion.

With the much greater hydrolytic stability of the TBDMS protecting group (which can survive aqueous workup), and the high reaction rate constant in the presence of TBD, it was selected as the silyl ether protecting group of choice for surface SuFEx. Dry MeCN was used to start the experiments, but no precautions were taken to exclude air or water in any of the PPM experiments. In the interest of widening the scope of molecules that can be attached to polymer brush coatings, we used SuFEx to graft a cross-section of moieties that are suitable for additional PPM reactions. After synthesizing the TBDMS protected versions, propargyl alcohol, mercaptoethanol, and furfuryl alcohol were all successfully reacted with brush surfaces via SuFEx. Table 1 shows the increase in thickness measured via spectroscopic ellipsometry and changes in the contact angle of the substrates for each PPM, along with the GATR-IR spectra in Figure 3.12(B-D). These functionalities can then be used for subsequent PPM through CuAAC, thiol-ene/yne, thio-Michael addition, and furan/maleimide Diels-Alder cycloaddition.

Table 3.1: Thickness increases and contact angle changes after PPM of p(FSPMA) brush surfaces with reactive molecules.

Substrate coating	Thickness increase (%)	Contact angle (°)
p(FSPMA) brush (25 nm)	N/A	78
propargyloxy	38	67
mercaptoethoxy	34	15
furfuryloxy	27	83

Conclusion

The use of SuFEx to functionalize polymer brushes is simple, quantitative and proceeds with rapid reaction kinetics. In fact, in our experience, surface PPM using SuFEx is even more facile to conduct than previously reported SuFEx in homogenous solution as the reaction proceeds rapidly with TBDMS derivatives at room temperature, which are considerably more hydrolytically stable than TMS derivatives. In addition, the surface reaction requires only minute amounts of catalyst and reagent. We have also confirmed that TBD, which is a commonly available commercial ring opening polymerization catalyst, is an excellent new choice for the expedient SuFEx functionalization of brushes. Using TBD, PPM is completed in just a few minutes and should replace DBU as an economical catalyst for these reactions, and perhaps in solution SuFEx as well. Sharpless *et al.* also noted the efficacy of BEMP, an exotic, extremely powerful, highly hindered phosphazene base as a catalyst for SuFEx bulk or solution polymerization²⁶, which was not explored in this study.

The selection of highly efficient, robust, and specific chemistries available for efficient PPM of polymer brush surfaces has generally been limited to systems with oxygen sensitivity or

incompatibility with free-radical polymerization conditions (CuAAc, Diels-Alder, thio-Michael addition, and thiol-ene/yne), hydrolytic instability (activated esters), or more difficult handling or synthesis (oximes and tetrazoles). SuFEx appears to be an alternative click chemistry with a broad functionality scope, tolerance to ambient conditions, easy synthesis, and compatibility with a wide variety of reaction conditions, most notably radical polymerization. The reaction is unidirectional, fast, high yielding, and produces only highly stable silyl fluorides as a byproduct. In addition, the functional group counterparts (TBDMS ethers and sulfonyl fluorides) can coexist in a dormant state under ambient conditions until activated by the addition of a catalyst. SuFEx is highly suitable for the addition of new functionalities to polymer brush backbones, especially other click moieties, which opens a vast library of compounds that can now be attached to polymer surfaces after a single facile PPM step.

References

1. Kolb, H. C.; Finn, M. G.; Sharpless, K. B., Click Chemistry: Diverse Chemical Function from a Few Good Reactions. *Angew. Chem. Int. Ed.* **2001**, *40*, 2004-2021.
2. Kolb, H. C.; Sharpless, K. B., The growing impact of click chemistry on drug discovery. *Drug Discovery Today* **2003**, *8*, 1128-1137.
3. Espeel, P.; Du Prez, F. E., “Click”-Inspired Chemistry in Macromolecular Science: Matching Recent Progress and User Expectations. *Macromolecules* **2015**, *48*, 2-14.
4. Nandivada, H.; Jiang, X.; Lahann, J., Click Chemistry: Versatility and Control in the Hands of Materials Scientists. *Adv. Mater.* **2007**, *19*, 2197-2208.
5. Iha, R. K.; Wooley, K. L.; Nyström, A. M.; Burke, D. J.; Kade, M. J.; Hawker, C. J., Applications of Orthogonal “Click” Chemistries in the Synthesis of Functional Soft Materials. *Chem. Rev.* **2009**, *109*, 5620-5686.
6. Sumerlin, B. S.; Vogt, A. P., Macromolecular Engineering through Click Chemistry and Other Efficient Transformations. *Macromolecules* **2010**, *43*, 1-13.
7. Nair, D. P.; Podgórski, M.; Chatani, S.; Gong, T.; Xi, W.; Fenoli, C. R.; Bowman, C. N., The Thiol-Michael Addition Click Reaction: A Powerful and Widely Used Tool in Materials Chemistry. *Chem. Mater.* **2014**, *26*, 724-744.
8. Hawker, C. J.; Fokin, V. V.; Finn, M. G.; Sharpless, K. B., Bringing Efficiency to Materials Synthesis: The Philosophy of Click Chemistry. *Aust. J. Chem.* **2007**, *60*, 381-383.
9. Barner-Kowollik, C.; Inglis, A. J., Has Click Chemistry Lead to a Paradigm Shift in Polymer Material Design? *Macromol. Chem. Phys.* **2009**, *210*, 987-992.

10. Barner-Kowollik, C.; Du Prez, F. E.; Espeel, P.; Hawker, C. J.; Junkers, T.; Schlaad, H.; Van Camp, W., “Clicking” Polymers or Just Efficient Linking: What Is the Difference? *Angew. Chem. Int. Ed.* **2011**, *50*, 60-62.

11. Senaratne, W.; Andruzzi, L.; Ober, C. K., Self-Assembled Monolayers and Polymer Brushes in Biotechnology: Current Applications and Future Perspectives. *Biomacromolecules* **2005**, *6*, 2427-2448.

12. Murata, H.; Prucker, O.; Rühe, J., Synthesis of Functionalized Polymer Monolayers from Active Ester Brushes. *Macromolecules* **2007**, *40*, 5497-5503.

13. Orski, S. V.; Fries, K. H.; Sheppard, G. R.; Locklin, J., High Density Scaffolding of Functional Polymer Brushes: Surface Initiated Atom Transfer Radical Polymerization of Active Esters. *Langmuir* **2010**, *26*, 2136-2143.

14. Xu, L. Q.; Wan, D.; Gong, H. F.; Neoh, K.-G.; Kang, E.-T.; Fu, G. D., One-Pot Preparation of Ferrocene-Functionalized Polymer Brushes on Gold Substrates by Combined Surface-Initiated Atom Transfer Radical Polymerization and “Click Chemistry”. *Langmuir* **2010**, *26*, 15376-15382.

15. Gevrek, T. N.; Bilgic, T.; Klok, H.-A.; Sanyal, A., Maleimide-Functionalized Thiol Reactive Copolymer Brushes: Fabrication and Post-Polymerization Modification. *Macromolecules* **2014**, *47*, 7842-7851.

16. Dübner, M.; Gevrek, T. N.; Sanyal, A.; Spencer, N. D.; Padeste, C., Fabrication of Thiol-Ene “Clickable” Copolymer-Brush Nanostructures on Polymeric Substrates via Extreme Ultraviolet Interference Lithography. *ACS Appl. Mater. Interfaces* **2015**, *7*, 11337-11345.

17. de los Santos Pereira, A.; Kostina, N. Y.; Bruns, M.; Rodriguez-Emmenegger, C.; Barner-Kowollik, C., Phototriggered Functionalization of Hierarchically Structured Polymer Brushes. *Langmuir* **2015**, *31*, 5899-5907.

18. Hensarling, R. M.; Doughty, V. A.; Chan, J. W.; Patton, D. L., “Clicking” Polymer Brushes with Thiol-yne Chemistry: Indoors and Out. *J. Am. Chem. Soc.* **2009**, *131*, 14673-14675.

19. Golas, P. L.; Matyjaszewski, K., Marrying click chemistry with polymerization: expanding the scope of polymeric materials. *Chem. Soc. Rev.* **2010**, *39*, 1338-1354.

20. Rahane, S. B.; Hensarling, R. M.; Sparks, B. J.; Stafford, C. M.; Patton, D. L., Synthesis of multifunctional polymer brush surfaces via sequential and orthogonal thiol-click reactions. *J. Mater. Chem.* **2012**, *22*, 932-943.

21. Arnold, R. M.; Patton, D. L.; Popik, V. V.; Locklin, J., A Dynamic Duo: Pairing Click Chemistry and Postpolymerization Modification To Design Complex Surfaces. *Acc. Chem. Res.* **2014**, *47*, 2999-3008.

22. Dong, J.; Krasnova, L.; Finn, M. G.; Sharpless, K. B., Sulfur(VI) Fluoride Exchange (SuFEx): Another Good Reaction for Click Chemistry. *Angew. Chem. Int. Ed.* **2014**, *53*, 9430-9448.

23. Huheey, J. E.; Keiter, E. A.; Keiter, R. L., Inorganic chemistry: principles of structure and reactivity. *Harper and Raw, New York* **1983**.

24. Gembus, V.; Marsais, F.; Levacher, V., An Efficient Organocatalyzed Interconversion of Silyl Ethers to Tosylates Using DBU and p-Toluenesulfonyl Fluoride. *Synlett* **2008**, *2008*, 1463-1466.

25. Arnold, R. M.; Sheppard, G. R.; Locklin, J., Comparative Aminolysis Kinetics of Different Active Ester Polymer Brush Platforms in Postpolymerization Modification with Primary and Aromatic Amines. *Macromolecules* **2012**, *45*, 5444-5450.

26. Dong, J.; Sharpless, K. B.; Kwisnek, L.; Oakdale, J. S.; Fokin, V. V., SuFEx-Based Synthesis of Polysulfates. *Angew. Chem. Int. Ed.* **2014**, *53*, 9466-9470.

27. Orski, S. V.; Sheppard, G. R.; Arumugam, S.; Arnold, R. M.; Popik, V. V.; Locklin, J.,
Rate Determination of Azide Click Reactions onto Alkyne Polymer Brush Scaffolds: A
Comparison of Conventional and Catalyst-Free Cycloadditions for Tunable Surface Modification.
Langmuir **2012**, *28*, 14693-14702.

CHAPTER 4

MULTIFUNCTIONAL SURFACE MANIPULATION USING ORTHOGONAL CLICK
CHEMISTRY ¹

¹ Yatvin, J.*; Brooks, K.*; McNitt, C. D.; Reese, R. A.; Jung, C.; Popik, V. V.; and Locklin, J. 2016. *Langmuir*. 32:6600-6605.

Reprinted with permission from publisher.

*Authors contributed equally to this work

Abstract

Polymer brushes are excellent substrates for the covalent immobilization of a wide variety of molecules due to their unique physicochemical properties and high functional group density. By using reactive microcapillary printing, poly(pentafluorophenyl acrylate) brushes with rapid kinetic rates toward aminolysis can be partially patterned with other click functionalities such as strained cyclooctyne derivatives and sulfonyl fluorides. This tri-reactive surface can then react locally and selectively in a one pot reaction via three orthogonal chemistries at room temperature: activated ester aminolysis, strain promoted azide-alkyne cycloaddition, and sulfur(VI) fluoride exchange, all of which are tolerant of ambient moisture and oxygen. Furthermore, we demonstrate that these reactions can also be used to create areas of morphologically distinct surface features on the nanoscale, by inducing buckling instabilities in the films and the grafting of nanoparticles. This approach is modular, and allows for the development of highly complex surface motifs patterned with different chemistry and morphology.

Introduction

The ability to pattern synthetic and biological molecules is useful for designing model surfaces to observe cell-surface interactions.¹⁻³ For instance, the growth of different tissues, such as bone,⁴ or neurons,⁵ can be guided and studied using patterned surfaces, which is critical in establishing structure/property relationships in the field of tissue engineering.^{6, 7} Such surfaces are also attractive for integration into multifunctional bio-sensors, which can be used to monitor biological responses from complex mixtures such as physiological fluids.⁸ In addition to the chemical content of a surface, the modulus⁹ and the micro- and nanomorphology of a surface coating have immense impact on the interactions between a live cell and a surface.^{10,11} Ultimately, with greater control of the spatial, chemical, and morphological complexity of synthetic surfaces, one can begin to mimic biological surfaces such as cell membranes and extracellular matrices.¹²⁻¹⁵

Reactive polymer brush coatings have become a common platform for the addition of densely packed chemical functionalities onto surfaces through post-polymerization modification, with click-type reactions being especially promising due to their fast kinetics, quantitative yields, and lack of side-reactions.¹⁶⁻¹⁸ The specificity inherent in click reactions also allows for the covalent addition of chemistries to the surface in an orthogonal manner from a complex mixture of components in solution. By employing different click reactions in localized areas of a substrate, a surface can be patterned with a variety of chemically distinct molecules.¹⁹⁻²³

In this work, three different surface chemistries have been used to pattern substrates in an orthogonal fashion: aminolysis of activated esters, strain promoted azide-alkyne cycloaddition (SPAAC), and silyl ether sulfur-fluoride exchange (SuFEx).^{20, 24-26} These reactions are premier click-type reactions that can all be performed under ambient conditions with rapid rates at room temperature, do not utilize metal catalysts, and produce zero or only innocuous by-products. By

using reactive microcapillary printing (R- μ CaP),²⁰ a highly adaptable and simple patterning technique, to add the initial SuFEx and SPAAC functionalities to the surface by aminolysis, tri-functional surfaces can easily be fabricated with high fidelity.

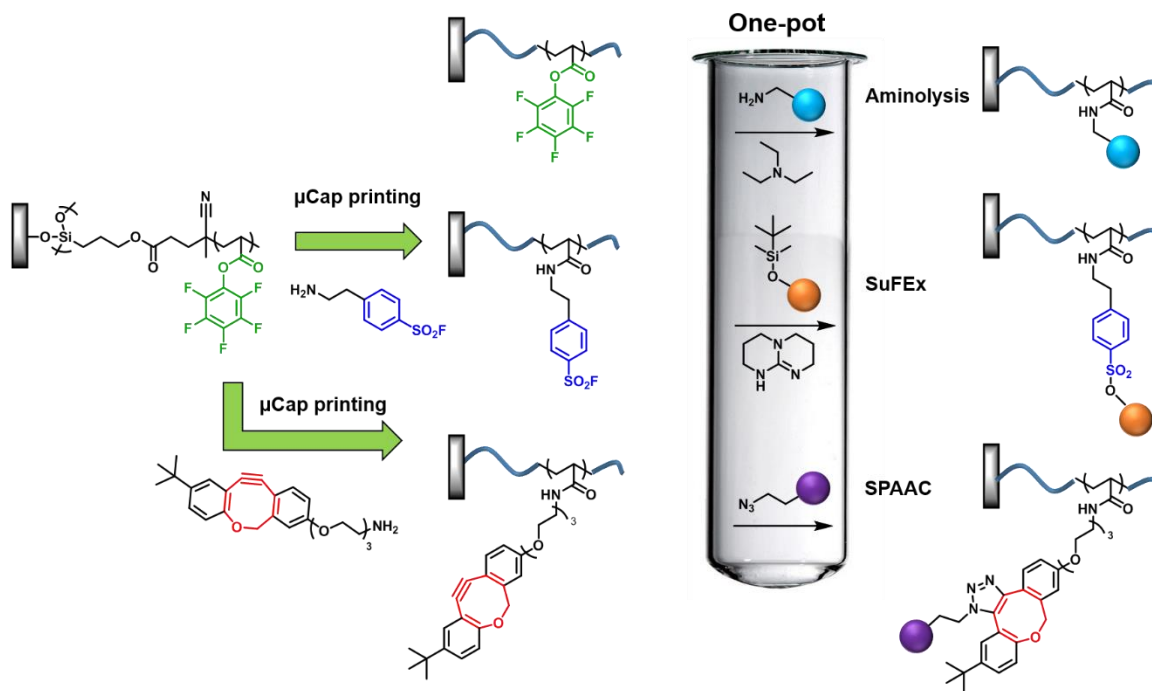


Figure 4.1. Reaction scheme for the formation of a tri-reactive surface, followed by the addition of 3 different molecules to the surface.

To illustrate the versatility of this method, two different types of tri-functional surfaces have been prepared. The first utilizes three different dyes to illustrate the high resolution of R- μ CaP functionalization, orthogonal reactivity, and the quantitative attachment of three different dye molecules to the surface from one solution (Figure 4.1). The second example uses reactive nanoparticles and stress-induced creasing with a reactive polymer to create three distinct morphological subdivisions on the surface.²⁷ For each tri-reactive substrate, the surface contains pentafluorophenyl acrylate (PFPA), oxa-dibenzocyclooctyne (ODIBO),²⁸ and an aryl sulfonyl

fluoride (PEFABLOC), which can undergo aminolysis, SPAAC, and SuFEx on the surface, respectively. The click functionality counterparts to these surface moieties (amines, azides, and silyl ethers) are easily accessible as commercial compounds or through straightforward synthesis from a variety of biological or synthetic substrates.

Experimental Section

Materials: Silicon wafers (orientation <100>, native oxide) were purchased from University Wafer. Jeffamine M-2070 was provided as a gift by Huntsman Chemical. All organic solvents were dried and freshly distilled before use. Tetrahydrofuran was distilled from sodium/benzophenone ketyl and dichloromethane was distilled from CaH_2 . Other reagents were obtained from Sigma-Aldrich, TCI, or VWR and used as received unless noted. Flash chromatography was performed using 40-63 μm silica gel. All NMR spectra were recorded in CDCl_3 unless otherwise noted using both 300 and 400 MHz instruments.

Polymer Brush Fabrication: PFPA was synthesized following previously reported methods.²⁹ It was further purified using a plug of neutral alumina with DCM as eluent to remove any residual acrylic acid. The AIBN-silane initiator was also prepared using previously reported methods and, after synthesis, stored immediately in an inert atmosphere glovebox.²⁶ Silicon wafers and glass microscope slides were cut using a diamond scribe and cleaned by sonication in hexanes, isopropyl alcohol, acetone, and deionized water for 1 min each. The slides were then cleaned using argon plasma for 5 min (Harrick Plasma PDC-32G) and subsequently placed in a slide stainer and transferred to an inert atmosphere glovebox (MBraun Labstar). A 10 mM solution of the AIBN-silane initiator was prepared in 20 mL of dry toluene in a scintillation vial. The vial was shaken vigorously to ensure full dissolution of the initiator and added to the slide stainer for 16 h. After 16 h, the initiator solution was removed and replaced with fresh toluene for storage until use. PFPA

was degassed by bubbling argon through a needle at 0 °C and transferred to an inert atmosphere glovebox. An initiator substrate was sonicated in fresh toluene to remove any physisorbed material. The substrate was then dried under a stream of nitrogen, cut into smaller pieces, and placed 10 mL vials, and transferred back into the glovebox. To the vials, 71.6 µL of dry dioxane and 291.4 µL of PFPA were added and subsequently Teflon taped and capped. The vials were removed and placed in a UV reactor for 2 h. After 2 h, the vials were removed from UV irradiation and sonicated in THF to remove the substrate from the glassy polymer formed. The glassy polymer was saved for subsequent analysis via gel permeation chromatography. Gel permeation chromatography (GPC) was conducted on a liquid chromatograph (Shimadzu LC-20AD series) equipped with a RID-10A refractive index detector. Polymer samples were diluted in a THF mobile phase and passed through three Phenomenex Phenogel (10E3A, 10E4A, and 10E5A) columns at 40 °C under a constant volumetric flow rate (1 mL min⁻¹). Molecular weight characteristics of the samples were referenced to polystyrene standards (Agilent Technologies EasiCal PS-2).

PDMS Stamp Fabrication: PDMS was made using the SYLGARD 184 silicone elastomer kit from Dow Corning. Microfluidic masks were designed on AutoCAD (Autodesk, Inc., San Rafael, CA) and printed on transparencies at 20000 dpi by CAD/Art services, Inc. (Bandon, ORD).

Individual Substrate Fabrication: Poly(PFPA) brushes on silicon wafers were functionalized in 40 mM solutions of 1-aminomethyl pyrene, ODIBO-amine, and PEFABLOC for 1 h in DMF with 80 mM of triethylamine. The substrates were then removed, rinsed vigorously with DMF, dried under a stream of nitrogen, and characterized via spectroscopic ellipsometry, drop shape analysis, and FTIR. The substrates functionalized with ODIBO-amine and PEFABLOC were then placed in 13 mmol Texas Red azide in 2 mL DMF and 0.1 mmol TBDMS-fluorescein methyl ester with 0.02 mmol TBD in 2 mL DMF respectively for 30 min. After 30 min, the slides were removed,

washed with DMF, dried under a stream of nitrogen, and characterized via spectroscopic ellipsometry, drop shape analysis, and FTIR.

UV/Vis Kinetic Traces: PEFABLOC brush functionalized glass slides were measured on a UV-Vis spectrometer using a slide holder accessory with a sample window area of 19.6 mm². The functionalized slide was immersed in a solution of 0.1 mmol TBDMS fluorescein methyl ester silyl ether (the solution is saturated at this concentration) and 0.02 mmol TBD in 2 mL MeCN for a predetermined amount of time. The slides were rinsed thoroughly with DMF and DCM prior to each measurement. The rate of substitution of fluorescein methyl ester onto the polymer brush was measured by monitoring the appearance of the dye peak with time, and a kinetic plot was generated using the linear portion of the absorbance plot. This procedure was repeated on poly(PFPA) brush with 40 mM 1-aminomethylpyrene with 80 mM triethylamine in DMF and again on an ODIBO brush with 4 mM azido-Disperse Red 1 in DMF.

Synthesis of ODIBO-amine:

ODIBO-amine was prepared by the Popik lab and the procedure is available in the Supplementary information of the submitted paper.

Fluorescein TBDMS Synthesis

Fluorescein methyl ester: Adapted from Adamczyk *et al.*²⁸ 2 g (5.3 mmol) of fluorescein sodium salt was suspended in 6 mL of MeOH at 0° C. 1.5 mL sulfuric acid was added slowly, then an addition funnel containing 3Å molecular sieves and a condenser were attached to the apparatus and the solution heated to reflux overnight. 15 mL of saturated NaHCO₃ was slowly added, and the resultant suspension filtered and rinsed with water. The orange powder was dried on high-vac for 1 hr at 110°C to give 0.8 g (43% yield) of red-orange powder. ¹H NMR (300 MHz, CDCl₃)

δ =8.28 (d, J = 7.5 Hz, 1H), 7.83 – 7.66 (m, 2H), 7.38 – 7.23 (m, 1H), 7.15 – 7.04 (m, 4H), 6.94 (d, J = 9.5 Hz, 2H), 3.61 (s, 3H).

TBDMS Fluorescein methyl ester: 0.200 g (0.46 mmol) of fluorescein methyl ester was suspended in 12 mL dry MeCN. 0.110 g (1.61 mmol) imidazole and 0.083 g (0.55 mmol) TBDMS-Cl was added and the reaction stirred at 50° C overnight. The next morning the MeCN was removed by evaporation and DCM was added. The DCM layer was washed twice with water, dried with MgSO₄, then the compound was concentrated in vacuo to give 95 mg (45% yield) of red-orange solid. ¹H NMR (300 MHz, CDCl₃) δ =8.25 (d, J = 7.6 Hz, 1H), 7.78 – 7.62 (m, 2H), 7.32 (d, J = 7.5 Hz, 1H), 6.95 (d, J = 9.2 Hz, 2H), 6.87 (s, 1H), 6.77 (d, J = 9.3 Hz, 2H), 3.62 (s, 3H), 0.91 (s, 9H), 0.08 (s, 6H). ¹³C NMR (75 MHz, CDCl₃) δ =175.99, 165.58, 157.78, 134.25, 132.62, 131.10, 130.46, 130.34, 129.82, 122.33, 120.75, 114.48, 103.46, 52.43, 29.94, 25.64, -3.59.

11-azidoundecanoic acid Synthesis: 11-azidoundecanoic acid: 2 g of 11-bromoundecanoic acid was added to 5 mL of DMF. NaN₃ was added and the solution turned orange. Reaction was stirred at 60° C overnight then room temperature for two days. DCM was added and the solution was extracted 4x with water then concentrated in vacuo to give 0.65 g (76% yield) of clear oil. ¹H NMR (300 MHz, CDCl₃) δ =3.25 (t, J = 6.9 Hz, 2H), 2.34 (t, J = 7.5 Hz, 2H), 1.69 – 1.50 (m, 4H), 1.40 – 1.20 (m, 12H).

Tri-Patterned Surface Fabrication: Using a poly(PFPA) brush grafted-from silicon dioxide by surface initiated radical photopolymerization described above, 2 μ L of 40 mM ODIBO-amine in DMF with 80 mM triethylamine (TEA) was printed using via micro-capillary printing (μ -CaP) using 100 μ m channels. The solution was allowed to evaporate fully. The PDMS stamp was then removed, washed with DMF, and dried under a stream of nitrogen. 40 mM of PEFABLOC in DMF

with 80 mM TEA was printed perpendicular to the printed ODIBO-amine via μ -CaP. The solution was allowed to evaporate, and then the stamp was removed, washed with DMF, and dried under a stream of nitrogen. The slide was then placed in a solution containing 0.006 mmol AMP, 0.012 mmol TEA, 0.1 mmol fluorescein-TBDMS, 0.02 mM TBD, and 9.8×10^{-4} mmol Texas Red azide for 30 minutes in 450 μ L of dry DMF. After 30 minutes, the substrate was washed and sonicated in DMF and dried under a stream of nitrogen. The substrate was then characterized via fluorescence microscopy.

Nanoparticle Synthesis: Azide coated iron oxide nanoparticles: Octadecene coated nanoparticles were prepared by thermal decomposition according to the procedure of Cowger *et al.*³⁰ 1 mL of the crude reaction mixture was dissolved in 3 mL of hexane then added to 20 mL of EtOH, and centrifuged down at 4400 rpm. The supernatant was decanted and the process repeated 2x to yield purified octadecene coated iron oxide nanoparticles. The purified particles were dissolved in 2 mL DCM, and 50 μ L of 11-azidoundecanoic acid was added. The reaction was shaken thoroughly then allowed to sit for 3 days. After ligand exchange, 20 mL of MeOH was added, and the particles centrifuged down at 4400 rpm. The supernatant was decanted and the process repeated 2x to yield purified 11-azidoundecanoic acid coated iron oxide nanoparticles. The presence of the azide peak at 2099 cm^{-1} was confirmed by FTIR.

Tri-Morphological Surface. A grafted from poly(PFPA) brush on silicon was patterned with ODIBO and PEFABLOC. The substrate was then placed in a vial containing azide-functionalized iron nanoparticles in DCM for 5 minutes and continuously shaken. After 5 minutes, the substrates were removed, vigorously washed with DCM, and dried under nitrogen. The substrate was then increased using a PDMS stamp and Jeffamine M-2070 using our previously reported methods.²⁷

Characterization. Fluorescent images were taken using a Nikon Eclipse NI-U, using a 10x objective lens. The filter set used were a DAPI filter set (395/460), GFP filter set (488/509), and a red filter set (560/590) for AMP, fluorescein, and Texas Red, respectively. The wrinkled morphologies of the substrates were collected using the Scanasyst program on Bruker Multimode AFM (Scanasyst-AIR, $k = 0.4$ N/m, resonant frequency (f_0) = 50-90 kHz Nanoscope Analysis Software (Bruker) was used to analyze the nanoparticle topography images. The infrared spectra of the substrates were taken using a Nicolet model 6700 with a grazing angle attenuated total reflectance accessory at 256 scans with a 4 cm^{-1} resolution. The thicknesses of the polymer brushes were measured using a M-2000 spectroscopic ellipsometer (J.A. Woollam Co., Inc.) with a white light source at three angles of incidence (65° , 70° , and 75°) to the silicon wafer normal. The data were modeled using a Cauchy layer fitting both the extinction coefficient and refractive index for the polymer brush layer. Contact angle measurements were collected using Krüss DSA 100 using a $1\text{ }\mu\text{L}$ drop of $18\text{ m}\Omega$ water ($\text{pH}=7$) and averaging the results over three experiments. Raman spectra of the three distinctly functionalized regions were acquired using a confocal Raman microscope (InVia, Renishaw, Inc., Gloucestershire, United Kingdom). A 632.8 nm HeNe laser excited the sample through a 50x objective (N.A.=0.75) with $\sim 3.1\text{ mW}$ of power (as measured at the sample). The resulting spot size had a diameter of $1\text{-}2\text{ }\mu\text{m}$. Spectra between 3100 and 1000 cm^{-1} were acquired with a 30s acquisition time and 10 accumulations.

Results and Discussion

As a base layer, poly(PFPA) brushes were synthesized by surface initiated photopolymerization from azo-initiator containing silane monolayers using previously reported

methods on Si/SiO₂ substrates with an average thickness of 48.9 nm and a grafting density of 0.093 chains/nm².²⁶ Each post-polymerization modification reaction was first carried out on individual substrates to both ensure full functionalization and to characterize the rate and extent of each reaction individually. The poly(PFPA) brushes were reacted with a solution containing 40 mM 4-(2-Aminoethyl)benzenesulfonyl fluoride hydrochloride (PEFABLOC) in DMF with 80 mM TEA and 40 mM ODIBO-amine in DMF with 80 mM TEA. The substrates were removed and washed with DMF, dried under a stream of nitrogen, and characterized via spectroscopic ellipsometry, drop shape analysis, and grazing incidence attenuated total reflectance Fourier transform infrared spectroscopy (GATR-FTIR). A change in thickness and contact angle occurred for each substrate, and are reported in Table 4.1.

Table 4.1. Thicknesses and Contact Angles of Individual PEFABLOC, ODIBO-amine, and Poly(PFPA) Substrates Before and After Functionalization and Reaction with Fluorescent Dye

	poly(PFPA) brush	reactive molecule	dye
AMP	47.13 nm, 118.0°	-	163.54 nm, 86.5°
PEFABLOC	44.49 nm, 116.1°	90.26 nm, 100.0°	244.79 nm, 90.4°
ODIBO	55.20 nm, 120.9°	262.46 nm, 91.3°	407.72 nm, 87.2°

The FTIR spectra also indicated full conversion, resulting in the loss of the characteristic PFPA C=O ester stretch at 1785 cm⁻¹ and C-C aromatic stretch at 1523 cm⁻¹ as well as the appearance of amide peaks at 1640 cm⁻¹ and 1540 cm⁻¹ in each spectra (Figure 4.2). Once the individual functionalizations were confirmed, a patterned surface combining the two reactions outlined above was fabricated. To generate a patterned tri-reactive surface, R-μCaP was performed on the

poly(PFPA) brush.²⁰ PDMS stamps with 250 μm channels were fabricated using conventional lithographic methods, sonicated in acetone, dried in a vacuum oven at 45°C, and further cleaned using Scotch tape. The stamps were placed directly on the brushes and 2 μL of 40 mM of ODIBO-amine in DMF with 80 mM TEA was wicked into the channels by capillary action. The solvent was allowed to evaporate, and the stamp was removed. Another PDMS stamp was then placed perpendicular to the initial pattern, and 2 μL of 40 mM solution of PEFABLOC was wicked into the stamp. The solvent was again allowed to evaporate, and the stamp was removed from the substrate, resulting in a surface that contained ODIBO (strained alkyne), PEFABLOC (sulfonyl fluoride), and activated ester functionality in a checkerboard pattern. To confirm the fidelity of the process, Raman spectroscopy was taken in each region using a Raman microscope (Figure 4.3). The spectra obtained in each area of the slide resulted in characteristic peaks for each reactive group. In the ODIBO-functionalized region, peaks were observed at 3067 cm^{-1} corresponding to the C-H aromatic, 2151 cm^{-1} (C≡C alkyne), 1605 cm^{-1} and 1564 cm^{-1} (C=C aromatic) were observed. In the PEFABLOC region, peaks were observed at 3061 cm^{-1} (C-H aromatic), 1597 cm^{-1} (C=C aromatic), and 1376 cm^{-1} (S=O). Finally, in the PFPA region, peaks were observed at 1788 cm^{-1} and 1652 cm^{-1} , corresponding to the C=O and C=C aromatic stretches. These characteristic peaks for each functionality were not observed in the other areas of the substrate, indicating reasonable fidelity with no indication of cross-contamination.

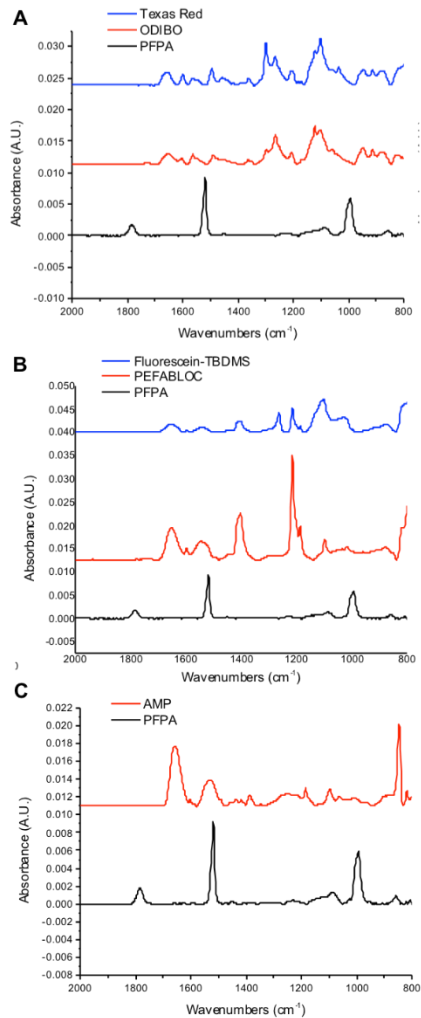


Figure 4.2. Infrared spectra of poly(PFPA) brushes functionalized with (A) ODIBO-amine, (B) PEFABLOC, and (C) AMP as well as ODIBO-amine clicked with Texas Red azide and PEFABLOC clicked with TBDMS fluorescein methyl ester.

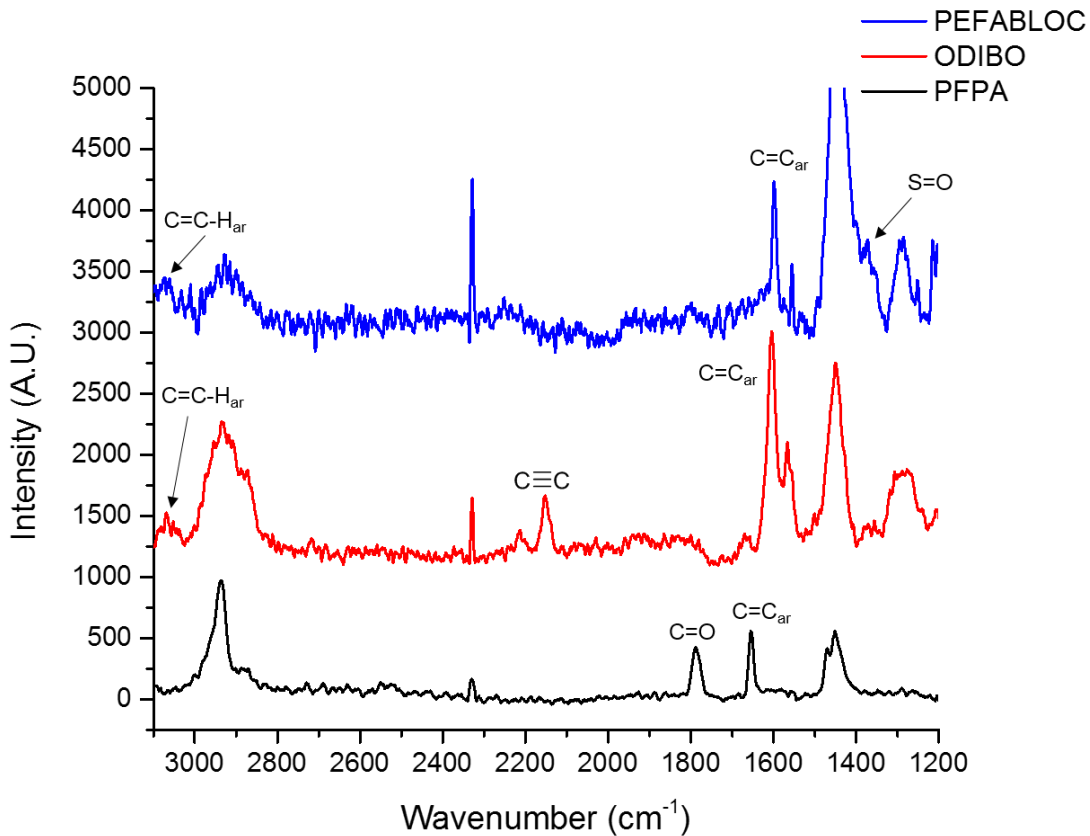


Figure 4.3. Raman spectra of the, poly(PFPA) (black), ODIBO (red) and PEFABLOC (blue) areas on a tri-reactive surface.

To further confirm the fidelity and orthogonal reactivity of these surface patterns, dyes containing the complementary click functionality were used to generate patterns that could be characterized using fluorescence microscopy. Individual reactions with dyes were first carried out on functionalized brushes and subsequently characterized via GATR-IR and DSA to confirm quantitative conversion. Individual ODIBO and PEFABLOC slides were clicked via SPAAC with Texas Red azide and SuFEx with a TBDMS fluorescein methyl ester, using a triazabicyclodecene (TBD) catalyst. Also, a poly(PFPA) brush slide was functionalized 40 mM aminomethylpyrene (AMP) with 80 mM TEA in 2 mL DMF with stirring. After 30 minutes, the substrates were washed with DMF, dried under a stream of nitrogen, and characterized. The contact angles, thicknesses,

and FTIR spectra reveal successful and near-quantitative conversions for both reactions (Table 4.1; Figure 4.2). Each dye reaction was allowed to stir for thirty minutes due to the observed kinetics of the reaction of an aryl sulfonyl fluoride and an aryl TBDMS derivative, which has a pseudo-first order rate constant of $k' = 0.0014 \text{ s}^{-1}$ (Figure 1A), an order of magnitude slower than the $k' = 0.04 \text{ s}^{-1}$ observed between alkyl sulfonyl fluorides and an

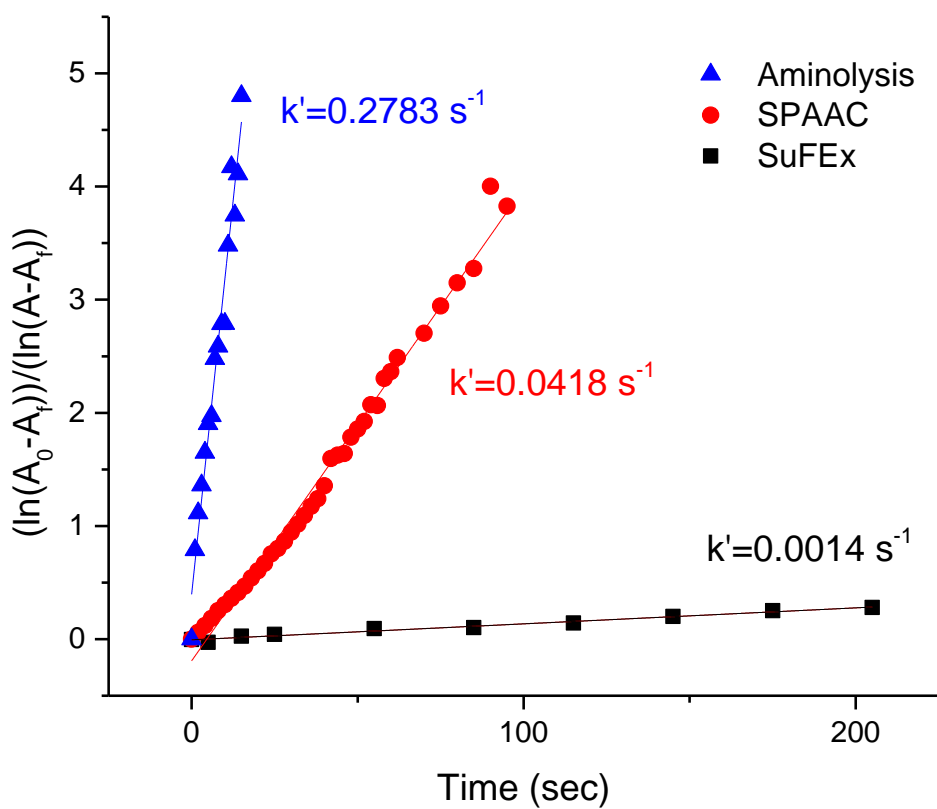


Figure 4.4. Pseudo-first order kinetic plots of aminolysis (blue),²⁶ SPAAC (red), and aryl silyl ether SuFEx (black) are shown.

alkyl TBDMS derivative in our previous work.²⁵ Although SPAAC ($k' = 0.0418 \text{ s}^{-1}$) and aminolysis ($k' = 0.2783 \text{ s}^{-1}$) are faster reactions, to closely mimic the one-pot orthogonal reaction with the tri-reactive surface, each slide was placed in the respective dye solution for a full thirty minutes. Since sulfonyl fluorides are known to react with amines at raised temperatures, a PEFABLOC functionalized surface was immersed in an AMP/TEA solution, where no functionalization with AMP was observed.

The true orthogonality of the surface chemistries was demonstrated using a one-pot, self-sorting reaction for post-polymerization modification. A tri-reactive surface was placed in a vial containing AMP, triethylamine (TEA), Texas Red azide, TBDMS fluorescein methyl ester, and TBD in 450 μL of DMF. The substrate was allowed to react for 30 minutes with agitation. It was then removed, washed thoroughly with DMF, and dried under stream of nitrogen. The patterned surface was then examined under a fluorescent microscope (Nikon Eclipse NI-U; 10x), using DAPI filter set (395/460), GFP filter set (488/509), and a red filter set (560/590) to excite AMP, fluorescein, and Texas Red, respectively. The obtained fluorescent images are shown in Figure 4.5. Figure 4.4A was obtained using the DAPI filter set and reveals the AMP derivatization; Figure 4.5B was obtained using the red filter set, where Texas Red is observed; and Figure 4.5C is the image obtained using the GFP filter set, which reveals the fluorescein substitution. Fluorescence in the AMP region was also observed using the GFP filter set likely due to the fact that densely packed AMP molecules lead to excimer formation.²⁹¹ Excimers occur in pyrene-containing materials as a result of a ground state pyrene ring and an excited state pyrene ring in close proximity forming an excited state dimer. In this system, the AMP functionalized polymer brushes are densely packed, resulting in conditions that promote excimer formation, which is observed at 484 nm.³⁰² A superposition of the images, shown in Figure 4.45, illustrates three distinct regions

with no noticeable cross-contamination, which corroborates the data obtained using Raman spectroscopy and demonstrates that sequential R- μ CaP results in a patterned surface that self-sorts with high fidelity.

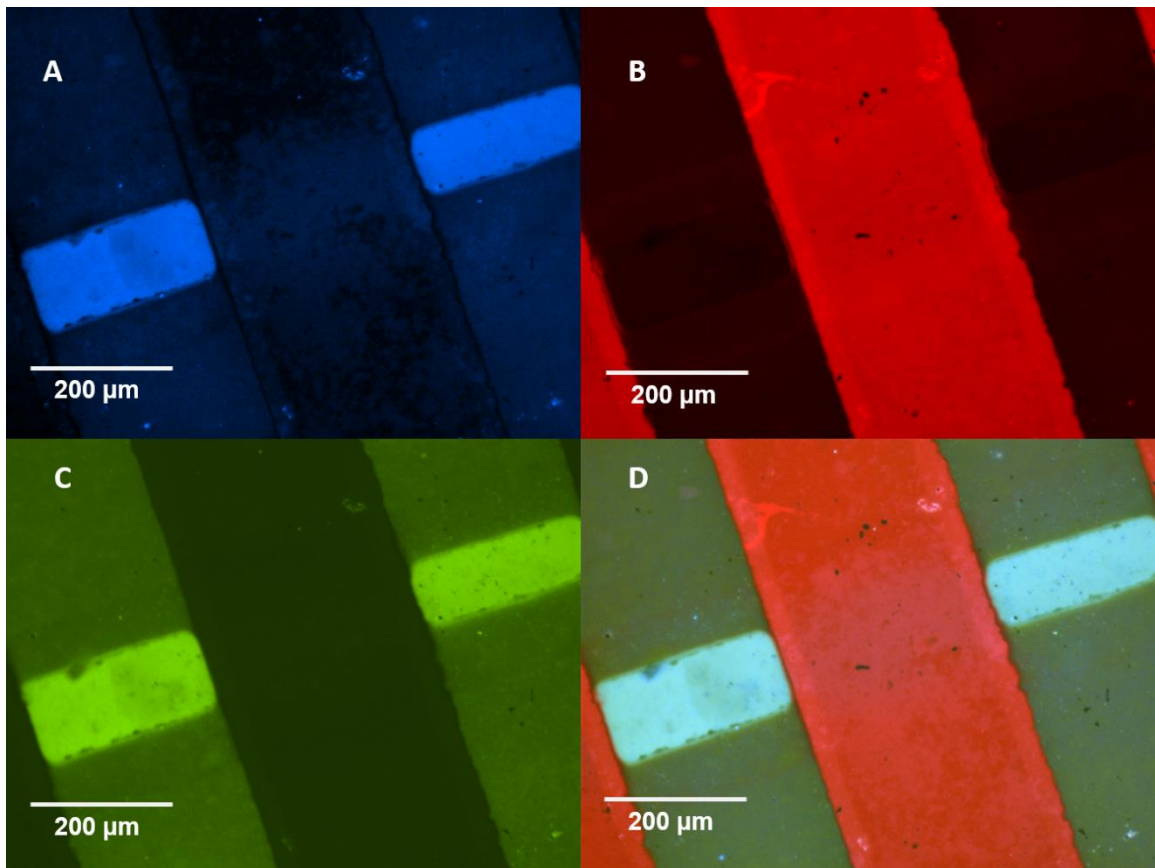


Figure 4.5. Fluorescence microscopy images for the tri-functional surface of AMP, Texas Red Azide, and TBDMS fluorescein methyl ester: (A) DAPI filter set (395/460) exciting AMP, (B) red filter set (560/590) exciting Texas Red, (C) GFP filter set (488/509), and (D) combined image of all three filter sets.

To further expand the utility of this technique, a surface with patterned morphologies was fabricated using a tri-reactive template. The tri-reactive surface, fabricated in the same fashion described above, was placed in a vial of azide-functionalized iron oxide nanoparticles (~20 nm) in DCM for 5 minutes with constant stirring. After 5 minutes, the substrate was washed with DCM

and dried under a stream of nitrogen. Then, using micro-contact printing (μ CP) with Jeffamine-M2070 (40 mM in toluene with 80 mM TEA), creases were generated in the remaining PFPA area of the pattern using our recently reported method.²⁷ Analysis was then performed using atomic force microscopy (AFM) (Bruker ScanAssyst) which is shown in Figure 4.6. Figure 4.6A shows the topography of the PFPA brush, which was creased using μ CP under confinement.²⁷ In Figure 4.6B, the azide-functionalized nanoparticles were observed only in the ODIBO-functionalized channel region. The average diameter of the surface bound nanoparticles (21.96 nm) is consistent with the diameter of the source particles. Finally, in Figure 4.6C, the PEFABLOC channel is shown, where a smooth, featureless morphology with a RMS roughness of 3.55 nm was observed, containing neither nanoparticle or crease contaminants. To our knowledge, this is the first example of using click chemistry to generate three distinct nanoscale morphologies using orthogonal post-polymerization, without cross-contamination or lithographic methods.

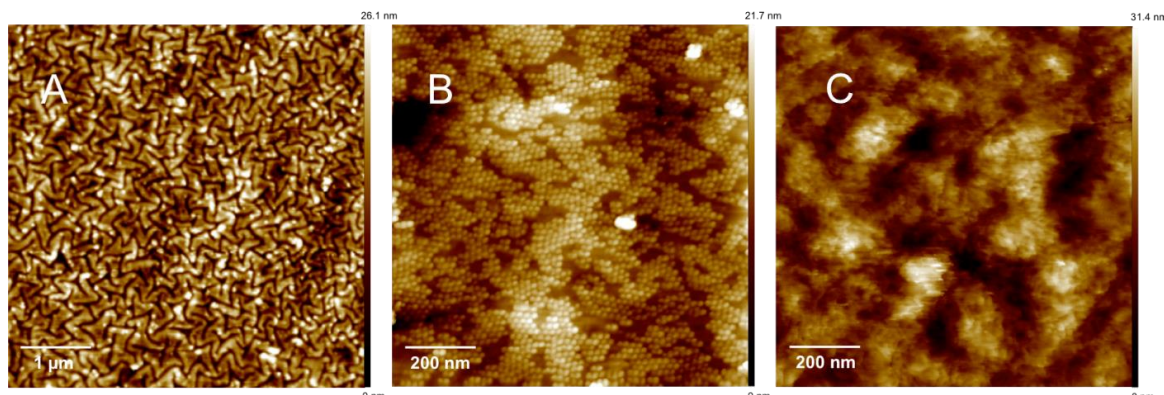


Figure 4.6. AFM topography images of a reacted tri-functional surface: (A) creases fabricated through μ CP with Jeffamine-M2070, (B) azide coated iron oxide nanoparticles clicked to ODIBO, and (C) unfunctionalized, smooth poly(PEFABLOC amide).

Conclusion

This work demonstrates a versatile method to create an orthogonal, self-sorting surface in which three different chemical and/or morphological functionalities can be generated from a complex one-pot reaction. The reaction conditions are compatible with environmental oxygen and water, and are highly functional group tolerant. These surfaces offer a wide array of possibilities as a scaffold in the fields of biological and biomedical engineering and provide a method to fabricate different localized morphological and molecular environments on a single substrate, with the ultimate goal of more closely mimicking the complexity observed in biological interfaces.

References

1. Mrksich, M.; Whitesides, G. M., Using self-assembled monolayers to understand the interactions of man-made surfaces with proteins and cells. *Annu. Rev. Biophys. Biomol. Struct.* **1996**, *25*, 55-78.
2. Yamato, M.; Konno, C.; Utsumi, M.; Kikuchi, A.; Okano, T., Thermally responsive polymer-grafted surfaces facilitate patterned cell seeding and co-culture. *Biomaterials* **2002**, *23*, 561-567.
3. Ito, Y., Surface micropatterning to regulate cell functions. *Biomaterials* **1999**, *20*, 2333-2342.
4. Thomas, C. H.; McFarland, C. D.; Jenkins, M. L.; Rezania, A.; Steele, J. G.; Healy, K. E., The role of vitronectin in the attachment and spatial distribution of bone-derived cells on materials with patterned surface chemistry. *J. Biomed. Mater. Res.* **1997**, *37*, 81-93.
5. Saneinejad, S.; Shoichet, M. S., Patterned glass surfaces direct cell adhesion and process outgrowth of primary neurons of the central nervous system. *Journal of Biomedical Materials Research* **1998**, *42*, 13-19.
6. Marx, V., Tissue engineering: Organs from the lab. *Nature* **2015**, *522*, 373-377.
7. Malchesky, P. S., Artificial Organ Technologies Around the World. *Artif. Organs* **2014**, *38*, 99-100.
8. Im, S. G.; Bong, K. W.; Kim, B.-S.; Baxamusa, S. H.; Hammond, P. T.; Doyle, P. S.; Gleason, K. K., Patterning Nanodomains with Orthogonal Functionalities: Solventless Synthesis of Self-Sorting Surfaces. *J. Am. Chem. Soc.* **2008**, *130*, 14424-14425.
9. Discher, D. E.; Janmey, P.; Wang, Y.-l., Tissue Cells Feel and Respond to the Stiffness of Their Substrate. *Science* **2005**, *310*, 1139-1143.

10. Boyan, B. D.; Hummert, T. W.; Dean, D. D.; Schwartz, Z., Role of material surfaces in regulating bone and cartilage cell response. *Biomaterials* **1996**, *17*, 137-146.

11. Huang, L.; Cao, Z.; Meyer, H. M.; Liaw, P. K.; Garlea, E.; Dunlap, J. R.; Zhang, T.; He, W., Responses of bone-forming cells on pre-immersed Zr-based bulk metallic glasses: Effects of composition and roughness. *Acta Biomater.* **2011**, *7*, 395-405.

12. Zhang, X.; Tanner, P.; Graff, A.; Palivan, C. G.; Meier, W., Mimicking the cell membrane with block copolymer membranes. *Journal of Polymer Science Part A: Polymer Chemistry* **2012**, *50*, 2293-2318.

13. Zhu, B.; Luo, S.-C.; Zhao, H.; Lin, H.-A.; Sekine, J.; Nakao, A.; Chen, C.; Yamashita, Y.; Yu, H.-h., Large enhancement in neurite outgrowth on a cell membrane-mimicking conducting polymer. *Nat Commun* **2014**, *5*.

14. Tibbitt, M. W.; Anseth, K. S., Hydrogels as Extracellular Matrix Mimics for 3D Cell Culture. *Biotechnology and bioengineering* **2009**, *103*, 655-663.

15. Geckil, H.; Xu, F.; Zhang, X.; Moon, S.; Demirci, U., Engineering hydrogels as extracellular matrix mimics. *Nanomedicine (London, England)* **2010**, *5*, 469-484.

16. Iha, R. K.; Wooley, K. L.; Nyström, A. M.; Burke, D. J.; Kade, M. J.; Hawker, C. J., Applications of Orthogonal “Click” Chemistries in the Synthesis of Functional Soft Materials. *Chem. Rev.* **2009**, *109*, 5620-5686.

17. Sumerlin, B. S.; Vogt, A. P., Macromolecular Engineering through Click Chemistry and Other Efficient Transformations. *Macromolecules* **2010**, *43*, 1-13.

18. Espeel, P.; Du Prez, F. E., “Click”-Inspired Chemistry in Macromolecular Science: Matching Recent Progress and User Expectations. *Macromolecules* **2015**, *48*, 2-14.

19. Arnold, R. M.; Patton, D. L.; Popik, V. V.; Locklin, J., A Dynamic Duo: Pairing Click Chemistry and Postpolymerization Modification To Design Complex Surfaces. *Acc. Chem. Res.* **2014**, *47*, 2999-3008.

20. Arnold, R. M.; McNitt, C. D.; Popik, V. V.; Locklin, J., Direct grafting of poly(pentafluorophenyl acrylate) onto oxides: versatile substrates for reactive microcapillary printing and self-sorting modification. *Chem. Commun.* **2014**, *50*, 5307-5309.

21. Broyer, R. M.; Schopf, E.; Kolodziej, C. M.; Chen, Y.; Maynard, H. D., Dual Click reactions to micropattern proteins. *Soft Matter* **2011**, *7*, 9972-9977.

22. Hensarling, R. M.; Hoff, E. A.; LeBlanc, A. P.; Guo, W.; Rahane, S. B.; Patton, D. L., Photocaged pendent thiol polymer brush surfaces for postpolymerization modifications via thiol-click chemistry. *Journal of Polymer Science Part A: Polymer Chemistry* **2013**, *51*, 1079-1090.

23. Spruell, J. M.; Wolffs, M.; Leibfarth, F. A.; Stahl, B. C.; Heo, J.; Connal, L. A.; Hu, J.; Hawker, C. J., Reactive, Multifunctional Polymer Films through Thermal Cross-linking of Orthogonal Click Groups. *J. Am. Chem. Soc.* **2011**, *133*, 16698-16706.

24. Dong, J.; Krasnova, L.; Finn, M. G.; Sharpless, K. B., Sulfur(VI) Fluoride Exchange (SuFEx): Another Good Reaction for Click Chemistry. *Angew. Chem. Int. Ed.* **2014**, *53*, 9430-9448.

25. Yatvin, J.; Brooks, K.; Locklin, J., SuFEx on the Surface: A Flexible Platform for Postpolymerization Modification of Polymer Brushes. *Angew. Chem. Int. Ed.* **2015**, *54*, 13370-13373.

26. Arnold, R. M.; Sheppard, G. R.; Locklin, J., Comparative Aminolysis Kinetics of Different Active Ester Polymer Brush Platforms in Postpolymerization Modification with Primary and Aromatic Amines. *Macromolecules* **2012**, *45*, 5444-5450.

27. Brooks, K.; Razavi, M. J.; Wang, X.; Locklin, J., Nanoscale Surface Creasing Induced by Post-polymerization Modification. *ACS Nano* **2015**, *9*, 10961-10969.

28. Adamczyk, M.; Grote, J.; Moore, J. A., Chemoenzymatic Synthesis of 3'-O-(Carboxyalkyl)fluorescein Labels. *Bioconjugate Chemistry* **1999**, *10*, 544-547.

29. Birks, J. B.; Christophorou, L. G., Excimer fluorescence spectra of pyrene derivatives. *Spectrochimica Acta* **1963**, *19*, 401-410.

30. Lehrer, S. S., Pyrene Excimer Fluorescence as a Probe of Protein Conformational Change. In *Proteins: Structure, Function, and Engineering*, Biswas, B. B.; Roy, S., Eds. Springer US: Boston, MA, 1995; pp 115-132.

CHAPTER 5

DURABLE DEFENSE: ROBUST AND VARIED ATTACHMENT OF NON-LEACHING POLY“-ONIUM” BACTERICIDAL COATINGS TO REACTIVE AND INERT SURFACES¹

Yatvin, J.; Gao, J.; and Locklin, J. 2014. *Chem. Commun.*, 50:9433-9442.

Reprinted with permission from publisher.

Abstract

Developing antimicrobial coatings to eliminate biotic contamination is a critical need for all surfaces, including medical, industrial, and domestic materials. The wide variety of materials used in these fields, from natural polymers to metals, require coatings that not only are antimicrobial, but also contain different surface chemistries for covalent immobilization. Alkyl “-onium” salts are potent biocides that have defied bacterial resistance mechanisms when confined to an interface. In this feature article, we highlight the various methods used to covalently immobilize bactericidal polymers to different surfaces and further examine the mechanistic aspects of biocidal action with these surface bound poly“-onium” salts.

Introduction

Surface contamination by microbes is a universal challenge in medical,^{2,3} domestic,⁴ and industrial settings.⁵ For example, contact contamination of methicillin resistant *Staphylococcus aureus* (MRSA) is a crisis in medical settings, tripling the stay time and costs for affected individuals, and quintupling the likelihood of death as of 2001.⁶ Food product contamination by MRSA is common, with one 2010 study finding that 24% of U.S. poultry and meat contains MRSA⁷. Because of these and many other examples, materials science and engineering has begun to address surface contamination by attempting to imbue or coat various substrates with chemistries that are antimicrobial and are self-sterilizing.

In terms of coating technologies, several different chemistries have been applied to address this problem, the most common of which release an antimicrobial agent such as triclosan,⁸ chlorine from N-halamines,⁹ silver ions,^{10,11} or conventional pharmaceutical antibiotics¹² slowly over time. While effective, these “leaching” strategies are hampered by depletion of the antimicrobial functionality from the coating unless they are actively replenished or “recharged.” These materials also have a tendency to contaminate their surroundings. A prime example of contamination by leaching triclosan, which has been found in significant concentrations in U.S. wastewater.¹³ Alongside these antimicrobial agents are membrane-disrupting “-onium” cations. The most extensively investigated “-onium” salts are alkyl ammonium and alkyl pyridinium compounds, whose small molecule versions are found in commercial disinfectants such as LysolTM. One advantage of these materials is that “-onium” salts are biocidal even when immobilized to different surfaces. This non-leaching behavior circumvents environmental contamination, and also minimizes the risk of organisms developing resistance to the “-onium” salt’s mechanism of biocidal action.

Bacterial membrane physiology

The biocidal activity of surface bound “-onium” salts is based on their ability to disrupt the bacterial cell membrane. Therefore, it is important to describe the physiology and chemical makeup of the membrane to better understand the mechanism of action. The bacterial cell membrane of a Gram-positive bacterium is primarily composed of two layers: the peptidoglycan layer and the lipid bilayer. The peptidoglycan layer consists of alternating N-acetylglucosamine and N-acetylmuramic acid chains, with a tetrapeptide extending off the N-acetylmuramic acids.¹⁴ The peptidoglycan layer is cross-linked via peptide interbridges between the tetrapeptides that form a protective barrier around the bacterium. The next layer is the lipid bilayer (LB), which consists of outwardly facing polar groups and inwardly facing long hydrocarbon chains. These phospholipids contain headgroups that are either zwitterionic, such as phosphatidylethanolamine and phosphatidylcholine, or negatively charged, as is the case with phosphatidylglycerol and phosphatidylserine. While the specific phospholipid content varies among organisms, and even changes with metabolic cycle, a bacterial cell membrane typically has a net negative charge. The membrane of a Gram-negative bacterium is more complex, consisting of an outer leaflet with lipopolysaccharides (LPS) that are anchored to the outer lipid membrane by the LPS lipid A domain,¹⁵ and an inner membrane consisting of phospholipids. Between these two lipid bilayers is the periplasm, an area of low density that contains a peptidoglycan layer similar in structure to that of Gram-positive bacteria, but usually much thinner.¹⁶

Mechanism of bactericidal action with leaching “-onium” salts

There are two main hypothesized mechanisms of action involving leaching alkyl “-onium” biocidal activity. Both rely on the electrostatic attraction between the net-negatively charged lipid bilayer surface and the positive charge of the “-onium” cations. First, the alkyl “-onium”

functionality must permeate through the peptidoglycan layer of Gram-positive bacteria, or through the LPS and peptidoglycan of Gram-negative bacteria. The first mechanism suggests an electrostatic interaction in which the alkyl “-onium” cations displace the divalent cations of the LB (primarily Mg^{2+} and Ca^{2+}) which serve as counterions to the anionic phosphate groups.¹⁷ This displacement damages the structural integrity and organization of the surface of the lipid bilayer, which increases its permeability and facilitates leaking of internal cellular content out of the cell.

The second proposed mechanism of biocidal action occurs when the hydrophobic alkyl functionalities are brought into close proximity to the membrane. These hydrophobic tail-groups intercalate into the phospholipid hydrocarbon chains and disrupt bilayer organization, which has the consequence of creating holes in the membrane.¹⁸ Work by Klibanov demonstrated that some bacteria, such as *P. aeruginosa*, that are immune to quaternary amines (QA) in solution,¹⁹ are still susceptible to similar functionalities that are tethered to a surface.²⁰ Klibanov also demonstrated that *S. aureus* and *E. coli* do not develop resistance to surface bound PQAs (polymer quaternary ammoniums).²¹ Based on this evidence, it is possible that the biocidal mechanism of action in surface bound, non-leaching “-onium” cations may deviate from that of free, solvated, “-onium” salts.

Mechanism of bactericidal action with non-leaching “-onium” salts

The Busscher group has recently demonstrated proof of a third mechanism of biocidal action that applies only to surface bound cationic antimicrobials.²² This study, which uses hyperbranched surface bound quaternary amine polymers, demonstrated powerful adhesive forces (~100 nN via bacterial probe atomic force microscopy) between the negatively charged bacterial cell membrane and the positively charged polymers. These electrostatic-based adhesive forces,

which are orders of magnitude higher than those ordinarily experienced by a bacterium, disrupt the bacterium's ability to grow and reproduce.

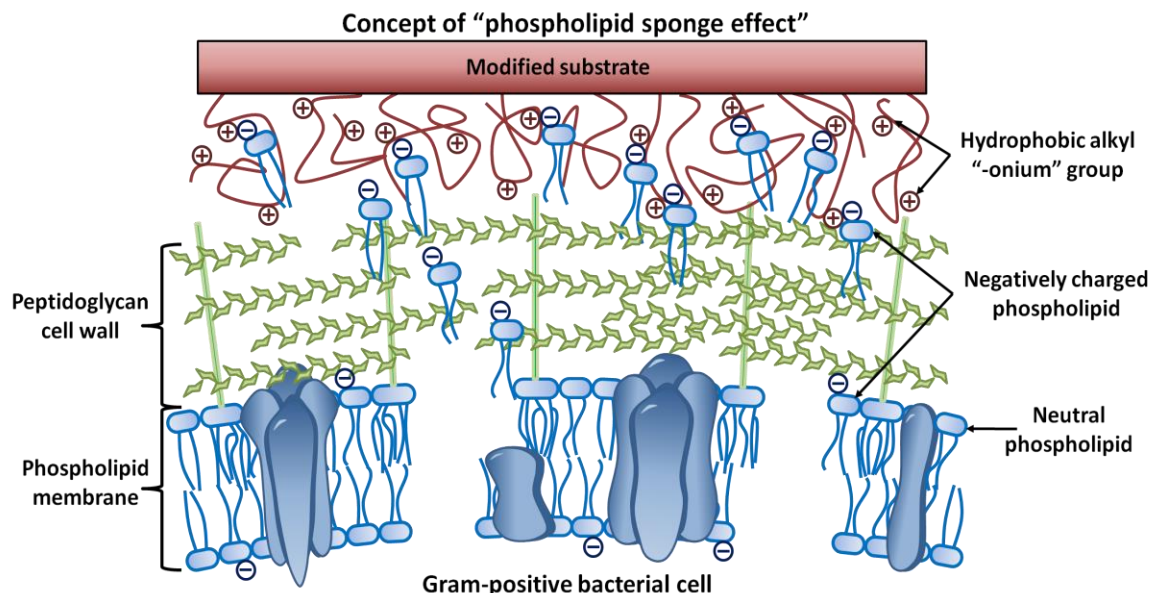


Figure 5.1. Schematic of the "phospholipid sponge" effect. Anionic phospholipids are being absorbed from the cell membrane and sequestered into the polymer matrix.

A related alternative to the electrostatic adhesive force hypothesis was put forward by Tiller, the "phospholipid sponge effect," which hypothesizes that the poly"-onium" films pull anionic phospholipids directly out of the bacterial membrane and sequesters them within the polymer matrix, causing the observed holes in the cellular membrane (Fig 5.1).²³ This hypothesis is also supported by research done by Li et al,²⁴ whose work offers a similar conclusion of "suctioning" off anionic phospholipids from bacteria and sequestering them within cationic hydrogels.

Attachment chemistry

There are numerous methods described in the literature that are used to coat surfaces with antimicrobial materials. In some cases the affinity of an antimicrobial compound to the surface (physisorption, either through electrostatic or hydrophobic forces) can be strong enough to resist

leaching, such as in Klibanov's pioneering work in which quaternized polyethyleneimines were painted onto glass,²⁵ which was one of the most critical developments for the field. However, many applications require more robust interactions, where it is necessary to use covalent attachment strategies (chemisorption) to ensure that the antimicrobial agent does not leach and remains confined to the surface. Depending on the nature of the functional groups available and the type of material, a wide variety of attachment chemistries have been employed. The most common is silane chemistry, which can react with -OH groups found on cellulose,²⁶ silicon oxide,²⁷ and certain metal oxides.²⁸ Hydroxyl and carboxylate attachment points can also be generated on inert materials by exposure to plasma²⁹ or chemical oxidants.³⁰ Broader nucleophilic substitution reactions, such as between an amine and a surface bound alkyl or acyl halides,³¹ have also been employed as a covalent grafting strategy. The chemical functionality employed in dying textiles, which occur mostly through condensation reactions with cellulose, can also be used to attach antimicrobials.³² Finally, more exotic attachment chemistries which employ reactions that form C-C or N-C bonds with inert surfaces,³³ or take advantage of powerful dopamine adhesion chemistry,^{34,35} have been used to tether antimicrobials to surfaces. Recently, several review articles have highlighted surface antimicrobial “-onium salts”.^{18, 36-41} In this feature article, we specifically focus on the robust attachment of non-leaching poly“-onium” salt-based antimicrobial compounds to surfaces, and pay special attention to non-traditional methods of attachment. We have chosen to exclude the attachment of “-onium” salts to nanoparticle surfaces,⁴²⁻⁴⁵ which are usually not themselves tethered to bulk surfaces, and therefore can leach into solution. The rest of this article is organized according to the general classes of surfaces and materials that have been coated: natural polymers, synthetic polymers, and inorganic surfaces such as metals and oxides.

Polymer surfaces

Natural textiles

The derivatization of natural textiles, primarily cellulose, with antimicrobial functionality is an enormous frontier for both medical and commercial applications. Antimicrobial wound care technologies represented 11% of the \$11.7 billion dollar global wound care market in 2013.⁴⁶ Commercial products which boast “anti-odor” properties due to antimicrobial agents engineered into fabrics are abundant, with a prominent example being triclosan- containing MicrobanTM coatings. The overwhelming majority of these coatings rely heavily on compounds that work via leaching mechanisms that are detrimental for the reasons described above, and therefore work on non-leaching antimicrobial textiles surfaces via poly“-onium” salts holds great promise.

One of the first reports using conventional cross-linkers to fix poly“-onium” cations to cellulose was described by Kim et al,⁴⁷ who employed a chitosan derivative, *N*-(2-hydroxy)propyl-3-trimethylammonium chitosan chloride (HTCC), as an antimicrobial functionality to derivatize cotton. The authors employed dimethyloldihydroxyethylene urea (DMDHEU), butanetetracarboxylic acid, and citric acid as a strategy to cross-link HTCC to cellulose through condensation using the -OH groups found on both HTCC and cellulose. While DMDHEU was ineffective, both polycarboxylic acids were successful in functionalizing cotton with HTCC. A 0.1% weight loading of cotton was found to be sufficient to reduce the population of *S. aureus* by $\geq 91\%$ even after 20 laundering cycles.

More precise methods of imbuing textiles with biocidal properties (which are likely also less scalable) have utilized “grafting from” polymerization techniques. Lee and Matyjaszewski demonstrated the functionalization of paper with a PQA derived from the post-polymerization quaternization of poly(2-(dimethylamino)ethyl) methacrylate (PDAEMA) using ethyl bromide.⁴⁸ The initiator, 2-bromoisobutyrlbromide, was covalently attached to the surface of filter paper via

condensation with the -OH groups. The PQA was then grown from the surface via surface initiated atom transfer radical polymerization (SI-ATRP). A ~6 cm² piece of paper functionalized with these coatings was able to kill up to 10⁹ bacteria in minutes. The coatings were ineffective after washing, since the substrate began to fragment and degrade under the stresses of washing. For this reason the authors used a more robust substrate, silicon wafers, to investigate the role of washing on the PQA. On SiO₂, it was noted that after exposure to bacteria, substrates washed with pure water became deactivated after two bacterial challenge/wash cycles. However, surfaces washed with a sodium dodecylsulfate detergent retained their efficacy. Furthermore, washing with detergent could be used to reactivate surfaces that had been rinsed with pure water and were deactivated through exposure to and killing of bacteria. The authors hypothesized that dead bacteria clogged the surface, and were responsible for deactivation. These bacterial carcasses could not be removed by rinsing with pure water. Detergents, however, were capable of dislodging the dead cells, which re-exposed the coating to the environment, and renewed biocidal activity.

Roy et al used a similar approach, and polymerized DAEMA via reversible addition-fragmentation chain transfer (RAFT).⁴⁹ The PDAEMA was then quaternized by post-polymerization modification with alkyl chains ranging from C₈ to C₁₆ in order to study the effects of substituent length on the biocidal efficacy of quaternized PDAEMA. The authors observed a trend of decreasing antimicrobial efficacy as the chain length of the alkyl group was increased

from C₈ to C₁₆. Maximum efficacy was observed with the C₈ polymer, which reduced an initial concentration from 10⁶ colony forming units (CFU) of *E. coli* per mL to <100 CFU/mL.

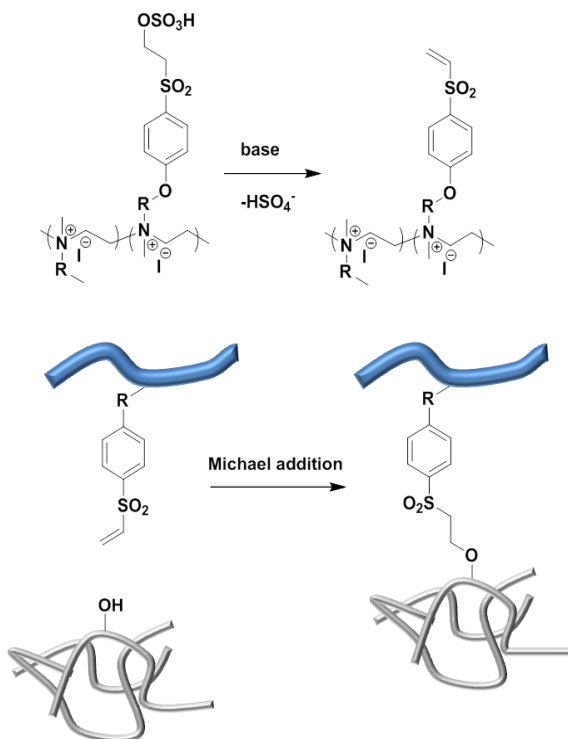


Figure 5.3. Creation of the reactive vinyl sulfone by exposure of pendant sulfate group to basic conditions, followed by attachment of the antimicrobial polymer to cellulose via Michael addition.

“Grafting to” approaches are another popular method of functionalizing fabrics, and the most relevant for industrial application. Our lab recently employed a polymer that used a tethering functionality that requires no pretreatment or separate crosslinkers to “graft to” cellulose. We synthesized a polyethyleneimine (PEI) polymer quaternized with C₁₂ chains and pendant phenylsulfonylethyl sulfate groups (Fig 3).³² The sulfate group undergoes elimination in the presence of base which produces a vinyl sulfone, that is susceptible to attack via Michael addition with soft nucleophiles,⁵⁰ like cellulose’s pendant –OHs. The polymer was tethered to cellulose

after exhaustion onto fabric at 45 °C from aqueous solution at pH 9. The resulting coating was shown to be effective against *E. coli* and *S. aureus*.

These previous results are interesting, and initiate discussion on the wider topic of alkyl chain length and its influence on biocidal activity involving alkyl “-onium” cations. The study by Roy makes a strong case that C₈ is the appropriate alkyl chain length necessary to maintain the hydrophobic/hydrophilic balance required for antimicrobial activity in surface confined polymers. They cite several studies, which observe this peak in efficacy with C₈ alkyl chains.⁵¹⁻⁵³ However, we argue that this assumption can lead to oversimplifications, and the resulting pendant group size strongly depends on the nature of the polymer backbone. For example, Klibanov found that with surface bound alkylated poly-4-vinylpyridine (P4VP) coatings, C₆ chains had the highest biocidal activity, with C₈ alkyl chains displaying ~8x less antimicrobial efficacy.²⁰ In the case of alkylated PEI derivatives, very long alkyl chains (C₁₂ and C₁₈) displayed the highest biocidal activity.⁴⁴ Specific we argue that alkyl chain length is not the primary factor that governs biocidal efficacy, but rather it is the net sum of all the hydrophobic/hydrophilic interactions in the polymer (backbone and side-chain) that determine the outcome. Each of these studies used different polymer backbones, ranging from hydrophobic (P4VP) to hydrophilic (PEI). As polymer architectures increase in complexity through eloquent design, predetermining factors such as pendant side-chain length becomes more difficult and can lead to materials with less than optimal efficacy.

Another critical factor in designing antimicrobial polymers is molecular weight. It has been demonstrated by Klibanov using quaternized polyethyleneimine (Q-PEI) that molecular weight plays a critical role in determining biocidal efficacy of surface coatings.²⁵ This work demonstrated that a 750 kDa, Q-PEI killed effectively all of the bacteria sprayed as an aerosol onto the surface,

with the biocidal efficacy decreasing when lower molecular weight Q-PEIs were used. As an example, a 2 kDa Q-PEI was shown to kill less than 50% of all microbes. This again illustrates that the overall composition and polymer architecture is important when designing materials with

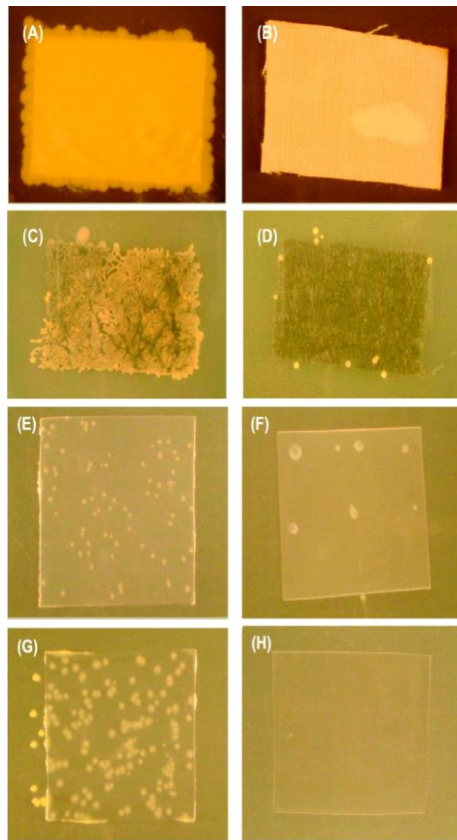


Figure 5.4. Digital pictures of the textiles and plastic substrates sprayed with *S. aureus*: (A) untreated cotton, (B) cotton spray-coated with 15 mg/mL BPAMP, (C) untreated polypropylene (nonwoven geotextile fabric), (D) polypropylene spray-coated with 15 mg/mL BPAMP, (E) untreated poly(vinyl chloride) substrate, (F) poly(vinyl chloride) substrate spray-coated with 15 mg/mL BPAMP, (G) untreated polyethylene substrate, and (H) polyethylene substrate spray-coated with 15 mg/mL BPAMP. Reprinted with permission from P. Dhende, S. Samanta, D. M. Jones, I. R. Hardin and J. Locklin, *ACS Appl. Mater. Interfaces*, 2011, **3**, 2830. Copyright 2011 American Chemical Society.

high biocidal efficacy.

Synthetic polymers

Polymers such as polypropylene and polystyrene have only alkyl and/or aryl functionalities and usually require harsh chemistry to produce synthetic “handles” that can be detrimental to the mechanical properties of the material. Our group has produced a Q-PEI with pendant benzophenone groups that allows the functionalization of *any material containing a C-H bond*.³³ Benzophenone can be excited with mild UV light (345-365 nm) to a diradicaloid triplet state that can abstract a hydrogen atom from a nearby C-H group, which creates a second carbon-centered radical. The two carbon radicals can then combine to form a new C-C bond.⁵⁴ We combined the photo-grafting ability of benzophenone with the biocidal activity of *N,N*-methyldodecyl Q-PEI to generate a benzophenone-containing antimicrobial polymer (BPAMP) that can be covalently attached to any surface that contains C-H or N-H bonds. After curing with 365 nm light, this coating renders a cross-linked network tethered to any plastic surface that serves as a permanent antimicrobial coating. To illustrate the wide applicability, we used BPAMP to coat cotton, polypropylene, polyvinyl chloride, and polyethylene, which rendered these materials antimicrobial in a single functionalization step (Fig 4). A relationship between coating thickness and bacterial kill effectiveness of *S. aureus* and *E. coli* was noted, with films 35 nm or thicker killing essentially all bacteria applied. There are two plausible explanations for this behavior. If the alkyl chain intercalation or ion exchange mechanisms are valid, then perhaps the polymer film must be thick enough for free polymer ends to burrow past the peptidoglycan layer, interact directly with the phospholipid bilayer, disrupt ionic integrity, and cause cell death. . Gram-negative bacteria generally have peptidoglycan layers of <10nm whereas Gram-positive bacteria usually have peptidoglycan layers of 20-80 nm.¹⁶ It is also possible that if the “phospholipid sponge” theory is

valid, a film must be sufficiently thick to have enough storage volume to absorb sufficient anionic phospholipids to damage the bacterial membrane.

As a compliment to the “grafting to” approach with benzophenone that was employed by our

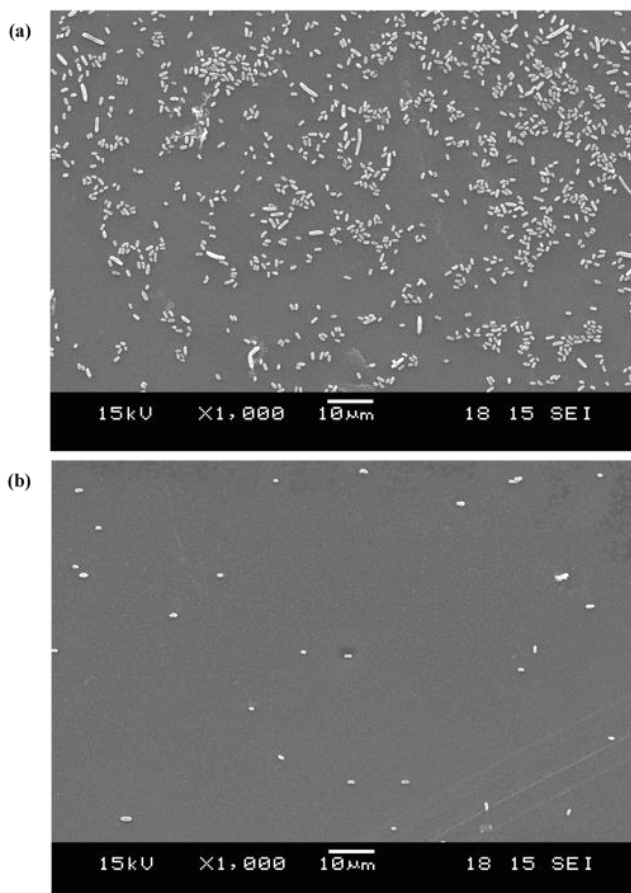


Figure 5.5. Scanning electron micrographs of (a) PET and (b) an alkylated P4VP film on PET after exposure to airborne *E. coli* subsequent incubation with solid growth agar for 24 h.

Reprinted with permission from L. Cen, K. G. Neoh and E. T. Kang, *Langmuir*, 2003, **19**, 10295.

Copyright 2003 American Chemical Society.

group, Huang et al used the reactivity of benzophenone to attach an ATRP initiator to polypropylene in the form of a benzophenonyl 2-bromo isobutyrate.⁵⁵ The benzophenone end of the molecule was tethered to the surface by UV excitation, generating a polypropylene surface coated with ATRP initiator. PDAEMA was then “grafted from” the surface using ATRP conditions that afforded several different molecular weights. The PDAEMA was then quaternized with ethyl bromide. As with Lee and Matyjaszewski’s previous antimicrobial coatings generated using SI-ATRP, a biocidal efficacy dependence on molecular weight was observed. In this system, biocidal

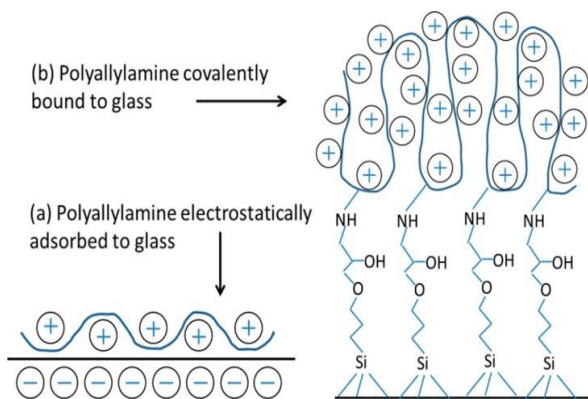


Figure 5.6. Morphology of a polycation that is electrostatically bound to glass versus one that is bound to the surface via silanes. Reprinted with permission from D. D. Iarikov, M. Kargar, A. Sahari, L. Russel, K. T. Gause, B. Behkam and W. A. Ducker, *Biomacromolecules*, 2014, **15**, 169. Copyright 2014 American Chemical Society.

efficacy correlated with the density of QA groups observed via the fluorescein dye method.⁵⁶ Coatings with >9800 molecular weight polymer brushes, corresponding to a surface QA density >14 QA/nm², killed essentially all bacteria exposed to these surfaces.

Klibanov extended his earlier work that coated glass using PEI derivatives to strategies for coating cotton by adding a pendant photoactive (4'-azido-2'-nitrophenylamino)hexanoyl (ANPAH) group to branched, Q-PEI.⁵⁷ The aryl azide of the ANPAH group can undergo excitation

upon exposure to UV light and form covalent bonds to cellulose. After coating a 2.5 cm² swatch of cotton with three layers of the ANPAH Q-PEI derivative, the swatch was effective in killing 4 x 10⁵ bacteria from a 10 mL solution. It is interesting that this work only described the functionalization on cotton, since aryl azides are known for similar photo-catalyzed nonspecific C-H insertion chemistries to benzophenone.^{58, 59, 60}

Another alternative and effective strategy is the use of plasma polymerization to derivatize inert polymer surfaces, such as polypropylene. Plasma polymerization generates a large amount of free radicals, which can also abstract a hydrogen from surface C-H bonds, and create a reactive carbon-centered radical which either terminates a nearby growing free polymer or initiates polymerization of a gas phase or aerosolized monomer. Wafa et al used this method to graft poly(glycidal methacrylate) (GMA) which was then reacted with HTCC.⁶¹ Several other compounds were also used to functionalize polypropylene, including several cyclodextrin-entrapped molecules, but HTCC was the most effective, displaying a 1.33 log reduction for *E. coli* and a 1.30 log reduction for *S. aureus*. The authors noted that lower concentrations of HTCC corresponded to stronger antimicrobial activity in the case of *E. coli*. The same effect was previously documented by Lim⁶² on HTCC functionalized cellulose, and was explained via a peculiar mechanism involving high surface concentrations of HTCC on a bacterial cell wall which formed a new barrier and prevented the leakage of cellular contents after the membrane has been disrupted by the polymer. An analogous approach was used by Wafa to also functionalize nylon 6,6.⁶³

The Kang group also used a plasma grafting approach to functionalize polyethylene terephthalate (PET) using three separate steps.⁶⁴ First, the PET surface was bombarded with argon plasma and exposed to air to create surface -OH and peroxy functionalities, from which P4VP was

grown in a UV reactor. Finally, the pyridines were converted to alkyl pyridinium salts by the addition of hexyl bromide. The functionalized surfaces were tested against both air and waterborne *E. coli*. The surface demonstrated a strong ability to reduce bacterial contamination. The study also provided SEM images that showed any remaining bacteria were small in size (~1 μm compared to 2-6 μm for healthy bacteria), sparsely distributed, and did not appear to be actively reproducing or growing (Fig 5). Huh et al used a similar procedure,⁶⁵ except that acrylic acid was polymerized, then crosslinked by direct condensation with a quaternized chitosan derivative.

Inorganic surfaces

Stainless steel

Direct functionalization of metals is an important application for antimicrobial functionalization, especially in the medical field where embedded implants, screws, and pins are a prime source of contamination. With conducting surfaces, electrografting is a well defined strategy for immobilizing organic molecules that contain a wide variety of functional groups.⁶⁶ Electrografting has also been used to initiate polymerization from electrode surfaces. Ignatova et al used electropolymerization and ATRP to create hyperbranched antimicrobial polymers grafted from stainless steel (SS).⁶⁷ The functionalization process begins with electropolymerization from the surface of SS using 2-(2-chloropropionate)ethyl acrylate (cPEA) as the monomer. ATRP was then employed using a secondary bromine containing monomer, resulting in a hyperbranched polymer with pendant alkyl halide groups. The alkyl halides were converted to pyridinium salts using pyridine. The group also created alkyl “-onium” salt coatings via electropolymerization of a monomer containing an N-hydroxy succinimide (NHS) ester. This NHS polymer was then reacted with branched PEI, creating a crosslinked PEI network polymer. The PEI was then alkylated with chlorooctane. Curiously, having created what appears to be a potent antimicrobial surface coating,

the study only examines the bacterial adhesion properties of the coatings. Their results certainly suggested lower bacterial adhesion, with the poly(cPEA) having 10^2 fewer colony forming units (CFU) and the PEI derivative having 2.5×10^3 fewer CFU than the control SS.

When functionalizing steel, corrosion prevention can be as high a priority as short-term antimicrobial efficacy. Biofilms speed up corrosion, so hybrid films that are both biocidal and corrosion preventing are a popular approach to functionalizing steel. An interesting combined antimicrobial/antifouling coating was established on SS by Yuan et al.⁶⁸ Poly(3-trimethoxysilyl)propyl methacrylate-b-poly(2-(dimethylamino)ethyl methacrylate) (PTMSPMA-b-DMAEMA)) was fabricated via consecutive SI-ATRP, a procedure adapted from earlier work by the Matyjaszewski group⁶⁹. The pendant tertiary amino groups of the outer PDMAEMA block were quaternized with hexyl bromide to form an alkyl ‘-onium’ salt. The inner PTMSPMA block containing trimethoxysilyl groups were hydrolyzed and condensed to form a cross-linked polysiloxane network, which provided enhanced anticorrosion capability. A significant increase in corrosion potential and decrease of corrosion current compared to pristine SS in Tafel polarization curves and electrochemical impedance spectra demonstrated the anticorrosion capabilities of the material. The biocidal functionality of the coatings was also demonstrated with a reduction in viable cell counts on the surface from 10^6 cells/cm² to 10^3 cells/cm² when challenged with *D. desulfuricans*.

The same group also used layer-by-layer deposition of TiO_2 capped with an ATRP initiator to

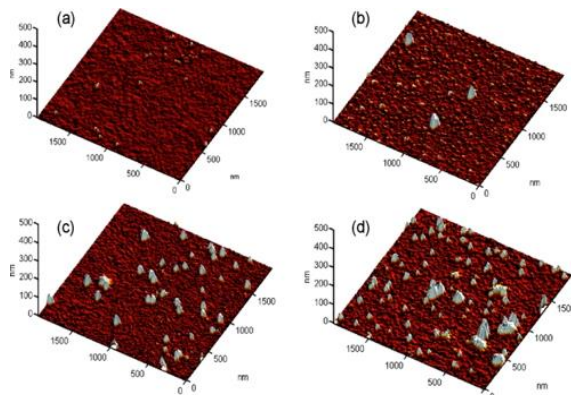


Figure 5.7. AFM images of glass surfaces after being immersed in the solution of $\text{PDMAEMA}_{97}\text{--PTMSPMA}_{60}$ in toluene ($C = 2.5 \text{ g/L}$) for (a) 2.5 h, (b) 7.0 h, (c) 19 h, (d) 70 h at 70 °C. Reprinted with permission from J. Huang, R. R. Koepsel, H. Murata, W. Wu, S. B. Lee, T. Kowalewski, A. J. Russell and K. Matyjaszewski, *Langmuir*, 2008, **24**, 6785. Copyright 2011 American Chemical Society.

establish a “handle” for functionalization of stainless steel while simultaneously taking advantage of the antifouling capabilities of titanium.³⁰ SS was activated by washing with Piranha solution to create surface –OHs, which were then exposed to Ti(IV) tert-butoxide under inert conditions. The substrate was washed with water to generate surface –OHs on the titanium, and exposed to the Ti(IV) tertbutoxide for four more cycles before the addition of a reactive silane ATRP initiator. P4VP was polymerized from the initiator via ATRP, then alkylated with bromohexane. The alkyl-P4VP surface demonstrated a reduction in the viable cell count of *D. desulfiricans*, while simultaneously obtaining good anticorrosion properties via Tafel plot and electrochemical impedance spectroscopy measurements.

SiO_2

The functionalization of glass or silicon substrates with antimicrobial polymers has proven useful in probing the mechanism of biocidal activity and the effectiveness of various functional

groups. In a single study, both the “grafting to” and “grafting through” motifs were examined by the Klibanov group on glass.²⁰ Poly(4-vinyl-N-alkylpyridinium bromide) were covalently attached to pendant -NH₂ coated glass slides using two different strategies. In the “grafting through” method, -NH₂ functionalized glass were acylated using acryloyl chloride, followed by free radical polymerization of P4VP, and subsequent post-polymerization alkylation. In the “grafting to” method, the -NH₂ glass were reacted with 1,4-dibromobutane, which could react with P4VP, along with subsequent alkylation of the bound polymer. Several different alkyl bromides were utilized for quaternization, with hexyl alkylated P4VP prepared by both methods demonstrating the highest bactericidal activity, killing over 94% of bacteria in a surface-aerosol test.

A notable example that stands out from hydrophobic “-onium” salts is work done by the Ducker group in which polyallylamine hydrochloride salt (PAA·HCl) was grafted to a silicon surface via a trimethoxy silane.⁷⁰ These amines are nonalkylated, and instead appear to derive their antimicrobial properties from the protonated amine functionality. This material was able to kill over 98% of *S. aureus* and *epidermidis* and 89% of *P. aeruginosa*, lending credence to the theory that alkylation is merely a method of balancing the hydrophobic/hydrophilic interactions, and that the cation is the prime mover of antimicrobial action. The group noted that it is possible to apply PAA·HCl to a glass surface and achieve only a physisorbed coating; however, this coating is not antimicrobial. They theorize that the positive charges of the material are interacting with the glass surface instead of being available to interact with bacterial cells walls. However, when the polymer is bound via a silane, the positive charges are more accessible and available for interaction, which leads to biocidal activity (Fig 6).

The Matyjaszewski group used ATRP to prepare a bifunctional block copolymer that contains a PTMSPMA surface anchoring segment and a PDAEMA biocidal segment.⁶⁹ “Grafting to”

immobilization of the block copolymer was achieved by reaction between PTMSPMA and silanol groups on activated glass slides, and antimicrobial activity was achieved by quaternization of the PDMAEMA block with ethyl bromide. The effects of the grafting density of the PQA, polymer chain length, and the ratio of PDMAEMA to PTMSPMA on biocidal efficacy were investigated. It was demonstrated that surfaces with higher grafting density possessed higher biocidal activity, however there was no relationship between polymer chain length or block ratio on biocidal activity. The most critical factor was determined to be the density of QAs on the surface. In fact, a direct surface QA to bacterium ratio was established for this system, with about 10^{10} QAs being necessary to kill one *E. coli* bacterium. During these studies, a “patchiness” phenomenon was noted for these polymers (Fig 7). The polymers aggregated and formed high density QA patches on glass which had superior biocidal activity. Furthermore, these patches were more effective than PQA grown via “grafting from” ATRP at the same overall charge density. This data implies that highly concentrated QAs over small areas are more effective than less concentrated QAs over a wider area. The use of dopamine as a coating functionality is also very appealing because of its ability to coordinate via the catechol group to metals or adhere strongly to a variety of substrates via polydopamine networks. Dopamine has been used to coat metals such as silver,^{34, 71, 72} metal oxides such as TiO₂,^{73, 74} silicon oxide,⁷⁵ and even highly inert surfaces like polyethylene and polytetrafluoroethylene.^{75, 76} The Kuroda group used this potent attachment chemistry to coat a poly(2-(dimethylamino)ethyl methacrylate-co-methoxyethyl acrylate-co-dopamineacrylamide

(PDAEMA-co-MEA-co-DMA) terpolymer onto glass, where the PDAEMA was quaternized with dodecyl chains.³⁴ After optimizing the ratio of these three monomers, a film was produced that killed nearly 100% of *E. coli* and *S. aureus*. Sum frequency generation spectroscopy (SFG) was used to study the polymer coated surface (Fig 8). The SFG spectrum indicated that in the dry state the dodecyl chains in the polymer aggregate at the surface. In solution, however, all surface organization is lost. This data indicates that the biocidal alkyl “-onium” functionality is presented at the surface in the dry state, not the MEA, catechol or polydopamine functionalities.

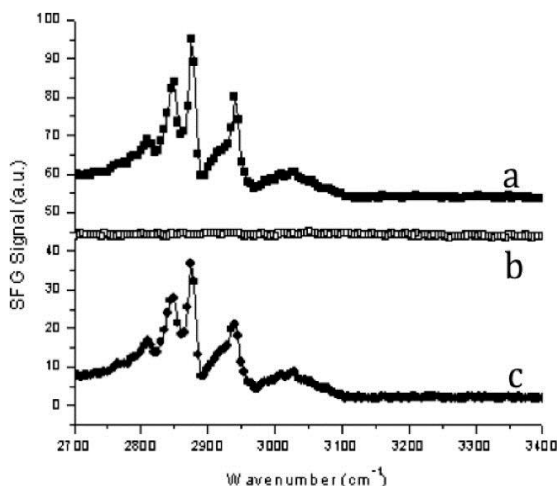


Figure 5.8. SFG spectra of the P2 coating surface (a) in air, (b) in contact with water, and (c) in air, after removal from water contact. Reprinted with permission from H. Han, J. Wu, C. W. Avery, M. Mizutani, X. Jiang, M. Kamigaito, Z. Chen, C. Xi and K. Kuroda, *Langmuir*, 2011, **27**, 4010. Copyright 2011 American Chemical Society.

Kim et al used a different polymer system to establish the robustness of catechol attachment chemistry on a wide variety of surfaces.³⁵ Chain transfer polymerization was used to synthesize a poly(dimethylaminoethyl) acrylate (PDMA) homopolymer, which was partially quaternized with 2-chloro-3'4'-dihydroxyacetophenone and bromododecane (Fig 9). Substrates consisting of Si wafer, titanium, quartz, Au, polystyrene, polyvinyl chloride, PET, polypropylene, and

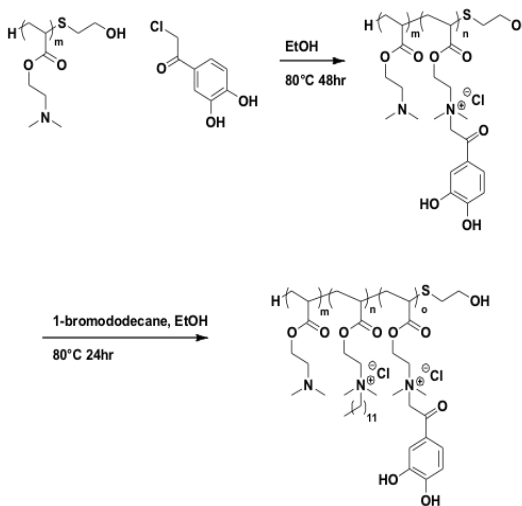


Figure 5.9. Synthesis of partially quaternized catechol antimicrobial polymer.

polycarbonate were soaked in a polymer solution for 24 hours at room temperature to allow for polymer attachment. The functionalized substrates were washed, and the presence of the polymer on the surface was confirmed via ellipsometry and contact angle measurements. The polypropylene surface was subjected to bacterial testing with *S. aureus* and *E. coli* to confirm the antimicrobial activity of the polymer, with their testing showing near 100% killing efficiency. Furthermore, the coating was aged for 60 days at 60°C, and no loss in activity was observed.

Conclusions

In this feature article, we have highlighted the wealth of options available for permanent attachment of antimicrobial functionality to surfaces. Each tethering motif is highly effective in attaching to a complementary surface, but most of the approaches outlined above require multiple steps and are highly complex, which lead to challenges on the industrial scale. Techniques such as SI-ATRP or post-polymerization modification are likely too costly, time consuming, and have limited scalability for many high-throughput processes. While these approaches provide valuable insight into the mechanism of biocidal activity, most fall short of providing an optimized

antimicrobial coating. The ideal coating should be synthetically accessible from low-cost starting materials and biocidal across a wide range of microbes and surface conditions, while remaining inactive towards mammalian cells. This material should also be stable under ambient conditions and be highly reactive towards the surface. It would also benefit from being non-specific, so that the same chemistry can be used across different surface chemistries.

In our opinion, another barrier to success in this field is the extreme heterogeneity of antimicrobial surface testing used by different researchers. For example, it is difficult to even compare the results of many of the studies described above, considering that they used different bacteria application methods, bacterial species, loading concentrations, solution versus aerosol application, application times, among other variables. Klibanov has initiated the standardization of this practice, and provided a method of testing antibacterial and antiviral activity of non-leaching flat surfaces which we strongly recommend.⁷⁷ Although this is an important step, standard methodologies for testing for other organisms such as fungi and three dimensional, non-leaching surfaces are still needed.

Finally, it is imperative that the mechanism of bactericidal action of these materials be more concretely determined in order to optimize interfacial design. Research has been performed on the hydrophobic/hydrophilic balance and its influence on surface antimicrobial efficacy, but this balance varies widely depending on molecular functionality and polymer architecture, and is highly qualitative in nature. There is also only a limited selection of research on the effects of these surface bound materials on fungi, viruses, and mammalian cells, a critical gap that needs to be addressed by the field. In our opinion, both Busscher's adhesive forces model and the "phospholipid sponge" concepts especially deserve additional investigation, since the concepts

appear promising by addressing the fact that solution and surface poly“-onium” antimicrobials appear to not be created equal.

References

1. Yatvin, J.; Gao, J.; Locklin, J., Durable defense: robust and varied attachment of non-leaching poly “-onium” bactericidal coatings to reactive and inert surfaces. *Chem. Commun.* **2014**, *50*, 9433-9442.
2. Curtis, L. T., Prevention of hospital-acquired infections: review of non-pharmacological interventions. *Journal of Hospital Infection* **2008**, *69*, 204-219.
3. Schabrun, S.; Chipchase, L., Healthcare equipment as a source of nosocomial infection: a systematic review. *Journal of Hospital Infection* **2006**, *63*, 239-245.
4. Scott, E.; Bloomfield, S. F., The survival and transfer of microbial contamination via cloths, hands and utensils. *Journal of Applied Bacteriology* **1990**, *68*, 271-278.
5. Leonid A. Kulakov, M. B. M., Kimberly L. Ogden, Michael J. Larkin, and John F. O'Hanlon, Analysis of Bacteria Contaminating Ultrapure Water in Industrial Systems. *Appl Environ Microbiol.* **2002**, *68*, 1548-1555.
6. Noskin, G. A.; Rubin, R. J.; Schentag, J. J.; J. Kluytmans; E.C Hedblom; M. Smulders; E. Lapetina; Gemmen, E., The burden of staphylococcus aureus infections on hospitals in the united states: An analysis of the 2000 and 2001 nationwide inpatient sample database. *Archives of Internal Medicine* **2005**, *165*, 1756-1761.
7. Andrew E. Waters, T. C.-C., Jordan Buchhagen, Cindy M. Liu, Lindsey Watson, Kimberly Pearce, Jeffrey T. Foster, Jolene Bowers, Elizabeth M. Driebe, David M. Engelthaler, Paul S. Keim, and Lance B. Price, Multidrug-Resistant Staphylococcus aureus in US Meat and Poultry. *Clin. Infect. Dis.* **2010**, *52*, 1227-1230.

8. McBride, M. C.; Karl Malcolm, R.; David Woolfson, A.; Gorman, S. P., Persistence of antimicrobial activity through sustained release of triclosan from pegylated silicone elastomers. *Biomaterials* **2009**, *30*, 6739-6747.

9. Hui, F.; Debiemme-Chouvy, C., Antimicrobial N-Halamine Polymers and Coatings: A Review of Their Synthesis, Characterization, and Applications. *Biomacromolecules* **2013**, *14*, 585-601.

10. Eckhardt, S.; Brunetto, P. S.; Gagnon, J.; Priebe, M.; Giese, B.; Fromm, K. M., Nanobio Silver: Its Interactions with Peptides and Bacteria, and Its Uses in Medicine. *Chem. Rev.* **2013**, *113*, 4708-4754.

11. D. Roe, B. K., N. Bonn-Savage, B. Gibbons, J. B. Roullet, Antimicrobial surface functionalization of plastic catheters by silver nanoparticles. *J Antimicrob Chemother* **61**, 869-876.

12. S. N. Davidoff, J. O. S., B. D. Brooks, D. W. Grainger, and A. E. Brooks, Evaluating antibiotic release profiles as a function of polymer coating formulation. *Biomed Sci Instrum* **2011**, *47*, 46-51.

13. Venkatesan, A. K.; Pycke, B. F. G.; Barber, L. B.; Lee, K. E.; Halden, R. U., Occurrence of triclosan, triclocarban, and its lesser chlorinated congeners in Minnesota freshwater sediments collected near wastewater treatment plants. *Journal of Hazardous Materials* **2012**, *229–230*, 29-35.

14. *Bacterial Membranes: Structural and Molecular Biology*. Caister Academic Press: Norfolk, **2014**.

15. Needham, B. D.; Trent, M. S., Fortifying the barrier: the impact of lipid A remodelling on bacterial pathogenesis. *Nat Rev Micro* **2013**, *11*, 467-481.

16. *Prokaryotic Cell Wall Compounds: Structure and Biochemistry*. Springer 2010.

17. Kügler, R.; Bouloussa, O.; Rondelez, F., Evidence of a charge-density threshold for optimum efficiency of biocidal cationic surfaces. *Microbiology* 2005, 151, 1341-1348.

18. Tiller, J. C., Antimicrobial Surfaces. In *Adv. Poly. Sci.* 2010; Vol. 240, pp 193-217.

19. A. Tabata, H. N., T. Maeda, K. Murakami, Y. Miyake, and H. Koura, Correlation between Resistance of *Pseudomonas aeruginosa* to Quaternary Ammonium Compounds and Expression of Outer Membrane Protein OprR. *Antimicrob Agents Chemother* 2003, 47, 20933-2099.

20. Tiller, J.; Liao, C.; Lewis, K.; Klibanov, A., Designing surfaces that kill bacteria on contact. *Proceedings of the National Academy of Sciences of the United States of America* 2001, 98, 5981-5985.

21. Nebojsa M. Milovic, J. W., Kim Lewis, Alexander M. Klibanov, Immobilized N-Alkylated Polyethylenimine Avidly Kills Bacteria by Rupturing Cell Membranes With No Resistance Developed. *Biotechnol. Bioeng* 2005, 90, 715-722.

22. Asri, L. A. T. W.; Crismaru, M.; Roest, S.; Chen, Y.; Ivashenko, O.; Rudolf, P.; Tiller, J. C.; van der Mei, H. C.; Loontjens, T. J. A.; Busscher, H. J., A Shape-Adaptive, Antibacterial-Coating of Immobilized Quaternary-Ammonium Compounds Tethered on Hyperbranched Polyurea and its Mechanism of Action. *Adv. Funct. Mater.* 2014, 24, 346-355.

23. Bieser, A. M.; Tiller, J. C., Mechanistic Considerations on Contact-Active Antimicrobial Surfaces with Controlled Functional Group Densities. *Macromol. Biosci.* 2011, 11, 526-534.

24. Li, P.; Poon, Y. F.; Li, W.; Zhu, H.-Y.; Yeap, S. H.; Cao, Y.; Qi, X.; Zhou, C.; Lamrani, M.; Beuerman, R. W.; Kang, E.-T.; Mu, Y.; Li, C. M.; Chang, M. W.; Jan Leong, S. S.; Chan-

Park, M. B., A polycationic antimicrobial and biocompatible hydrogel with microbe membrane suctioning ability. *Nat Mater* **2011**, *10*, 149-156.

25. Park, D.; Wang, J.; Klibanov, A. M., One-Step, Painting-Like Coating Procedures To Make Surfaces Highly and Permanently Bactericidal. *Biotechnology Progress* **2006**, *22*, 584-589.

26. Xie, Y.; Hill, C. A. S.; Xiao, Z.; Militz, H.; Mai, C., Silane coupling agents used for natural fiber/polymer composites: A review. *Composites Part A: Applied Science and Manufacturing* **2010**, *41*, 806-819.

27. Ulman, A., Formation and Structure of Self-Assembled Monolayers. *Chem. Rev.* **1996**, *96*, 1533-1554.

28. Moses, P. R.; Wier, L. M.; Lennox, J. C.; Finklea, H. O.; Lenhard, J. R.; Murray, R. W., X-ray photoelectron spectroscopy of alkylaminesilanes bound to metal oxide electrodes. *Analytical Chemistry* **1978**, *50*, 576-585.

29. Os, M. V., *Surface Modification by Plasma Polymerization: Film Deposition, Tailoring of Surface Properties, and Biocompatibility*. University of Twente: Enschede, **2000**.

30. Yuan, S. J.; Pehkonen, S. O.; Ting, Y. P.; Neoh, K. G.; Kang, E. T., Inorganic–Organic Hybrid Coatings on Stainless Steel by Layer-by-Layer Deposition and Surface-Initiated Atom-Transfer-Radical Polymerization for Combating Biocorrosion. *ACS Appl. Mater. Interfaces* **2009**, *1*, 640-652.

31. Lin, J.; Qiu, S.; Lewis, K.; Klibanov, A. M., Mechanism of bactericidal and fungicidal activities of textiles covalently modified with alkylated polyethylenimine. *Biotechnology and Bioengineering* **2003**, *83*, 168-172.

32. Locklin, J. Synthesis and application reactive antimicrobial copolymers for textile fibers. US20130036558 A1, 2013.

33. Dhende, V. P.; Samanta, S.; Jones, D. M.; Hardin, I. R.; Locklin, J., One-Step Photochemical Synthesis of Permanent, Nonleaching, Ultrathin Antimicrobial Coatings for Textiles and Plastics. *ACS Appl. Mater. Interfaces* **2011**, *3*, 2830-2837.

34. Han, H.; Wu, J.; Avery, C. W.; Mizutani, M.; Jiang, X.; Kamigaito, M.; Chen, Z.; Xi, C.; Kuroda, K., Immobilization of Amphiphilic Polycations by Catechol Functionality for Antimicrobial Coatings. *Langmuir* **2011**, *27*, 4010-4019.

35. Kim, S.; Nam, J. A.; Lee, S.; In, I.; Park, S. Y., Antimicrobial activity of water resistant surface coating from catechol conjugated polyquaternary amine on versatile substrates. *J. Appl. Polym. Sci.* **2014**, n/a-n/a.

36. Neoh, K. G.; Kang, E. T., Combating Bacterial Colonization on Metals via Polymer Coatings: Relevance to Marine and Medical Applications. *ACS Appl. Mater. Interfaces* **2011**, *3*, 2808-2819.

37. Williams, G. J., Antimicrobial Surfaces. In *Russell, Hugo & Ayliffe's*, Wiley-Blackwell2013; pp 485-499.

38. Nigmatullin, R.; Gao, F., Onium-functionalised Polymers in the Design of Non-leaching Antimicrobial Surfaces. *Macromol. Mater. Eng.* **2012**, *297*, 1038-1074.

39. Kenawy, E.-R.; Worley, S. D.; Broughton, R., The Chemistry and Applications of Antimicrobial Polymers: A State-of-the-Art Review. *Biomacromolecules* **2007**, *8*, 1359-1384.

40. Alexander, M. K., Permanently microbicidal materials coatings. *J. Mater. Chem.* **2007**, *17*.

41. Green, J.-B. D.; Fulghum, T.; Nordhaus, M. A., A review of immobilized antimicrobial agents and methods for testing. *Biointerphases* **2011**, *6*, MR13-MR28.

42. Beyth, N.; Yudovin-Farber, I.; Perez-Davidi, M.; Domb, A. J.; Weiss, E. I., Polyethyleneimine nanoparticles incorporated into resin composite cause cell death and trigger biofilm stress in vivo. *Proceedings of the National Academy of Sciences of the United States of America* **2010**, *107*, 22038-22043.

43. Botequim, D.; Maia, J.; Lino, M. M. F.; Lopes, L. M. F.; Simões, P. N.; Ilharco, L. M.; Ferreira, L., Nanoparticles and Surfaces Presenting Antifungal, Antibacterial and Antiviral Properties. *Langmuir* **2012**, *28*, 7646-7656.

44. Lin, J.; Qiu, S.; Lewis, K.; Klibanov, A. M., Bactericidal Properties of Flat Surfaces and Nanoparticles Derivatized with Alkylated Polyethylenimines. *Biotechnol. Prog.* **2002**, *18*, 1082-1086.

45. Song, J.; Kong, H.; Jang, J., Bacterial adhesion inhibition of the quaternary ammonium functionalized silica nanoparticles. *Colloids and surfaces. B, Biointerfaces* **2011**, *82*, 651-656.

46. *Worldwide Wound Management, Forecast to 2021: Established and Emerging Products, Technologies and Markets in the Americas, Europe, Asia/Pacific and Rest of World*; 2013; p 376.

47. Kim, Y. H.; Nam, C. W.; Choi, J. W.; Jang, J., Durable antimicrobial treatment of cotton fabrics using N-(2-hydroxy)propyl-3-trimethylammonium chitosan chloride and polycarboxylic acids. *J. Appl. Polym. Sci.* **2003**, *88*, 1567-1572.

48. Lee, S. B.; Koepsel, R. R.; Morley, S. W.; Matyjaszewski, K.; Sun, Y.; Russell, A. J., Permanent, Nonleaching Antibacterial Surfaces. 1. Synthesis by Atom Transfer Radical Polymerization. *Biomacromolecules* **2004**, *5*, 877-882.

49. Roy, D.; Knapp, J. S.; Guthrie, J. T.; Perrier, S., Antibacterial Cellulose Fiber via RAFT Surface Graft Polymerization. *Biomacromolecules* **2007**, *9*, 91-99.

50. Meadows, D. C.; Gervay-Hague, J., Vinyl sulfones: Synthetic preparations and medicinal chemistry applications. *Medicinal Research Reviews* **2006**, *26*, 793-814.

51. Ignatova, M.; Voccia, S.; Gilbert, B.; Markova, N.; Mercuri, P. S.; Galleni, M.; Sciannamea, V.; Lenoir, S.; Cossement, D.; Gouttebaron, R.; Jérôme, R.; Jérôme, C., Synthesis of Copolymer Brushes Endowed with Adhesion to Stainless Steel Surfaces and Antibacterial Properties by Controlled Nitroxide-Mediated Radical Polymerization. *Langmuir* **2004**, *20*, 10718-10726.

52. Akihiko, K.; Tomiki, I.; Takeshi, E., Novel polycationic biocides: Synthesis and antibacterial activity of polymeric phosphonium salts. *Journal of Polymer Science Part A: Polymer Chemistry* **1993**, *31*.

53. Lenoir, S.; Pagnoulle, C.; Detrembleur, C.; Galleni, M.; Jérôme, R., New antibacterial cationic surfactants prepared by atom transfer radical polymerization. *Journal of Polymer Science Part A: Polymer Chemistry* **2006**, *44*, 1214-1224.

54. J. N. Turro, *Modern Molecule Photochemistry* **1991**.

55. Huang, J.; Murata, H.; Koepsel, R. R.; Russell, A. J.; Matyjaszewski, K., Antibacterial Polypropylene via Surface-Initiated Atom Transfer Radical Polymerization. *Biomacromolecules* **2007**, *8*, 1396-1399.

56. Ledbetter, J. W.; Bowen, J. R., Spectrophotometric determination of the critical micelle concentration of some alkyldimethylbenzylammonium chlorides using fluorescein. *Analytical Chemistry* **1969**, *41*, 1345-1347.

57. Hsu, B. B.; Klibanov, A. M., Light-Activated Covalent Coating of Cotton with Bactericidal Hydrophobic Polycations. *Biomacromolecules* **2010**, *12*, 6-9.

58. Kym, P. R.; Carlson, K. E.; Katzenellenbogen, J. A., Evaluation of a Highly Efficient Aryl Azide Photoaffinity Labeling Reagent for the Progesterone Receptor. *Bioconjugate Chemistry* **1995**, *6*, 115-122.

59. Soundararajan, N.; Platz, M. S., Descriptive photochemistry of polyfluorinated azide derivatives of methyl benzoate. *The Journal of Organic Chemistry* **1990**, *55*, 2034-2044.

60. Scriven, E. F. V., *Azides and Nitrenes: Reactivity and Utility*. Academic Press: Orlando, **1984**.

61. Wafa, D. M.; Breidt, F.; Gawish, S. M.; Matthews, S. R.; Donohue, K. V.; Roe, R. M.; Bourham, M. A., Atmospheric plasma-aided biocidal finishes for nonwoven polypropylene fabrics. II. Functionality of synthesized fabrics. *J. Appl. Polym. Sci.* **2007**, *103*, 1911-1917.

62. Lim, S.-H.; Hudson, S. M., Synthesis and antimicrobial activity of a water-soluble chitosan derivative with a fiber-reactive group. *Carbohydr. Res.* **2004**, *339*, 313-319.

63. Gawish, S. M.; Ramadan, A. M.; Cornelius, C. E.; Bourham, M. A.; Matthews, S. R.; McCord, M. G.; Wafa, D. M.; Breidt, F., New Functionalities of PA6,6 Fabric Modified by Atmospheric Pressure Plasma and Grafted Glycidyl Methacrylate Derivatives. *Text. Res. J.* **2007**, *77*, 92-104.

64. Cen, L.; Neoh, K. G.; Kang, E. T., Surface Functionalization Technique for Conferring Antibacterial Properties to Polymeric and Cellulosic Surfaces. *Langmuir* **2003**, *19*, 10295-10303.

65. Huh, M. W.; Kang, I.-K.; Lee, D. H.; Kim, W. S.; Lee, D. H.; Park, L. S.; Min, K. E.; Seo, K. H., Surface characterization and antibacterial activity of chitosan-grafted poly(ethylene terephthalate) prepared by plasma glow discharge. *J. Appl. Polym. Sci.* **2001**, *81*, 2769-2778.

66. Belanger, D.; Pinson, J., Electrografting: a powerful method for surface modification. *Chem. Soc. Rev.* **2011**, *40*, 3995-4048.

67. Ignatova, M.; Voccia, S.; Gabriel, S.; Gilbert, B.; Cossement, D.; Jérôme, R.; Jérôme, C., Stainless Steel Grafting of Hyperbranched Polymer Brushes with an Antibacterial Activity: Synthesis, Characterization, and Properties. *Langmuir* **2008**, *25*, 891-902.

68. Yuan, S. J.; Pehkonen, S. O.; Ting, Y. P.; Neoh, K. G.; Kang, E. T., Antibacterial Inorganic–Organic Hybrid Coatings on Stainless Steel via Consecutive Surface-Initiated Atom Transfer Radical Polymerization for Biocorrosion Prevention. *Langmuir* **2009**, *26*, 6728-6736.

69. Huang, J.; Koepsel, R. R.; Murata, H.; Wu, W.; Lee, S. B.; Kowalewski, T.; Russell, A. J.; Matyjaszewski, K., Nonleaching Antibacterial Glass Surfaces via “Grafting Onto”: The Effect of the Number of Quaternary Ammonium Groups on Biocidal Activity. *Langmuir* **2008**, *24*, 6785-6795.

70. Iarikov, D. D.; Kargar, M.; Sahari, A.; Russel, L.; Gause, K. T.; Behkam, B.; Ducker, W. A., Antimicrobial Surfaces Using Covalently Bound Polyallylamine. *Biomacromolecules* **2013**, *15*, 169.

71. Liao, Y.; Wang, Y.; Feng, X.; Wang, W.; Xu, F.; Zhang, L., Antibacterial surfaces through dopamine functionalization and silver nanoparticle immobilization. *Materials Chemistry and Physics* **2010**, *121*, 534-540.

72. Jiang, Y.; Lu, Y.; Zhang, L.; Liu, L.; Dai, Y.; Wang, W., Preparation and characterization of silver nanoparticles immobilized on multi-walled carbon nanotubes by poly(dopamine) functionalization. *J Nanopart Res* **2012**, *14*, 1-10.

73. Geiseler, B.; Fruk, L., Bifunctional catechol based linkers for modification of TiO₂ surfaces. *J. Mater. Chem.* **2012**, *22*, 735-741.

74. Wu, H.; Zhang, C.; Liang, Y.; Shi, J.; Wang, X.; Jiang, Z., Catechol modification and covalent immobilization of catalase on titania submicrospheres. *Journal of Molecular Catalysis B: Enzymatic* **2013**, *92*, 44-50.

75. Lee, H.; Dellatore, S. M.; Miller, W. M.; Messersmith, P. B., Mussel-Inspired Surface Chemistry for Multifunctional Coatings. *Science* **2007**, *318*, 426-430.

76. Zhu, L.-P.; Jiang, J.-H.; Zhu, B.-K.; Xu, Y.-Y., Immobilization of bovine serum albumin onto porous polyethylene membranes using strongly attached polydopamine as a spacer. *Colloids and Surfaces B: Biointerfaces* **2011**, *86*, 111-118.

77. Haldar, J.; Weight, A.; Klibanov, A., Preparation, application and testing of permanent antibacterial and antiviral coatings. *Nature Protocols* **2007**, *2*, 2412-2417.

CHAPTER 6

CONCLUSIONS AND OUTLOOK

Analysis and future prospects

Sulfonyl azide chemistry is a unique and underutilized method of C-H insertion on surfaces. Ruhe and Prucker have been virtually the sole users of this chemistry in the last decade aside from our earlier discussed Kevlar work.¹ However, they have focused on the use of sulfonyl azides to graft to fairly ordinary alkyl-containing substrates such as polystyrene. Sulfonyl azides have much more promise with surface grafting chemistry due to the extreme reactivity of the nitrene intermediate. Other inert surfaces such as metals, metal oxides, silicon and silica, and fluorinated surfaces should be investigated for their reactivity with sulfonyl nitrenes.

The future of SuFEx seems extremely promising, with expansions further into the field of materials chemistry very likely.. Analogues of novel materials made using CuAAC and thiolene/yne should be investigated using SuFEx chemistry with sulfonyl fluorides/fluorosulfates and silyl ethers. Among the approaches that should be explored are end group functionalization, clicking together homopolymers to make block copolymers and clicking monofunctional polymers to multifunctional small molecules to make star polymers.

The use of SuFEx and other orthogonal click chemistries on the surface allows us to prepare carefully controlled biomimetic and biosensing surfaces. The ability of biology to attain nearly perfect fidelity with various lock and key reactions is ideal and unattainable presently, but as we invent more reactions of the click variety which have high degrees of orthogonality, we can start to make attempts to imitate complex biology in structure and function.

Dong and Sharpless have already established that SuFEx can be used to make a sulfate analogue of polyethylene terephthalate.² This approach barely scratches the surface of polymers that could be made using SuFEx polymerization. Sulfates are an interesting linker with possible biological activity, and sulfonates made from sulfonyl fluorides present another linker with potential biological relevance. There is a possibility that sulfate and sulfonate connected polymers, which are typically quite stable to acids and bases, may also be biodegradable, which presents fascinating opportunities for biodegradable analogues of commercial polymers.

An important step in realizing these advances in SuFEx chemistry is elucidating the mechanism by which the reaction between a sulfonyl fluoride and a silyl ether occurs. Thus far, no published work has investigated it. Gembus mentions the concept of a sulfonyl-ammonium intermediate, but presents no evidence of such an intermediate forming.³ While NMR and other solution techniques may be able to produce information about the mechanistic pathway, the use of surface chemistry and analytical techniques could also yield critical insight into the SuFEx mechanism.

Conclusions

In conclusion, this work demonstrates two different approaches to surface functionalization: creating reactive polymers that can graft to highly inert surfaces through unique nitrene chemistry and brush based functionalization for the attachment of more complex, delicate, or difficult to polymerize moieties. Both approaches yield unique chemistries that broaden our toolbox for the functionalization of surfaces. Moreover, it is also my hope that the nascent field of SuFEx chemistry can lead to an array of fascinating new materials technologies.

References

1. Körner, M.; Prucker, O.; Rühe, J. Kinetics of the Generation of Surface-Attached Polymer Networks through C, H-Insertion Reactions. *Macromolecules* **2016**.
2. Dong, J.; Sharpless, K. B.; Kwisnek, L.; Oakdale, J. S.; Fokin, V. V. SuFEx-Based Synthesis of Polysulfates. *Angew. Chem. Int. Ed.* **2014**, *53* (36), 9466-9470.
3. Gembus, V.; Marsais, F.; Levacher, V. An Efficient Organocatalyzed Interconversion of Silyl Ethers to Tosylates Using DBU and p-Toluenesulfonyl Fluoride. *Synlett* **2008**, *2008* (10), 1463-1466.